TAMPEREEN TEKNILLINEN YLIOPISTO
TAMPERE UNIVERSITY OF TECHNOLOGY

Syed Fahad Yunas

Capacity, Energy-Efficiency and Cost-Efficiency Aspects of Future Mobile Network Deployment Solutions

Julkaisu 1323 • Publication 1323

Tampere 2015

Tampereen teknillinen yliopisto. Julkaisu 1323
Tampere University of Technology. Publication 1323

Syed Fahad Yunas

Capacity, Energy-Efficiency and Cost-Efficiency Aspects of Future Mobile Network Deployment Solutions

Thesis for the degree of Doctor of Science in Technology to be presented with due permission for public examination and criticism in Tietotalo Building, Auditorium TB224, at Tampere University of Technology, on the 9th of October 2015, at 12 noon.

Tampereen teknillinen yliopisto - Tampere University of Technology
Tampere 2015

Supervisor

Mikko Valkama, Dr. Tech., Professor
Vice Head of Department of Electronics and Communications Engineering
Vice Dean of Faculty of Computing and Electrical Engineering
Tampere University of Technology
Tampere, Finland

Co-supervisors

Jukka Lempiäinen, Dr. Tech., Professor
Head of Laboratory of Radio Network Planning
Department of Electronics and Communications Engineering
Tampere University of Technology
Tampere, Finland

Jarno Niemelä, Dr. Tech.
Service Manager
Elisa Oyj
Espoo, Finland

Pre-examiners

Jyri Hämäläinen, Dr. Tech., Professor
Dean of School of Electrical Engineering
Aalto University
Espoo, Finland

Preben Mogensen, Ph.D., Professor
Department of Electronic Systems
Aalborg University
Aalborg, Denmark

Opponent

Mario Garcia-Lozano, Ph.D., Associate Professor
Department of Signal Processing and Communications
Polytechnic University of Catalonia
Barcelona, Spain

ISBN 978-952-15-3581-9 (printed)
ISBN 978-952-15-3594-9 (PDF)
ISSN 1459-2045

Abstract

Recent data analytics from the mobile broadband networks have revealed an exponentially rising trend of mobile data traffic for the past five years. It is predicted that by 2020 the overall data traffic will increase by a factor of 1000x. This traffic growth is caused both by the increased adoption of smartphones and tablets, and by the increased usage of multimedia rich services, such as video streaming. Furthermore, most of this demand is likely to come from indoor users. In order to be able to meet the increased capacity needs, network densification has been identified as a viable pathway for mobile operators to evolve their networks. Network densification can be achieved by either densifying the existing legacy deployments, e.g. by deploying more macrocell sites or street-level microcells, or by deploying new indoor low-power sites, or both. Furthermore, different distributed antenna solutions offer an additional interesting aspect in network densification and deployments.

This doctoral dissertation addresses network densification from alternative deployment strategies' perspective, in particular, when individual densification solutions are pushed to their capacity limits, such that all the network elements operate at full load. It evaluates and compares the performance of different deployment strategies in terms of *capacity-*, *energy-* and *cost- efficiency*. The performance evaluations are carried out using propagation modeling based analysis and are based on a system-independent approach, integrating not only the classical capacity and spectral efficiency aspects, but also energy- and cost-efficiency perspectives, through realistic power consumption and investment cost models. The energy-efficiency aspects are seen particularly important when moving towards the era of green communications, under clear trends and incentives to save energy at all levels of society. Furthermore, the analysis integrates some of the recent findings related to substantially increased building penetration losses, through the use of more energy-efficient building materials.

The obtained results indicate that the indoor femtocell-based solutions with densely deployed femto-cells are much more spectrally-, energy- and cost efficient approach to

address the enormous indoor capacity demands of the 5G era and beyond, compared to densifying the outdoor legacy deployment solutions, when the network is pushed to the extreme limit. This is particularly so when the building penetration losses are high, as has been recently observed in actual field measurements. Furthermore, the dynamic outdoor DAS concept, studied also in this thesis, offers an efficient and capacity-adaptive solution to provide outdoor capacity, on-demand, in urban areas. In general, this thesis work provides tools, results, understanding and insight of both technical and techno-economical aspects of long-term evolutionary perspectives of different mobile network deployment and densification solutions, which can be used by network vendors, operators and device manufacturers.

Preface

The research work performed for this thesis was carried out during the years 2011-2015 at the Department of Electronics and Communications Engineering, Tampere University of Technology, Finland. I would like to thank all the current and earlier personnel of the Department of Electronics and Communications Engineering, for providing the most inspiring and pleasant working environment.

First of all, I would like to express my deepest gratitude to my supervisor Prof. Mikko Valkama for providing the opportunity to do my doctoral research under his supervision. His continuous guidance, support, and forensic scrutiny of my technical writing has been invaluable. He has always found the time to propose consistently excellent improvements. I owe a great debt of gratitude during the research work leading to this thesis.

I am also grateful to my co-supervisors Prof. Jukka Lempiäinen and Dr. Jarno Niemelä. Their patience, encouragement, and immense knowledge were key motivations during the course of my doctoral studies. Dr. Jarno Niemelä is a great mentor and friend, from whom I have learnt the vital skill of disciplined critical thinking. I would like to thank Dr. Tero Isotalo for offering thorough and excellent feedback on earlier versions of this thesis. Dr. Tero Isotalo also provided valuable technical discussions during the initial stages of my doctoral studies.

I want to acknowledge the dissertation pre-examiners, Prof. Jyri Hämäläinen from Aalto University and Prof. Preben Mogensen from Aalborg University for their valuable comments and suggestions for improving the dissertation.

A special thanks is dedicated to my past and present colleagues in the Laboratory of Radio Network Planning with whom I had the pleasure to work with: D. Sc. Panu Lähdekorpi, D. Sc. Jussi Turkka, D. Sc. Usman Sheikh, M. Sc. Joonas Säe and M. Sc. Sharareh Naghdi. Thanks guys for memorable events and discussions that I was able to share with you.

The research work was financially supported by the University of Engineering and

Technology, Peshawar Pakistan, in the initial stages of my doctoral studies, and afterwards by the Finnish Funding Agency for Technology and Innovation (Tekes, under the project "Energy-Efficient Wireless Networks and Connectivity of Devices - Systems (EWINE-S)"), all of which are gratefully acknowledged.

When it comes to practical matters, I would like to extend my thanks to the past and present secretaries of our department: Ms. Tarja Erälaukko, Ms. Soile Lönnqvist and also Ms. Sari Kinnari. A big thank you to Ms. Ulla Siltaloppi for being so nice and helpful in numerous practical and administrative matters inside and outside the university. My sincere appreciation also goes to our department's financial secretary Ms. Heli Ahlfors for sorting out the financial matters related to official travels, during my doctoral studies.

For all my friends from Pakistani community living here in Finland, I would just like to say; '*Thank you for your friendship and all the laughs, lovely memories, and nice time we have had together - Dera Manana! [Pashto]*'.

Finally, I wish to express my warmest and deepest thanks to my parents for their parenting, guidance, and love throughout my life. I am eternally gratefully to them. I would like to express my love to all my sisters.

I dedicate this thesis to a brave little superhero; my nephew (*your smile and laughter is the only thing that makes us happy in the family - Always be happy no matter what*).

"***In loving memory of my late elder sister, my brother-in-law and my sweet niece* - You will always be in my heart**".

Tampere, Finland
September 2015.

Syed Fahad Yunas

Table of Contents

List of Abbreviations

3D	3-Dimensional
2G	Second Generation
3G	Third Generation
4G	Fourth Generation
5G	Fifth Generation
3GPP	The Third Generation Partnership Project
ADSL	Asynchronous Digital Subscriber Line
AE	Antenna Element
AP	Access Point
B4G	Beyond Fourth Generation
BPL	Building Penetration Loss
BS	Base Station
BTS	Base Transceiver Station
CAPEX	Capital Expenditure
Cm-wave	Centimeter-wave
CSG	Closed Subscriber Group
C-RAN	Centralized Radio Access Network
DAS	Distributed Antenna System
DCF	Discounted Cash Flow
DenseNets	Dense Networks
DPM	Dominant Path Model
DSP	Digital Signal Processor
EHF	Extremely High Frequency
EIRP	Effective Isotropic Radiated Power
eNode B	3GPP term for evolved UMTS base station
EU	European Union
FAP	Femtocell Access Point

FBR	Front-to-Back Ratio
FM	Frequency Modulation
FPGA	Field-Programmable Gate Array
FTTH	Fiber-to-the-Home
GSM	Global System for Mobile communications
HCS	Hierarchical Cellular Structure
HetNet	Heterogeneous Network
HPBW	Half Power Beamwidth
ICIC	Interference Cell Interference Coordination
IP	Internet Protocol
ISD	Inter-site Distance
KPI	Key Performance Indicator
LOS	Line of Sight
LTE	Long Term Evolution
MIMO	Multiple Input Multiple Output
Mm-wave	Millimeter-wave
MS	Mobile Station
NLOS	Non Line of Sight
Node B	3GPP term for UMTS base station
NPV	Net Present Value
NSC	Neighborhood Small Cell
OA&M	Operation, Administration and Maintenance
ODAS	Outdoor Distributed Antenna System
OLOS	Obstructed Line of Sight
OPEX	Operational Expenditure
OSG	Open Subscriber Group
PA	Power Amplifier
QoE	Quality of Experience
QoS	Quality of Service
RAN	Radio Access Network
RF	Radio Frequency
RT	Ray Tracing
SBR	Shooting and Bouncing Ray
SHF	Super High Frequency
SLL	Side Lobe Level
SINR	Signal to Interference+Noise Ratio
SNR	Signal to Noise Ratio

TCO	Total Cost of Ownership
TRX	Transceiver
UE	User Equipment
UHF	Ultra High Frequency
UMTS	Universal Mobile Telecommunications System
UTP	Unshielded Twister Pair
UTRA FDD	UMTS Terrestrial Radio Access Frequency Division Duplex
WCDMA	Wideband Code Division Multiple Access
WLAN	Wireless Local Area Network
WPL	Wall Pentration Loss

Chapter 1

Introduction

1.1 Background and Motivation

With the exponentially increasing global data traffic volume together with a projected massive increase in the number of connected devices in near-future, it is envisioned that the current generation of cellular networks may already soon reach their capacity limits. According to a recent data analytics report [1], the amount of mobile data traffic, worldwide, has been annually doubling since 2010. With this annual growth rate trend, the industry experts predict a significant 1000x increase in the total data capacity demand in near future, with some of the experts and network vendors suggesting that the 1000x mark might be reached by year 2020 [2–4]. Most of this demand is expected to come from the surge in smart phones, tablets and laptop users with wireless broadband connectivity, accessing the ever increasingly rich multimedia contents over the Internet[1]. As a preemptive solution, to deflect the danger of running into a capacity crunch, the mobile industry is already working towards the 5^{th} generation (5G) of wireless cellular networks, which is conceived to address the growing capacity demand in a sustainable and cost-effective manner with substantially lowered energy consumption per transferred bit. 5G networks will not be just about enhancements in the radio access network (RAN) part but will rather represent an eco-system of interoperable technologies and network layers, working as a whole to provide ubiquitous high speed connectivity.

To tackle the '*1000*x *Data Challenge*', as some of the industry leaders name it [5], the network vendors and mobile operators have to focus on two partially related key

[1]Some projected figures from Cisco VNI Global Mobile Data Traffic Forecasts 2014 report [1]:

- 10 billion mobile-ready devices and connections by 2018 (approx. 3 billion more than in 2013).
- 5 billion global mobile users by 2018, up from more than 4 billion in 2013.
- Global mobile IP traffic to reach upto 190 exabytes in 2018, up from less than 18 exabytes in 2013

aspects:

- High bit rate service provisioning, and
- Ubiquitous - *anywhere anytime* – service provisioning

The first strategy is a traditional approach which the industry has been following till date i.e. increasing the cell level capacities by improving the air-interface efficiency through *advanced digital transmission techniques*, (e.g., higher-order modulation and coding, advanced antenna systems etc.,) and *utilization of larger spectrum chunks*. Although such improvements at the air-interface significantly improve the cell level capacities, they are still not able to provide the needed *network level gains*. Hence, a very different approach is needed on a system level to meet the imminent explosive growth in data traffic demands.

The second strategy focuses on providing ubiquitous '*anywhere any time*' service to the masses, i.e., increasing the network level capacity to support more users and devices in a given area. One of the most obvious ways to increase the capacity of a wireless network is by spatially reusing the existing allocated spectrum as frequently as possible throughout the network service area, in other words, by increasing the base station density. As such, the capacity of a cellular network is considered to be proportional to the base station density. The idea of enhancing the system capacity through network densification can be dated back to late 1940s when the cellular concept was introduced [6]. The initial adoption of the concept, however, was slow at the beginning but started to gain serious attention when 2G networks were introduced. Since then, network densification has been viewed as a feasible pathway towards network evolution.

While a significant amount of time and effort in the last two decades was dedicated by the industry and academia to improve the spectral efficiency of wireless networks, more recently, the focal point of the industry has started to expand towards including energy and cost efficiency aspects into its domain. To cope with the current rate of 'exponentially' increasing capacity demand, deployment of several magnitudes more base stations will be required, which is considered by the industry to be a feasible pathway. However, this strategy is known to significantly increase the cost and energy consumption of the cellular networks [7]. According to some studies conducted in 2007/2008, the radio access networks alone had a share of around 0.3% - 0.5% in the global CO_2 emissions [8, 9] and out of this roughly 80% came from the base stations [10]. As the worldwide awareness regarding global warming increases, political initiatives at the international level have started to put stringent requirements on the operators and manufacturers to lower the gas emissions of com-

munications networks [11]. This has led the telecommunication industry, especially the standardization and regulatory bodies, to focus their attention towards building 'greener' wireless networks.

Another recent trend, stemming from increased awareness of global warming and the resulting requirements to save energy and cut down on CO_2 emissions, is to improve the thermal insulation of commercial and residential buildings. A good example is the recent European Union (EU) directive [12], which states:

***"Member states shall ensure that by 31st December 2020 all new buildings are nearly zero-energy buildings"* - Directive 2010/31/EU, Article 9**.

As a result, the construction industries have started to develop, manufacture and utilize modern construction materials, that provide a greater degree of thermal insulation, thereby reducing the load on heating and cooling systems and hence the carbon emissions and energy consumption. Although at first sight this has seemingly nothing to do with radio communications and mobile networks, however, it has recently been reported that such new construction materials have a significant impact on the radio signal propagation, most notably in the form of highly increased building penetration losses (BPL) [13, 14]. Due to the lack of coordination and communication between mobile network and construction industries, this has started to pose serious concerns for mobile operators who are still heavily relying on traditional macro layer to provide indoor coverage and capacity. A concrete example is that the typical building penetration loss values used by mobile network operators and radio network planners till date, in dimensioning their networks, have been in the range of 5-15 dB [15, 16]. However, very recent works based on actual RF measurements in modern residential buildings have reported a drastic increase in these values, with peak BPL values reaching 35 dB [13, 14].

1.2 Scope of the Thesis

This dissertation looks into dense networks or *DenseNets* from an alternative deployment strategies' perspective, in particular, *when individual densification solutions are pushed towards their capacity limits.* It starts by looking into a conventional methodology of network densification used by the operators, mostly based on legacy macro-/micro-cellular deployment solutions, analyzing and discussing the limitations of such approaches, and then proceeding towards newer deployment paradigms that enable successful realization of *DenseNets* concepts. Particular emphasis, in the anal-

ysis and presentation, is placed on the *network-level spectral-efficiency* as well as *network energy-efficiency* and *cost-efficiency*, when different deployment solutions, namely densified macro network, extremely dense small-cell network, and distributed antenna systems (DAS) based network, are pushed to the limits such that all the network elements operate at full load. Special attention is given to the differences between indoor and outdoor user equipments (UEs) under these different deployment solutions, strongly motivated by the recent observations e.g. in [13, 14, 17] that the wall penetration losses of both residential and commercial buildings can peak up to 35 dB or so, due to new construction materials with high thermal insulation, impacting also radio signal propagation.

The main objective of the thesis is to gain technical insight and understanding of different solutions and to draw critical conclusions on the choice of deployment schemes that would assist mobile operators in deciding the best evolution strategy for their network in the future. As a systematic technology-independent study case, the thesis focuses on a concrete example scenario of 20 MHz carrier bandwidth at 2.1 GHz center-frequency. Naturally, the same methodology can be applied to other carrier bandwidths and center-frequencies as well. Furthermore, it is pertinent that although the results from the dense small-cell network study only considers femtocell deployment solutions, the analysis can be generalized to deployment solutions based on indoor WiFi.

1.3 Related Work in the Literature

1.3.1 A brief look at the history

The idea of enhancing the network capacity through densifying the network elements is something not novel, rather, it can be dated back to the late 1940's when the concept of *cellular system* was informally introduced by D. H. Ring [18, 19]. Several publications later went on to discuss the cellular concept as a possible solution to solve the problem of spectral congestion and increased user capacity demands [20–24]. Furthermore, different cell deployment layouts and the idea of cell sectorization, as coverage and capacity enhancing technique, were proposed in the late 70s; see [6, 25]. The concept of street-level cellular deployment, also known as *microcells*, was proposed in mid-1980s, which took the network densification one step further; see [26–29]. The basic concept behind the microcells was to address capacity demand in hot-spot areas especially in urban locality. All the cellular deployments prior to 1990 utilized unshileded twisted pair (UTP) or coaxial cables for backhaul transmission. However,

with the advancement in the optical fiber technology, microcellular concept utilizing fiber-optic, as a high capacity and low latency transmission medium, was introduced in the beginning of 1990s; see [30–32]. Research problems related to microcell site placement, location and size and resource management between macro and micro cell layers have been addressed in [33–39].

The initial adoption of the network densification idea through joint macro-/micro-cellular deployments, also known as heterogeneous network, was slow at first but started to gain serious attention when data capabilities were introduced in 2G networks. With the advent of 3G networks, the heterogeneous network deployments or 'hierachical cellular structure (HCS)' gained even more interest from the mobile operators.

During the last decade, mobile data traffic volume increased at an exponential rate, thanks to the availability of high speed mobile broadband services with flat-rate pricing and rapid proliferation of smart phones, tablets etc. The telecom industry realized that such massive increase in capacity demand could not be sustained by legacy wireless infrastructure, hence, efforts were put into finding a cost-efficient solution. In recent years, low power base stations have received much attention. The idea of having a compact, self-optimizing home cell site was first reported in 1999 by Alcatel [40]. Around 2005, the term *femtocell* was adopted by the industry to refer to operator managed, self-configuring and stand-alone home base station. The standardization activities related to femtocells started in 2007 with the start-up of Femto Forum (now Small Cell forum) [41]. Initially, many of the standarization activities focused around residential femtocells, however, lately heterogeneous small cell deployments with a wider focus have been gaining ground e.g. enterprise femtocells, outdoor urban femtocells and rural femtocells [42–44]. 3GPP has also been incorporating the introduction of femtocells, or Home (e)Node B, in its Releases 8 - 11 [45–49].

1.3.2 Recently reported work

Several studies have been undertaken in the past couple of years with wide ranging scope related to network densification utilizing legacy and modern heterogeneous deployment solutions. This section provides some recently reported work on network densification that are most relevant to this thesis.

Capacity performance related studies

In [50], the performance of base station densification with different transmission schemes has been compared to a network employing base station coordination al-

gorithms. The study concentrates on various techniques that can maximize the minimum spectral efficiency of the served users. In addition, a constant user density, irrespective of the network size, is assumed, resulting in a partially loaded system where some of the base stations are kept in sleep mode to avoid over provisioning of the network capacity. The findings from the study indicate that the cell spectral efficiency increases as the network is densified to a certain point and then saturates. In [51], the average cell spectral efficiency is shown to increase linearly with network densification, in partially loaded system. The impact of macrocell densification on the network throughput and power consumption in both homogeneous and heterogeneous network environments has been studied in [52, 53]. The study considers a fully loaded network, where all the base stations are continuously transmitting at full power. However, the maximum transmit power per base station is systematically reduced as the network is densified. The findings in [52] follow the outcomes of [51] i.e., in a homogeneous macrocell network, the cell spectral efficiency tends to improve with increasing network density. In [54, 55], the performance of different heterogeneous network deployment alternatives has been examined from uplink and downlink point of view. The analysis takes a slightly different approach by introducing variable user traffic and analyzing the system capacity performance of different deployment strategies in busy hour. Unlike in [50–52], where only an outdoor environment is assumed, the studies in [54, 55], also take into account the indoor environment with buildings and users distributed among different floors. Nevertheless, the findings therein indicate an increase in the served area traffic per busy hour as the network is densified.

Energy-efficiency related studies

As a result of recent worldwide awareness on global warming, considerable number of studies have been conducted and published in the recent years. The focus has been on quantifying the energy consumption of the wireless networks by establishing different metrics for evaluation of the energy efficiency, proposing power consumption models for different base station types and ways to improving the power consumption of the networks while maintaining decent quality of service and system throughput. Studies emphasizing on the importance of having a holistic framework for evaluating the energy efficiency of the wireless networks have been reported in [56, 57]. In [10], a new metric, area power consumption, is proposed to evaluate and compare the energy efficiencies of networks with different cell site densities per km^2. The impact of cell size on the power consumption, for different deployment strategies, can be found in [51, 58–60]. The energy-efficiency aspects of network densification in various deployment scenarios have been reported in [53]. Unlike the previous studies in [51, 58–60], which

fail to take into account the impact of interference and system throughput while evaluating the energy efficiency, the studies in [53] investigate the relation between energy efficiency, area capacity and cell size by taking into consideration both the interference and noise, and takes relates the energy efficiency in terms of system throughput. Moreover, in [61], the study investigates the energy-savings that can be achieved when co-channel femtocells are introduced into existing macrocellular network deployment. The findings in the paper indicate significant savings in the energy consumption can be achieved in macro-femto network, compared to macro-only network, when the capacity demand is high. The total power consumption of different network densification alternatives in LTE context has been reported in [62], which concludes that under low discontinuous transmission (DTX), the macrocell densification is the most power efficient solution.

Cost-efficiency related studies

The economics of introducing femtocells into LTE macrocellular networks, with open access and closed access femto mode, have been studied in [63]. In [64], comparative cost-capacity studies have been conducted while also taking into account the impact of typical wall penetration losses in the order of 10-20 dB. A similar study focusing on capacity, cost and energy efficiency of macro and femto based solutions for indoor service provisioning have been done in [65].

1.4 Author's Contribution and Thesis Outline

The research work for the thesis was conducted at the Department of Electronics and Communications Engineering, Tampere University of Technology, Finland, under the supervision of Prof. Mikko Valkama, Prof. Jukka Lempiäinen and Dr. Jarno Niemelä. Furthermore, also Dr. Tero Isotalo has contributed substantially through various technical discussions. Results obtained from the research have been reported in seven academic publications in form of conference papers and journal articles; [66–72]. This thesis gathers all the obtained results from these publications into a monograph form. It may be noted that for all the results presented in the following chapters, the author was solely responsible for simulations and post-processing, while the post-analysis of the results was done jointly with supervisors and colleagues. The outline of the thesis and the corresponding contributions of the author in each of the chapters can be summarized as follows:

- Chapter 2 provides the fundamentals of mobile communications systems and the cellular network concept. This is followed by a general description of the analysis methodology, key assumptions and general simulation parameters used in the studies reported in the following chapters.

- Chapter 3 looks at the performance of network densification based on classical deployment solutions namely; macrocellular and microcellular solutions, in a homogeneous and heterogeneous deployment scenarios. The results and analysis presented in the chapter are based on the publications [66, 67]. The author was responsible for simulations and post-processing of the simulation results. The deployment scenarios for the simulations and the post-analysis of the results leading to the publications were jointly carried with co-supervisor Dr. Jarno Niemelä and colleague Dr. Tero Isotalo. Prof. Jukka Lempiäinen participated in various technical discussions around the topic area, offering his technical insight and guidance.

- Chapter 4 looks at the techno-economical performance of denseNets based on indoor femtocell deployment solutions in urban and suburban environments. The results and analysis presented therein are based on the publications reported in [68, 69, 72]. The deployment scenarios for the simulations and the post-analysis of the results were jointly carried with supervisor Prof. Mikko Valkama and co-supervisor Dr. Jarno Niemelä. Dr. Tero Isotalo provided his valuable suggestions and key inputs for techno-economical analysis studies reported in [69]. MSc. Ari Asp provided the measurement results for different wall penetration losses, recently measured in old town house and modern buildings, as reported in [13, 14].

- Chapter 5 looks at the performance of outdoor distributed antenna system (ODAS) as an alternative solution for outdoor service provisioning. The performance of two deployment strategies for implementing the traditional ODAS are evaluated and compared with standalone small cells. Afterwards, a Dynamic DAS concept is introduced which aims to offer dynamic capacity based on outdoor data capacity demand. The results and analysis presented therein are based on the publications reported in [70–72]. The deployment scenarios for the simulations and the post-analysis of the results, reported in [70–72], were jointly carried with supervisor Prof. Mikko Valkama and co-supervisor Dr. Jarno Niemelä.

- Chapter 6 provides the concluding remarks and possible future work for enhancing/improving the analysis studies presented in this dissertation.
- A list of references for further reading is given at the end.

In summary, the thesis author has been the primary author of all reported work. He has carried out all the performance simulations, post-processing and analysis by himself, with natural supervision and guidance from the supervisors. Furthermore, the thesis author has written all the associated papers [66–72] as the first author, and composed majority of the text in all the articles.

Chapter 2

Mobile Communications Fundamentals, Analysis Methods and Assumptions

2.1 Mobile Communications Fundamentals

The design objective of early mobile communication systems was to have a single high power transmitter (base-station), installed on a high mast, that could provide coverage to a large geographic area. One such example was the Bell mobile system in New York in the 1970's. The system was able to support 12 simultaneous calls up to thousand square miles [73]. Initially, this coverage based strategy was performing well. However, as the subscriber base started to increase, the call blocking probability also increased correspondingly (due to system resource unavailability). Thus, in order to cope with the increasing capacity demand, a new strategy had to be formulated.

Wireless communication channel, like every other transmission medium, has a cap on its maximum capacity. This capacity limit was presented in 1945 by Claude E. Shannon in his ground breaking paper 'A Mathematical Theory of Communication'. Shannon showed that for any communication channel with certain bandwidth and Gaussian noise characteristics, the maximum channel capacity, C, is given by [74]:

$$C\,[\text{bps}] = W \cdot log_2(1 + SNR) \tag{2.1}$$

where, W is the channel bandwidth in Hertz and SNR is the signal to noise ratio.

Thus, from (2.1), one way of increasing the capacity of the channel is by increasing the channel bandwidth. Unfortunately, the RF spectrum is a scarce resource. The spectrum in the ultra-high frequency band, where most of the radio communications take place (i.e., from 300 MHz - 3 GHz), is severely congested. Serious

competition among the stakeholders (usually mobile operators) drive the price of the spectrum higher. Hence, increasing the channel bandwidth in the UHF band is not necessarily a viable business option for operators. More recently, communications in the extremely high frequency (EHF) band is being considered for inclusion in the 5G technology standard [75]. Mm-wave communications occur in the underutilized microwave spectrum (30 GHz to 300 GHz) thus providing huge chunk of spectrum bandwidth. The downside, however, is that in such extremely high frequency range, natural phenomenons like atmospheric absorption start to have significant impact of the radio signals thereby severely limiting the communications distance. As a possible solution, antennas with high gain tend to overcome the coverage limitation problem. Another proposal is to utilize the super high frequency (SHF) band which ranges from 3 GHz to 30 GHz [76]. In the SHF band, the impact of atmospheric absorption on the radio signals is reduced sigificantly. This allows non line of sight (NLOS) communications between transmitter and receiver, which is not possible in EHF band.

A second method to enhance the capacity of a wireless communications system is by improving the efficiency of the air-interface, i.e., transmitting more bits per Hertz. This is a traditional approach that the wireless industry has been following till date. Such a method can be realized by utilizing higher modulation and coding techniques, which in turn require higher SNR at the receiving end to de-modulate the signal with acceptable bit-error rate. However, with LTE (Long Term Evolution), the wireless channel capacity is already practically at par with the shannon capacity bounds. Hence, for future capacity requirements, some of the telecommunication industry players believe that upcoming generations of broadband cellular systems will not be defined by a single radio interface only, but rather encompass a suite of different technologies [77].

The third method involves utilizing spatial multiplexing techniques through the use of advanced antenna systems. MIMO (Multiple Input and Multiple Output) system is a type of advanced antenna system that utilizes multiple antennas at the transmitter and receiving end to achieve multiple independent radio links for transferring multiple streams of data at a single time instant. This method is shown to significantly increase the cell level capacity. Nevertheless, in order to realize multiple links, the level of uncorrelation between individual path has to be high enough; higher the degree of uncorrelation translates to higher MIMO channel gain and vice versa. Massive-MIMO is another key technology that is being considered as a candidate for upcoming 5G [78, 79]. However, in the current UHF band, due to the size of the antenna elements, it might not be feasible for the operators to deploy a large antenna array in urban downtowns, where, e.g., zoning restrictions apply.

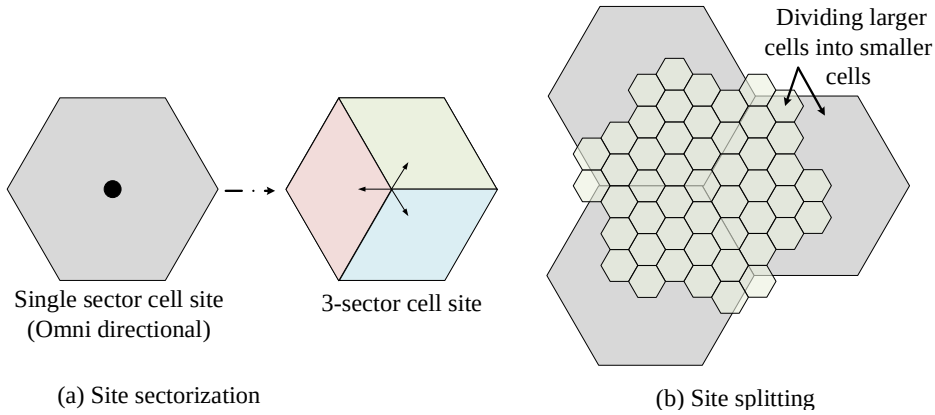

Figure 2.1 Illustration of (a) *Site sectorization* and (b) *Site splitting* techniques for network capacity enhancement.

The techniques described so far help in enhancing the cell level capacities. However, for network level capacity gain extensive spatial reuse of the frequency spectrum is required throughout the network coverage area. A high degree of spatial re-use can be achieved by *network densification*. As such, based on (2.1), the network level capacity, C_{net}, over an area can be roughly approximated as:

$$C_{net}\left[\text{bps/km}^2\right] = N_T \cdot [W \cdot log_2(1 + SINR)] \tag{2.2}$$

where, N_T is the number of co-channel transmitters re-using the same spectrum resource in a given area. It is pertinent to note in (2.2), that with the introduction of co-channel transmitters within the area, the SNR from (2.1) is now $SINR$ which is simply the ratio of *useful signal* (signal received from the serving transmitter) and *Guassian noise* plus *total interference*. The *total interference* is the sum of all other signals coming from non-serving transmitters in the given area. $SINR$ defines the instantaneous radio channel condition at a given location. Higher value of N_T translates into higher *total interference* and hence lower $SINR$. In an ideal scenario, a higher network level capacity is achieved with simultaneous maximization of N_T and $SINR$.

Network densification can be achieved either by *site sectorization* or by *site splitting*. *Site sectorization* involves increasing the number of logical sectors or cells within a base station serving area. Each of the logical sectors then serves a portion of the coverage area. Whereas, *Site splitting* involves dividing larger cells into small cells by reducing the cell sizes. Fig. 2.1 shows *Site sectorization* and *Site splitting* tech-

niques. The idea of enhancing system capacity through cell site densification was first proposed by D. H. Ring in 1940 to solve the spectrum congestion and increased user capacity demands [18], and it still is considered as a feasible pathway for mobile operators to cost-effectively enhance the system capacity. Ultra-dense networks take the network densification to a whole new level, where thousands of base stations are deployed to fulfill the exponentially rising user capacity demand. As such ultra-dense networks are also one of the key flavors of 5G systems and hence form a dominant theme of this dissertation.

2.2 Cellular Network Concepts and Evolution

2.2.1 Basic concepts

Current cellular networks are inherently heterogeneous in terms of network deployments. A heterogeneous network is formed by a combination of different base station types, each having its own characteristics. The classification is typically done based on site location, transmission power of the base transceiver station (BTS) and backhaul connectivity. Some of the main classes of different cell types are given below:

- *Macrocellular base stations*: These types of base stations are normally used for wide area coverage. The antennas are deployed above the average roof-top level in order for the signals to propagate further. Typical transmission power of macrocellular base station can vary from 20 W to 60 W [80]. The cell size can range from a few hundred meters (in dense urban environment) to as much as 35 km (in rural areas). Deployment requires proper RF (radio frequency) planning.

- *Microcellular/pico base stations*: These types of base stations are normally used for local area coverage. The antennas are deployed well below the average roof-top level, typically on a street-level. Typical transmission power of microcellular base station can vary from 100 mW to 10 W [80, 81]. However, in practical outdoor deployment scenarios, the transmit power may range from 250 mW to approximately 2 W [82], depending upon the vendor and intended area to be served. The cell size, due to street-level deployment and lower transmission power, can range from a few hundred meters (in dense urban environment) to 2 km (in urban areas). Microcells can be deployed as a standalone cell site or in form of distributed antenna systems (where the remote antenna nodes are deployed over a given area to provide seamless coverage). Deployment requires

proper RF (radio frequency) planning.

- *Femtocellular base stations*: Femtocell access points (FAPs) are typically deployed inside residential or office environment. Unlike macrocell and microcells base stations, FAPs are deployed by the end users in a plug-and-play fashion similar to WLAN (wireless local area networks) access points [83]. Due to being located inside the building the need for proper RF planning is eliminated. The maximum output power of femtocells access points equals 100 mW [80, 81]. Unlike traditional cellular base stations, the femtocell access points utilize the residential broadband connection (ADSL, FTTH) to connect to the mobile operator's core network. Furthermore, to regulate/control the access to the residential femtocells, the FAPs can be configured to work either in *open subscriber group* (OSG) mode which enables public access to the FAP, or *closed subscriber group mode* (CSG) to restrict the access to certain listed users, or it can be configured to work in hybrid mode, which allows public access to the FAP but preference/priority is given to listed users [84].

2.2.2 Network evolution

In the past and still today, mobile operators have been building their networks using the *Outside-In* approach, i.e. relying primarily on outside macro base stations. Looking at the network evolution, initially, the network is designed from the coverage perspective by deploying macrocell sites to serve both outdoor and indoor locations with certain minimum quality of service. As the number of devices accessing the network increases, it transitions from coverage limited to capacity limited state, thus, necessitating for denser deployments. The densification of the network is done gradually i.e., in the initial stages, the mobile operator tries to accomodate the network capacity demands by densifying the macro-layer itself by installing more macro base-stations. As the network matures, and the number of devices accessing the services keeps increasing, several capacity-limited local hotspot areas within the network begin to appear. These hotspots, limited in size and scattered throughout the network service area, are then covered by deploying street-level microcells. Thus forming what is typically known as a *hierarchical cellular structure*; where macrocells provide the umbrella coverage and microcells aim to fulfill the capacity demands in local hotspot areas. However, as the demand for further capacity increases (mostly coming from indoor locations) the achievable network capacity from densifying the outdoor layers begin to saturate and the operators are forced to transition towards indoors i.e., start deploying *dedicated indoor solutions*. This shifts the network provisioning paradigm

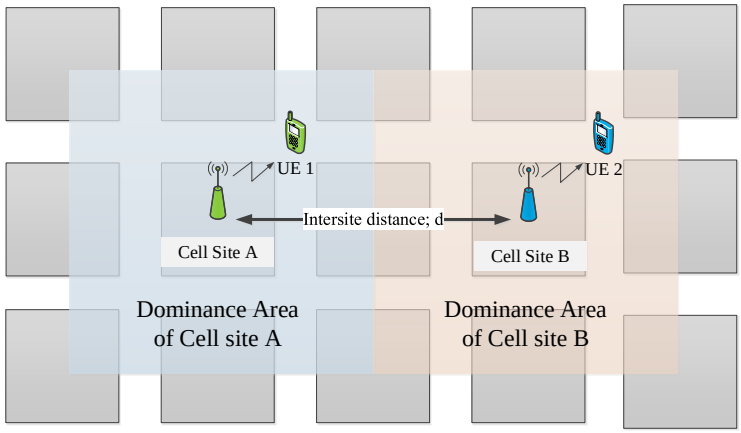

Figure 2.2 Homogeneous environment. Note: The square shape of the dominance area, as shown in the figure, is just for illustration purpose. The actual dominance area depends on the deployed infrastructure (macro-/micro-cell etc.) and cell plan.

from *outside-in* to *inside-in*, wherein a dedicated indoor solution caters for indoor capacity requirements.

2.3 Overview of the Analysis Methodology

An overview of the key assumptions used in the performance analysis of different deployment and densification solutions, in this dissertation, are highlighted below:

- A homogeneous propagation environment is assumed i.e., all the cell sites experience similar radio propagation conditions. As such, the dominance areas of all the cell sites are identical, as shown in Fig. 2.2. Hence, for the performance evaluation of different deployment strategies, the receiver points from the dominance (*best server*) area of the center cell site are considered for statistical analysis while other cells or transmission points are treated as interference.

- For simulating a continuous cellular network effect, the dominant interfering tiers that contribute significantly to the interference level in the dominance area of a serving cell are taken into account.

- The distribution of receiver points outdoors and across all the buildings (floors) is uniform.

- A full cell load over the network is assumed i.e., all the cells are transmitting at full power, which is the worst case scenario and also a typical methodology that is used for network capacity dimensioning. As such the different deployment solutions are thus pushed to their ultimate limits in a systematic manner.

The metrics and and general simulation parameters used in the performance evaluation studies are described in the following sections.

2.3.1 Cell and network area spectral efficiency

For a network operating at a full load, i.e., all the base stations transmitting at full power, the *cell spectral efficiency*, η_{cell}, is defined as the aggregate bit rate per Hz that an individual cell can support, under given radio channel and interference conditions. The average *network area spectral efficiency*, in turn, is defined as:

$$\bar{\eta}_{area}\left[\text{bps/Hz per km}^2\right] = \rho_{cell} \times \bar{\eta}_{cell} \tag{2.3}$$

where ρ_{cell} is the cell density (number of cells per km^2) and $\bar{\eta}_{cell}$ is the average cell spectral efficiency [bps/Hz] which is given by the Shannon capacity bound:

$$\bar{\eta}_{cell} = \langle log_2(1+\Gamma)\rangle\,. \tag{2.4}$$

The quantity Γ in (2.4) refers to the instantaneous signal-to-interference-noise ratio (*SINR*), which defines the radio channel conditions while $\langle . \rangle$ denotes averaging across receiver points. From (2.4) it is evident that the cell/network spectral efficiency depends directly on the distribution of Γ. The level of useful signal and interference that a user equipment (UE) receiver experiences at a given time is largely determined by the deployed network architecture. This will be explained in the following chapters where the mathematical expression for *SINR* will be formulated for each of the underlying deployment strategies.

2.3.2 Energy efficiency

One of the most commonly used metric for assessing the energy efficiency of a network is by evaluating the bits-per-energy ratio, i.e., the amount of bits communicated per unit energy. On a network level, this relates to the aggregate data rate that is achievable while consuming a given power, e.g. 1 kW. This methodology is appropriate for assessing the energy efficiency of a network operating under full load condition [56].

Hence the *network energy-efficiency* is defined as:

$$E_{\text{eff}}\,[\text{bps/Hz/kW}] = \frac{\bar{\eta}_{area}}{P_{area}} \tag{2.5}$$

where $\bar{\eta}_{area}$ is the average area spectral efficiency [bps/Hz per km^2] given by (2.3) and P_{area} is the area power consumption of the access network elements (base stations) within a nominal 1 km^2 geographical area. As already established in (2.5), the energy efficiency of a network depends on network area spectral efficiency and normalized power consumption, P_{area}, also known as the area power consumption measured in W/km^2. A similar performance metric has also been used e.g. in [56,85–87]. As such, the area power consumption of a wireless access network depends on the dominance area of a site, A_{site} (which is $3 \times A_{cell}$ for a 3-sectored site), and the individual power consumption of a base station, P_{BS}, and is given by:

$$P_{area}\left[\text{W/km}^2\right] = \frac{P_{BS}}{A_{site}} \tag{2.6}$$

In general, a base station site comprises of a base station unit, also known as the base transceiver station (BTS), which has the capability to transmit and receive radio signals to and from the mobile subscribers. Due to the clearly different deployment purposes, the different classes of base stations (macrocell, microcell, femtocell etc.) vary in their internal architectures which consequently have significant impact on their overall power consumption. For a correct estimation of area power consumption, it is thus important that the power consumption of an individual base station is modelled accurately. Hence, the power consumption models for legacy deployment solutions (macrocell/microcell) are introduced in Chapter 3, while the power consumption model for indoor femtocell access point is introduced in Chapter 4.

2.3.3 Cost efficiency

Cost efficiency analysis, or cost-benefit analysis, is one of the key methodologies that provide a general picture of the cost structure of an evolutionary pathway for a certain technology or system and whether or not it is a feasible option for investment. In this section the cost modelling methodology used in the analysis studies is described.

The cost efficiency is defined as the cost incurred in transmitting one bps/Hz and is calculated as following:

$$C_{\text{eff}}\,[\text{bps/Hz/k€}] = \frac{\bar{\eta}_{area}}{T_{cost/km^2}} \tag{2.7}$$

where $\bar{\eta}_{area}$ is the average area spectral efficiency [bps/Hz per km^2] given by (2.3) and T_{cost/km^2} is the total area cost i.e., the total cost of the base stations normalized over 1 km^2 area. Here the term base station may refer to macro-/micro- cellular base stations or even femtocell access point (FAP), depending upon the type of deployment.

The cost of deploying a cellular network can be broadly divided into two types; (*i*) Investment cost or CAPEX (capital expenditure), and (*ii*) Running/operational costs or OPEX (operational expenditure). The CAPEX consists of equipment costs like radio base station, transmission equipment, antennas, cables, and site build out and installation cost. OPEX consists of site rental, transmission or leased line, and OA&M (operation, administration & maintenance). In addition to these, there can be cost components such as radio network planning, core network and marketing costs whose impact can be modeled and taken into account as part of the radio network costs [88]. However, in the frame of the analysis studies in this dissertation, the scope is limited to items listed for CAPEX and OPEX as they typically depend very strongly on the number of deployed radio units. Combining CAPEX and OPEX gives the total cost of ownership (TCO) value of the deployed network. The total cost structure of a mobile operator is dominated by the accumulated running costs i.e. the OPEX [89], which spans over the life-time of the network, while the CAPEX is considered during the initial network roll-out phase or when the network is upgraded. Thus, in the cost analysis studies, a standard economical method known as discounted cash flow (DCF) analysis has been used in order to account for both the CAPEX and OPEX in finding the 'total cost per base station'. The net present value (NPV) of the base station cost is then found by summing up the discounted annual cash flow expenditure for a given study period (in years) [89, 90]. Mathematically;

$$BS_{NPV} = \sum_{i=0}^{Y} \frac{c_i}{(1+r)^i} \tag{2.8}$$

where Y is the study period in years (typically 8 years for base stations value depreciation), c_i is the total annual expenditure per base station (total annual cost which includes running cost and may include investment cost) in the i$^{\text{th}}$ year and r is the discount rate which is assumed to be equal to 10%. Furthermore, it is assumed that the mobile operator deploys its network as a Greenfield project i.e., the whole network is deployed in the first year. Hence, when calculating the NPV of the base station, the CAPEX is only considered in the first year while in the following years the cost from operating expenditures is only considered.

Like power consumption, the cost structure for the different base station classes

also vary significantly because of the underlying base station system architecture as well as the deployment setup. Hence, the cost-elements for legacy deployment solutions (macrocell/microcell) are introduced in Chapter 3, while the cost-elements for indoor femtocell access point are introduced in Chapter 4.

2.3.4 General simulation parameters

This section lists the simulation parameters that have been used throught the analysis covered in the following chapters. It is pertinent to mention that only the general simulation parameters, common to all the studies, are listed here while more specific parameters for different deployment strategies are given in the respective chapters.

- The operating frequency for the different deployment strategies is 2.1 GHz, which is chosen from the UMTS-FDD/LTE Band 1 and is commonly used by mobile operators in Europe. All the studies in this dissertation have been carried out at this center-frequency/cellular band in order to have a common ground and be able to compare the results.

- Assuming a 9 dB receiver noise figure and a 20 MHz bandwidth (which is nominal for long term evolution, LTE), the receiver noise floor level is calculated to be -92 dBm. 9 dB noise figure is also the baseline assumption in 3GPP studies [91].

- For modeling the outdoor and indoor radio channels, deterministic ray based radio propagation models are deployed. More information on the models is given in Section 2.5.

2.4 Antenna Model

To model a directional antenna, an extended 3GPP antenna model based on [92] was adopted for simulations. The proposed version extends the original model of [93], which only considers the horizontal plane, to include a vertical antenna pattern model with an option to set the electrical downtilt. The horizontal (azimuth) pattern, G_h, is given by:

$$G_h(\varphi) = -min\left[12\left(\frac{\varphi}{HPBW_h}\right)^2, FBR_h\right] + G_m \tag{2.9}$$

where $\varphi, -180° \leq \varphi \leq 180°$ is the azimuth angle relative to the main beam direction, $HPBW_h$ is the horizontal half power beamwidth [°], FBR_h is the front-to-back ratio

[dB] and G_m is the maximum gain of the antenna [dBi]. The vertical (elevation) pattern, G_v, is given by:

$$G_v(\phi) = -max\left[-12\left(\frac{\phi - \phi_{etilt}}{HPBW_v}\right)^2, SLL_v\right] \tag{2.10}$$

where $\phi, -90^\circ \leq \phi \leq 90^\circ$ is the negative elevation angle relative to horizontal plane (i.e., $\phi = -90^\circ$ is the upward plane relative to the main beam, $\phi = 0^\circ$ is along the main beam direction, and $\phi = 90^\circ$ is the downward plane relative to the main beam), ϕ_{etilt} is the electrical downtilt angle [°], $HPBW_v$ is the vertical half power beamwidth [°], and SLL_v is the side lobe level [°] relative to the maximum gain.

The antenna parameter values for FBR_h and SLL_v, were adopted from [92] i.e., the value for FBR_h was set at 30 dB, while for SLL_v the value was fixed at -18 dB. The rest of the input parameter values for the antenna model are given in each chapter seperately.

2.5 Description of the Applied Propagation Models

Accurate modelling of the radio propagation channel is one of the key elements for making reliable simulations of wireless communications networks. Several radio propagation models exist, ranging from empirical, semi-empirical to deterministic models, each with their own pros and cons. For the simulation studies in this dissertation, deterministic models were selected, due to their high-level of accuracy as compared to the other models.

2.5.1 3D ray-tracing model (3D RT)

A commercial radio wave propagation tool, Wireless InSite [94], was used for the studies covered in Chapter 3. The outdoor and indoor radio channels are modelled using a deterministic 3D propagation model. The model employs a ray-launching technique based on 'Shooting and Bouncing Ray' (SBR) method to find the propagation paths through the 3D building geometry between a transmitter and receiver [95]. Rays are shot from the emitting source in discrete intervals and traced correspondingly as they reflect, diffract and transmit (penetrate) through and around the obstacles. Each ray is traced independently and the tracing continues until the maximum number of interactions (reflections, transmissions, diffractions) per ray is reached. Once all the propagation paths have been computed and stored, the field strength for each ray path is then calculated using Uniform Theory of Diffraction (UTD) [96].

The accuracy of a 3D propagation model is dependent upon the input data and the total number of reflections, transmissions (or wall penetrations) and diffractions a single ray can encounter. Although, the propagation tool allows up to a maximum of 30 reflections and transmissions per ray path, setting higher number of interactions per ray path can significantly increase the complexity and hence the computation time. According to [94], the computation time is roughly proportional to: $\frac{(N_R+N_T+1)!}{N_R!\times N_T!}$, where N_R is the total number of reflections and N_T is the total number of transmissions (or penetrations) a single ray can undergo. Furthermore, the computation time also increases with higher number diffractions allowed per ray path.

An optimum number of interactions varies with propagation environment. Hence, in order to limit the calculation time, an empirical 'hit-and-trial' method was used, which involves simulating with a smaller number of interactions, and then re-simulating the same scenario by steadily increasing interactions and comparing the results. Once the results start to converge with insignificant change, those settings were then selected. This was observed at 10 reflections, 1 diffraction and 1 transmission (penetration inside obstacles).

2.5.2 Dominant path model (DPM)

Although, limiting the number of interactions per ray path has noticeable impact on the the overall computation time for ray tracing models, nevertheless, it still takes considerable amount of time for simulating a propagation environment with large number of transmitters. Hence, during the course of the doctoral studies a new propagation simulator, ProMan, was procured. ProMan is a tool within the WinProp Software Suite [97] that includes different propagation models ranging from empirical to deterministic models. Besides having the traditional ray-optical model, the tool offers a novel deterministic model based on dominant path between a transmitter and a receiver. The performance evaluation studies covered in Chapter 4 and 5 utilize this model for outdoor/indoor channel modeling.

The basic premise behind the Dominant Path Model (DPM) is that in a typical propagation scenario, only two or three ray paths contribute 90% of the total energy at the receiver end [98]. The DPM determines these dominant paths between the transmitter and each receiver pixel, thereby significantly reducing the computation time compared to ray tracing while maintaining the accuracy nearly identical to ray tracing algorithms.

The computation of the path loss in DPM is based on the following equation [99]:

$$L = 20log_{10}\left(\frac{4\pi}{\lambda}\right) + 10nlog_{10}(d) + \sum_{i=0}^{k} f(\varphi, i) + \Omega - g_t \tag{2.11}$$

where d is the distance between a transmitter and a receiver, n is the path loss exponent, λ is the wave length (depends upon the operating frequency), The sum of individual interaction losses function, $\sum_{i=0}^{k} f(\varphi, i)$, is due to diffraction for each interaction i of all k with φ as the angle between the former direction and the new direction of propagation. Ω is the wave-guiding (tunneling) effect for considering the effect of reflections (and scattering). The quantity Ω is empirically determined and is described in detail in [100], g_t is the gain of the transmitting antenna in the receiver's direction.

For path loss exponent, n, the recommended values depends on the propagation environment (Urban, Suburban, Indoor) and also on the height of the transmitter (macro, micro). Tables [2.1, 2.2 and 2.3] list the recommended path loss exponent values, taken from [97], for different types of propagation environment. The path loss exponent values quite nicely conforms to what have been reported in e.g., [15, 101].

Table 2.1 Example path loss exponent values for macrocell and microcell in urban environment

Environment	**Macro**	**Micro**
Line-of-Sight (LOS) before breakpoint	2.4	2.6
Line-of-Sight (LOS) after breakpoint	3.6	3.8
Obstructed Line-of-Sight (OLOS) before breakpoint	2.6	2.8
Obstructed Line-of-Sight (OLOS) after breakpoint	4.0	4.0

Table 2.2 Example path loss exponent values for macrocell and microcell in suburban/rural environment

Environment	**Macro**	**Micro**
Line-of-Sight (LOS) before breakpoint	2.0	2.2
Line-of-Sight (LOS) after breakpoint	3.6	3.8
Obstructed Line-of-Sight (OLOS) before breakpoint	2.1	2.3
Obstructed Line-of-Sight (OLOS) after breakpoint	4.0	4.0

Table 2.3 Example path loss exponent values for indoor environment

Environment	**Empty building**	**Filled building**
Line-of-Sight (LOS)	2.0	2.1
Obstructed Line-of-Sight (OLOS)	2.1	2.3
Non Line-of-Sight (NLOS) before breakpoint	2.2	2.5

- In Line-of-Sight (LOS) connection, a clear propagation path exists between a transmitter and a receiver, without any obstruction.
- In Obstructed Line-of-Sight (OLOS) connection, a clear propagation path does not exist between a transmitter and a receiver due to obstruction present in between. As such, the radio waves propagate via reflections and diffractions.
- In Non Line-of-Sight (NLOS) connection, the propagation path between a transmitter and a receiver is obstructed in such a way that the only means of communication is via wave penetration/transmission through the obstruction.

Chapter 3

Densification of Legacy Deployment Solutions

THIS chapter looks into network densification of legacy deployment solutions that have been used by the mobile operators till date. First, the performance of a densified homogeneous macrocellular deployment with different intersite distances (ISD), is investigated in Section 3.1. The performance is evaluated based on the metrics defined in Chapter 2 i.e., in terms of *network spectral efficiency*, *energy efficiency* and *cost efficiency*. Next, Section 3.2 examines the performance of densified homogeneous microcellular deployments with different cell plans, resulting in varying cell densities per km^2. Finally, the impact of heterogeneous co-channel macro-/microcellular deployment on the overall capacity performance is analyed in Section 3.3.

The study aims to answer the following questions:

- *How much system capacity gain can be achieved through network densification using legacy deployment solutions?*
- *Is the capacity gain sufficient to lower the energy per bit and cost per bit in order to make the legacy deployment solutions energy and cost efficient?*

The presented results in this chapter are based on radio propagation simulations which take into account both outdoor and indoor receiver points in a dense urban area with high-rise buildings. All the results and analysis presented in this chapter are based on the author's published work in [66, 67].

3.1 Macrocellular Densification

Macrocellular networks have been and still continue to be the basis for cellular network deployments globally. High power transmitters with highly elevated and directive antenna structures are superior in terms of wide-area coverage provisioning. They also

play a major role in fulfilling the mobility demands of cellular users, and hence, are assumed to maintain their position in the future as well. Moreover, it is envisioned that macrocell networks will continue to provide the outdoor coverage layer with small cells satisfying the local outdoor and indoor capacity demands. Current cellular networks are inherently heterogeneous in terms of network configuration and this trend is building towards an even denser heterogeneous configuration as new small cell technology and different indoor network solutions become more and more common.

In this section, the downlink capacity performance of macrocellular network densification is investigated in a full load condition, which is the worst case scenario and also a typical methodology that is used for network capacity dimensioning. The system model and simulation assumptions used in the analysis are described first. This is followed by capacity-, energy- and cost- efficiency analysis and results.

3.1.1 System model and assumptions

Scenario description

The analysis is done in a dense urban area. Hence, to imitate such an environment a Manhattan grid city model is utilized, as shown in Fig. 3.1. The model has been widely used for simulation of urban environment, e.g. [102, 103]. Each building has dimensions of 110 m x 110 m, a height of 40 m and comprises of 8 floors. The street width between two consecutive buildings within a block is taken to be 30 m, which also corresponds to inter-block separation. For the indoor floor plan, an open space is considered with no internal wall partitions i.e. no hard obstructions for the signal propagation except for the ceiling/floor and exterior walls. Furthermore, in order to model a modern building, an average building penetration loss (BPL) of 25 dB is assumed. This assumption is inline with what has been recently reported of wall penetration losses in modern construction, see e.g. [13, 14, 17].

ISDs (cell density) and electrical tilt

The cell density depends upon the average ISD ($\bar{d}_{site}$), which further specifies the dominance area of a cell. In the study, the dominance area is defined as the region where a cell provides highest signal level as compared to the rest of the cells. Altogether five different ISDs were considered. These were calculated from the center of the building (except in the average ISD of 170 m case, where it is calculated based on average inter cell distance owing to the square layout of the buildings). Assuming

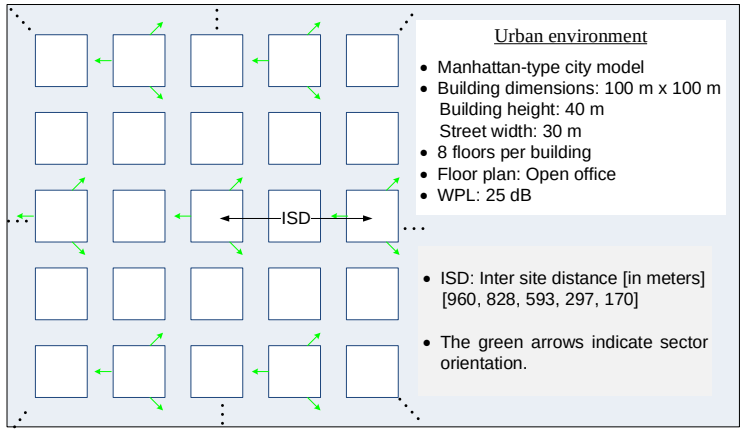

Figure 3.1 Manhattan grid city model (aerial view). The green arrows show sector antenna positions and orientations (example case: ISD 297 m). Note that only the first interfering tier is illustrated. The number of interfering tiers considered for each ISD in the simulations is given in Table 3.1.

a regular hexagon cell, the dominance area of a cell, A_{cell} is given by:

$$A_{cell}\left[\mathrm{km}^2\right] = \frac{\sqrt{3}}{6}(\bar{d}_{site})^2 \tag{3.1}$$

The cell density, ρ_{cell}, per km^2 is defined as $1/A_{cell}$.

In order to improve the cell edge coverage and avoid unnecessary interference into neighboring cells, the macrocell sector antennas are required to be downtilted such that the main beam of the antenna points at the cell border region [15, 104]. As such, the electrical tilt angle depends on the ISD as it defines the maximum cell range. Knowing the base station (BS) antenna height (h_{BS}), the mobile station (MS) antenna height (h_{MS}) and the cell range (r_{cell}), the tilt angle can be calculated geometrically as:

$$\phi_{etilt} = arctan\left(\frac{h_{BS} - h_{MS}}{r_{cell}}\right) \tag{3.2}$$

For a three sectored hexagonal cell site, the r_{cell}, can be calculated as $\frac{2}{3}\bar{d}_{site}$. In some of the reported studies, for example [105], a small correction factor to (3.2) in order to consider the 3 dB vertical beamwidth. However, for simplicity, that factor is ignored in this thesis.

Table 3.1 lists the average ISD and the corresponding electrical tilt angles, cell areas and the cell densities per km^2 for different levels of pure macrocellular network

Table 3.1 ISD, electrical tilt, cell area and cell density

$\bar{d}_{site}$	ϕ_{etilt}	A_{cell}[km^2]	ρ_{cell}[per km^2]	Interfering Tiers
960 m	3.5°	0.26	3.8	2
828 m	4.1°	0.20	5.1	2
593 m	5.8°	0.10	9.9	3
297 m	11.4°	0.03	39.3	4
170 m	47.5°	0.008	119.9	4

Table 3.2 General simulation parameters for macrocellular densification

Parameter	Unit	Value
Operating frequency	[MHz]	2100
Bandwidth, W	[MHz]	20
Transmit power per macrocell sector	[dBm]	43
BS antenna beamwidth, $HPBW_{h/v}$	[°]	Directional (65°/6°)
MS antenna type		Halfwave dipole
BS antenna gain	[dBi]	18
MS antenna gain	[dBi]	2
BS antenna height, h_{BS}	[m]	42
MS antenna height, h_{MS}	[m]	2
Receiver noise figure	[dB]	9
Receiver noise floor level, P_n	[dBm]	-92
Propagation environment		Manhattan
Propagation model		3D ray tracing
Building dimensions	[m]	110×110
Building height	[m]	40
Street width	[m]	30
Indoor layout		Open office
Outdoor-to-indoor wall penetration loss	[dB]	25

densification. ISD 170 m represents an extreme deployment scenario, wherein the macrocell sites are deployed on top of every buillding.

General simulation parameters

The rest of the simulation parameters are gathered in Table 3.2. Typically for LTE based macrocells, the transmit power ranges from 43-48 dBm (i.e., 20 - 60 W) [106]. The antennas are modeled using (2.9) and (2.10). Each sector of a 3-sectored macrocell site uses a directional antenna with 65° horizontal beamwidth, 6° vertical beamdwidth and a gain of 18 dBi, taken from [92]. Hence, the effective isotropic radiated power (EIRP) in the maximum antenna gain direction is 43 dBm + 18 dBi = 61 dBm.

3.1.2 Capacity efficiency analysis

Methodology for capacity efficiency analysis

This section expands on the analysis methodology and capacity efficiency metrics described in Chapter 2.

In a homogeneous deployment scenario, the *SINR*, at a j^{th} receiver point (both outdoor and indoor) is calculated using the following relation:

$$\Gamma_j = \frac{S_j}{\sum_{j \neq i} I_i + P_n} \tag{3.3}$$

where S_j is the received signal power of the center cell site at j^{th} receiver point. $\sum_{j \neq i} I_i$ is the sum of the received powers from all the other cells acting as interferers at j^{th} receiver point, and P_n is the noise floor level which includes the noise figure of the receiver as well.

In a multi-cellular scenario, a cell having the strongest signal level is considered as the serving cell and the rest are treated as interferers. For a set of i cells reachable at the j^{th} receiver, the best serving signal can be found, mathematically, as following:

$$S_j = arg \underset{i}{max} \left(Pr_{ij}\right) \tag{3.4}$$

where Pr_{ij} is the received power from the i^{th} cell at the j^{th} receiver.

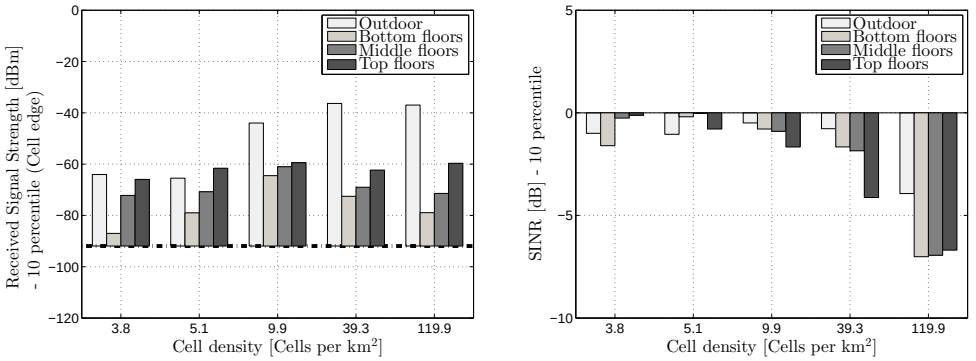

Figure 3.2 10^{th} percentile (cell edge) values for (a) Coverage, and (b) Signal-to-Interference Noise ratio, for pure macrocellular deployment with different cell densities. The black dashed line in (a) indicates the thermal noise floor at -92 dBm.

Capacity efficiency results and analysis

The general target of radio network planning is to design a network that provides sufficient coverage and maximizes overall capacity of the network with minimal costs. One of the most obvious methods for enhancing the network capacity is to increase the number of cells. However, the achievable average *SINR* values that eventually define the capacities (or 'cell spectral efficiency') in the cell level depend heavily on the network configuration. In this section, the results from the simulations, in terms of coverage, radio channel conditions and capacity, are analyzed and discussed. From the overall cell site capacity perspective, the improvement in the cell edge performance is of significance, as these regions, due to being away from the serving base station, experience worse radio propagation conditions. The improvement in the cell edge conditions can be achieved with a proper radio network deployment that eventually minimizes the inter-cell interference caused by the overlap between adjacent or neighboring cells, hence resulting in higher average cell level capacity.

Fig. 3.2 shows the statistical 10^{th} percentile values for the received signal levels (i.e., coverage) and *SINR*, respectively, for the outdoor and different indoor floor levels. The x-axis indicates the cell density per km^2 and y-axis the corresponding received signal strength [dBm] or *SINR* [dB]. For analysis, the indoor floor levels have been grouped into three classes; the bottom floors, middle floors and the top floors. The bottom floors bar presents the average of the 10^{th} percentile values on the 1^{st}

and the 2^{nd} floor, the middle floors bar indicate the average of the 10^{th} percentile values on the 4^{th} and the 5^{th} floor, while the top floors bar shows the average of the 10^{th} percentile values on 7^{th} and 8^{th} floor. From Fig. 3.2a it can be seen that the outdoor receiver points experience quite high signal levels from the very beginning as compared to the indoor floors. The received signal levels are relative to receiver noise floor level which is at -92 dBm (as shown by the dashed line). For less densified configurations, the receiver points in the lower floors experience high signal losses as compared to ones on the top floors. However, as a result of densification of the network, the overall coverage levels start to improve. The improvement in the coverage level comes from the deployment of more base stations together with antenna down tilt that results in smaller cell sizes, thereby reducing the path losses. Subsequent densification of the network does not bring any further improvement in the indoor coverage, while the outdoor receiver points experience a moderate improvement in the average signal levels. In the extreme case of 120 cells/km^2 (or average ISD of 170 m), the average signal levels saturate for receivers in outdoor and top floors, whilst the signal levels in the middle and lower floors start to experience coverage limitations. This is due to very high antenna tilt angles that cause signal losses in the lower floors.

Fig. 3.2b shows the 10^{th} percentile values i.e., the statistics from the cell edge, for *SINR* in outdoor and indoor environment for different cell densities. Although the coverage conditions on the top floor are better than in the middle and lower floors, the *SINR* performance degrades quite abruptly on top floor as the cell density increases. This is due to the rising interference conditions that become more prominent on the top floors as the network is densified. On the other hand, as a result of coverage improvement, the radio conditions in the lower and middle floor improve slightly when the network is densified to the level of 5 cells/km^2 (or average ISD of 828 m). For more densified configurations, lower and middle floors start to become coverage and clearly interference limited. Table 3.3 provides the 10^{th} percentile values for the cell spectral efficiency versus cell densities, for the outdoor and different indoor floor levels. The *SINR* values under the dominance area of the center site are directly mapped to the cell spectral efficiency. In a full load condition, the cell efficiency is shown to decrease as the network is densified. Initially (3.8 cells/km^2), the cell edge spectral efficiency is at the level of 0.84 bps/Hz and reduces to the level of 0.49 bps/Hz (42 % reduction) for outdoor locations when network is densified to the level of 120 cells/km^2. For the indoor floor levels, the overall cell edge efficiency is higher on the middle and top floors as compared to the lower floor levels and even outdoor location. However, as the network is densified to 120 cells/km^2, the cell spectral efficiency reduces to approximately 0.27 bps/Hz (70 % reduction) on all the floor levels.

Table 3.3 Cell edge (10^{th} percentile) capacity [bps/Hz] performance of pure macrocellular densification

		Cell spectral efficiency [bps/Hz]			
d_{site} [meters]	ρ_{cell} [Cells per km^2]	Outdoor	Bottom floors	Middle floors	Top floors
960	3.8	0.84	0.76	0.96	0.98
828	5.1	0.84	0.97	1	0.88
593	9.9	0.92	0.88	0.86	0.75
297	39.3	0.88	0.75	0.73	0.47
170	119.9	0.49	0.26	0.27	0.28

Table 3.4 Average cell and network area spectral efficiency for different ISDs

		$\bar{\eta}_{cell}$ [bps/Hz]		$\bar{\eta}_{area}$ [bps/Hz/km^2]	
d_{site} [meters]	ρ_{cell} [Cells per km^2]	Outdoor	Indoor	Outdoor	Indoor
960	3.8	2.7	2.67	15.1	14.96
828	5.1	2.65	2.61	22.42	22.06
593	9.9	2.57	2.05	36.05	28.74
297	39.3	2.09	1.99	92.81	88.06
170	119.9	1.65	0.88	289.2	153.9

The higher degree of resource reuse due to denser deployments results in an increase of the network area spectral efficiency as shown in Table 3.4. The impact of outdoor and indoor location on the network spectral efficiency is observed to be quite marginal in the beginning (ISD of 960 m and 828 m), but as the network is densified, the difference in the network capacity gain starts to become more visible. For the cell spectral efficiency, the effect tends to get more recognizable when the network is densified beyond the level of 5 cells/km^2 (or average ISD of 828 m). This is attributed to the deteriorating indoor coverage, mainly on the bottom floors, which negatively affects the indoor radio channel conditions (*SINR*).

In mobile communications industry, it has been widely speculated that around 60-85% of the overall network traffic originates from indoor users [107]. Hence, to properly dimension its network a mobile operator has to consider service provisioning from the indoor perspective. *However, the results indicate that macrocellular network densification in urban Manhattan environment clearly suffers from inefficiency indoors.* If the radio network planning target is limited to coverage provisioning for outdoor users only, the densification efficiency is higher (as shown in Table 3.4). On

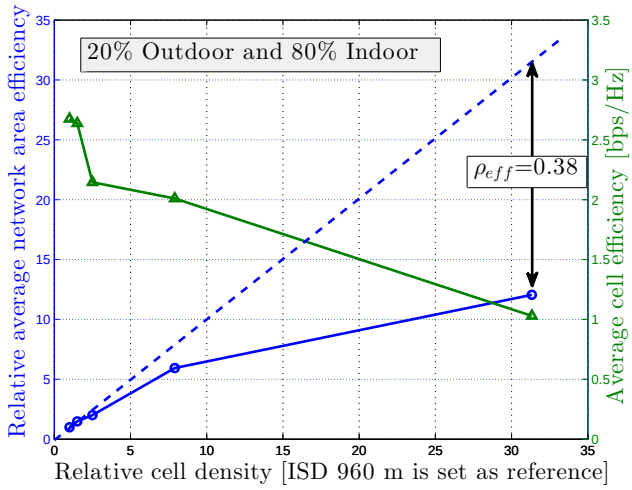

Figure 3.3 Relative network area efficiency (blue line) and average cell efficiency (green line) vs. relative cell density (the dashed line indicate a linearly increasing network spectral efficiency curve in an ideal case).

the other hand, if networks are planned for indoor coverage (as in practice), the efficiency is clearly lower. To illustrate this for a practical outdoor/indoor user distribution, Fig. 3.3 shows the capacity analysis in a slightly different way, where the relative network area spectral efficiency for a network with different cell densities per km^2 has been depicted. The network capacity values are relative with respect to nominal site density (3.8 cells/km^2). The dashed line illustrates 100 % densification efficiency (ρ_{eff}) line, whereas the solid line shows the improvement of the network area spectral efficiency for 20/80 % outdoor/indoor receiver point distribution. For less densified configuration, there can be observed a linearly increasing trend in the network spectral efficiency. The densification efficiency is still roughly 0.8 for 9.9 cells/km^2 (or average ISD of 597 m). However, beyond that point the efficiency can be observed to deteriorate significantly due to increase of inter-cell interference resulting from network densification, and abruptly drops down to 0.38 (62 % degradation) for 119.9 cells/km^2 scenario. These results clearly illustrate the inefficiency of macrocellular network densification with a more practical user distribution.

3.1.3 Energy efficiency analysis

Power consumption model for Macrocell base station

For evaluating the energy efficiency of different levels of macrocellular densification, a correct estimation of area power consumption is imperative which depends on the acurate modeling of the power consumption of an individual base station. The power consumption model for macrocellular base station, proposed in [85], considers the impact of external and internal components of the base station power consumption while at the same time also taking into account the impact of hourly network load. As such the power consumption of a macro base station site, P_{BS}^{Macro}, is given by:

$$P_{BS}^{Macro}\,[\mathrm{W}] = P_{const} + P_{load} \cdot F \tag{3.5}$$

where P_{const} is the total load-independent power contribution stemming from rectifier, P_{Rect}, microwave link for backhaul connectivity, P_{MLink}, and site air conditioning unit, $P_{Air-Cond}$, as given in (3.6). P_{load}, in turn, is the total load-dependent power consumption share stemming from power amplifier, P_{Amp}, transceiver, P_{TRX}, and digital signal processing units, P_{DSP}, as given in (3.7). F is the load factor, varying between 0 (no load) and 1 (high/peak load). As the network is assumed to be operating at full load, i.e., all the base stations transmitting at full power, therefore F is assumed to be 1.

$$P_{const}\,[\mathrm{W}] = (n_{sect} \cdot P_{Rect}) + P_{MLink} + P_{Air-Cond} \tag{3.6}$$

$$P_{load}\,[W] = n_{sect} \cdot [P_{Amp} + P_{TRX} + P_{DSP}] \tag{3.7}$$

In general, the contributions of P_{Amp}, P_{TRX} and P_{Rect} scale with the number of sectors, n_{sector}, per base station site. The power consumption of the power amplifier, in turn, depends mainly on the input power requirements of the antenna, P_{TX} and the power amplifier efficiency, η_{Amp}, and can be modelled and evaluated as:

$$P_{Amp} = \frac{P_{TX}}{\eta_{Amp}} \tag{3.8}$$

Table 3.5 summarizes the input parameters for the macro base station power consumption model. The parameters are approximate values taken from [85], except for power amplifier efficiency. With the advancements in power amplifier (PA) technologies e.g., Doherty PA with advanced signal conditioning algorithms, PA efficiencies in the range of 35 % to 65 % can be achieved when the network is operating in full

Table 3.5 Input parameters for the macrocellular BS power consumption model

Component/Equipment	Unit	Value
Number of sectors,		3
Transmit power at the antenna	[Watts]	20
Power consumption of DSP card	[Watts]	100
Power Amplifier efficiency	[%]	45
Power consumption of Transceiver	[Watts]	100
Power consumption of Rectifier	[Watts]	100
Power consumption of Air-conditioning unit	[Watts]	0
Power consumption of Microwave-Link unit	[Watts]	80

load, as reported e.g. in [56, 108, 109], hence, a 45 % PA efficiency is asumed in the analysis. Moreover, new outdoor pole mounted BTS's are also making their way into the markets, which don't require power consuming air-conditioning [110]. Hence, a 0 Watt contribution is assumed from the air conditioning unit in this study. Based on the parameters in Table 3.5, the total power consumption of a macro base station can be evaluated yielding approximately 1113 W ($\sim$ 1.11 kW). It is emphasized over here that many legacy macro-base stations can have still substantially higher total power consumption values, but the focus here is primarily on modern higher-efficiency equipment to understand the energy behavior of macro densification in the future.

Energy efficiency results and analysis

The power consumption per km^2 increases with the increase in the cell density over an area. This is because the area power consumption depends on the coverage area of the base station. Using the input parameters from Table 3.5, the energy efficiency of macrocellular deployment with varying cell densities have been calculated using (2.5). Table 3.6 gives the area power consumption of pure macrocellular deployment with different cell densities. As one can note from the results, the power consumption per km^2 increases with the increase in the cell density. In other words, densification of the network leads to increased power consumption per area proportionally with the increase in number of base stations. By densifying the network, the spectrum resources are reused more frequently, which thereby improves the network area spectral efficiency. However, looking at the impact of site densification on the energy efficiency of the network, as shown in Fig. 3.4, it is noted that although increasing the number of bps/Hz/km^2, the energy needed to transmit 1 bps/Hz also increases as the network is densified, especially in the indoor environment. Considering the initial

Table 3.6 Area power consumption of pure macrocellular deployment over different ISDs

ISD [meters]	ρ_{cell} [Cells per km^2]	P_{km^2} [kW/km^2]
960	3.8	1.4
828	5.1	1.9
593	9.9	3.7
297	39.3	14.5
170	119.9	44.4

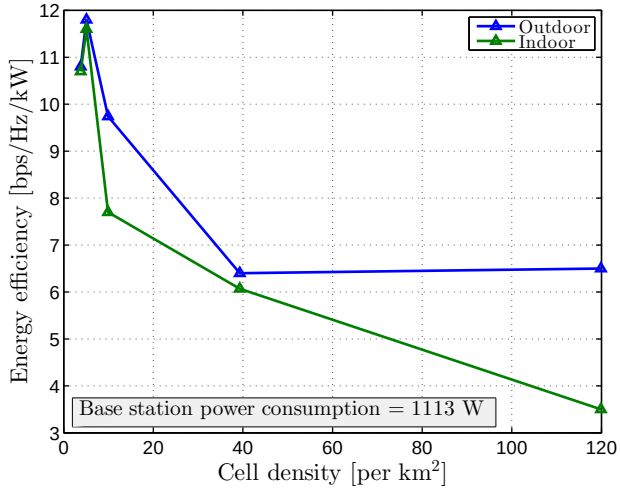

Figure 3.4 Energy efficiency [bps/Hz/kW] of pure Macrocellular network densification.

case of 3.8 cells/km^2 (ISD 960 m), where the average network area spectral efficiency is almost the same for both outdoor and indoor environment. In this case, the total power consumed per km^2 is approximately 1.4 kW, which leads to energy efficiency of approximately 10.8 bps/Hz/kW for outdoor and 10.7 bps/Hz/kW for indoor environment. Upon decreasing the inter-site distance to 828 m (i.e., 5.1 cells/km^2), a slight improvement can be observed in the energy efficiency (11.8 bps/Hz/kW for outdoor and 11.6 bps/Hz/kW for indoor). This improvement comes from the fact that in the initial stages of densification, the macrocellular network is slightly coverage limited. Hence, by densifying the network, the coverage levels improve in both outdoor and indoor environment, thereby improving the radio channel conditions and hence permitting higher cell spectral efficiency. Subsequent densification down to ISD 593 m

Table 3.7 CAPEX and OPEX costs for macrocellular base station deployment

CAPEX (*Initial costs*)	**Macrocell BS**
Base station equipment	10 k€
Site deployment cost	5 k€
Total CAPEX	*15 k€*
OPEX (*Running costs*)	**Macrocell BS**
Site rent (lease)	5 k€/year
Leased Line rent (backhaul)	2.25 k€/year
Operation and Maintenance	5 k€/year
Total OPEX	*12.25 k€/year*

and 297 m starts to degrade the energy efficiency performance as the network becomes more and more interference limited. The impact of degradation is more visible in the indoor environment due to relatively low rate of spectral efficiency improvement as compared to the outdoor environment. Eventually, when the network is further densified to an extreme case (ISD 170 m case or 120 cells/km^2), given approximately 32 times more cells/km^2 as compared to initial ISD 960 m case, the area power consumption increases also increases proportionally (i.e. 32 times more). However at this stage, a slight improvement in the outdoor energy efficiency can be observed, but for the indoor environment the degradation in the energy efficiency performance extends even further. The reason is attributed to the indoor capacity inefficiency at this level of densification which is not able to offset the high area power consumption.

3.1.4 Cost efficiency analysis

Table 3.7 gives the various cost items related to CAPEX and OPEX and their approximate values for macrocell cell site taken from [64,111]. Using the cost values in Table 3.7, the total cost for a 3-sectored macrocellular base station in NPV is estimated to be 104 k€, using (2.8).

The cost efficiency analysis results for different macrocellular cell densities are shown in Fig. 3.5. As evident, the total cost of deployment per km^2 increases as the base station density increases. However, the important metric to investigate is not the aggregate cost but the cost per bit efficiency, i.e., the relative gain that can be achieved from densification. In other words, the question is *whether the macrocellular densification can provide decent capacity gain to offset the incurred cost of deployment and hence bring down the cost per bit to make macrocellular densification a viable business*

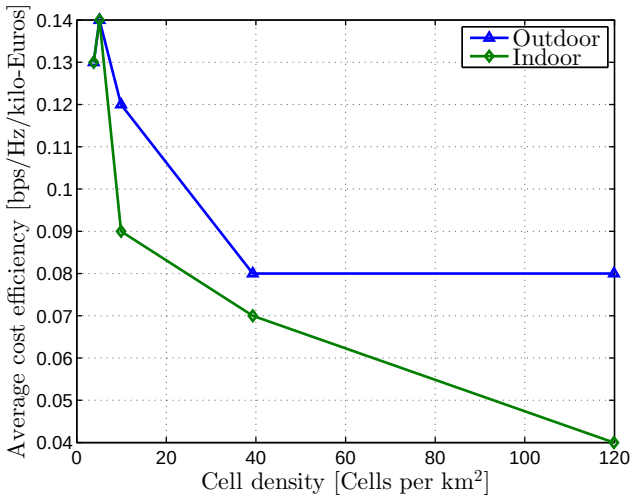

Figure 3.5 Cost efficiency [bps/Hz/k€] of pure macrocellular network densification.

case for investment?

In general, looking at the cost efficiency trend in Fig. 3.5, it can be seen that it follows the energy efficiency performance pattern. In the initial stages (increasing the cell density from 3.8 to 5.1 cells/km^2), there is a slight improvement in the cost efficiency performance for both outdoor and indoor environment. However, further densification not only degrades the cost efficiency performance but also the difference between outdoor and indoor environment starts to become more noticeable. This is, as mentioned previously, attributed to the inefficiency of pure macrocellular network densification in the indoor environment. As evident from (2.7), the cost efficiency depends on the area spectral efficiency. Hence, the more the network is densified, the smaller capacity gain in the indoor environment is achieved due to capacity inefficiencies associated with macrocellular densification strategy. This in turn results in higher cost per bit. For the outdoor environment, increasing the base station density to the extreme case (i.e., 120 cells/km^2) results in relatively higher area capacity gain than the indoor environment, which results in slightly improved cost efficiency. However, the efficiency still lags behind the cost efficiency of ISD 960 m. *Hence, it can be concluded that the pure macrocellular densification suffers from cost inefficiency especially in indoor environment in dense urban area.*

3.2 Microcellular Densification

Microcells have been a popular choice among mobile operators as a cost effective means of overcoming the capacity demand in their networks. Microcells are small base stations, mounted below the roof top level (e.g., 5 to 10 m above the ground), with a coverage radii smaller than the one of macrocell. Traditionally, they have been used to complement the macrocellular layer, by offloading the traffic in hot spot areas. In the previous section it was shown that the densification of macrocellular networks suffer from network area capacity saturation in dense urban environment, especially in indoors. This is due to very high levels of interference originating from the neighboring sites as they come closer together (reduced intersite distance). Microcells are thus identified with the technical solutions proposed to cope with the aforementioned problem. Bringing the base station antenna down below the average roof-top level can help reduce the overall interference, as the surrounding environment acts as a shield by limiting the propagation. Although, microcells allow for much tighter reuse scheme than macrocells, their performance is still limited by co-channel interferers mostly in LOS (line of sight) streets. Moreover, in urban environment, the signal originating from a cell site might leak and cause interference into neighboring non-LOS streets due to so called *tunneling effect*. Hence, proper cell planning is required to overcome this problem and increase the overall capacity performance of the system.

In this section, the downlink performance of microcellular network densification is investigated, in a full load condition. The section starts by outlining the *deployment cell plans* for microcells in urban type of environment. The different cell plans are based on microcellular inter-site distances (network densification) and site location. Next, the analysis methodology and general simulation parameters are described followed by results and analysis of microcellular densification.

Microcellular deployment cell plans

For microcell site deployment, the symmetric cell plans, *full block* and *half block* proposed in [112], have been used as the basis and further extended. Depending upon the site placement, the cell plans are classified into two groups; *square cell plans* and *rectangular/linear cell plans*. In the square cell plan, the sites are placed at the intersection of two streets, whereas in the linear cell plan, the sites are located in between two buildings, hence the overall LOS interferers are reduced as depicted in Fig. 3.6.

Based on the intersite distance (ISD), the square cell plans are categorized as:

Table 3.8 Cell plans and corresponding ISDs, Site areas and Site densities.

Cell plan	$\bar{d}_{site}$**[m]**	$\boldsymbol{A}_{cell}$**[km^2]**	$\rho_{\mathbf{cell}}$**[per km^2]**	**Interfering tiers**
Full square	280	0.0392	26	3
Half square	140	0.0196	51	6
Quarter square	70	0.00751	129	9
Linear-A	189.5	0.0196	51	3
Linear-B	119.5	0.0098	102	6

- *Full square (FS) cell plan*; A single sector site is placed at every second street intersection. Furthermore, each site covers one full building block in all four directions along the street (Fig. 3.6a).
- *Half square (HS) cell plan*; A single sector site is placed at every street intersection. Each site covers half of a block in all four directions along the street (Fig. 3.6b).
- *Quarter square (QS) cell plan*; This is the densest layout which is a combination of *Half square cell plan* and *Linear-B cell plan*, which is introduced next. In this cell plan, a site is placed at every intersection and also between two intersections (Fig. 3.6c).

whereas, the rectangular/linear cell plans, based on the ISD, are categorized as:

- *Linear-A (Lin-A) cell plan*; This cell plan is more or less the same as *Full square* cell plan, where a site is located at every other block, but with the only difference that instead of being located at the intersection, the site is placed between two intersections (Fig. 3.6d).
- *Linear-B (Lin-B) cell plan*; This is the more dense layout in linear cell plans where a site is located at every block and between two intersections (Fig. 3.6e).

Table 3.8 lists the average inter-site distance (ISD) and the corresponding cell areas, cell densities per km^2, and the number of co-channel microcell interfering tiers considered in the simulations. The cell density depends upon the average ISD ($\bar{d}_{site}$), which further specifies the dominance area of a cell. The dominance area is defined as the region where a serving cell provides highest signal level as compared to the rest of the cells, see (3.4).

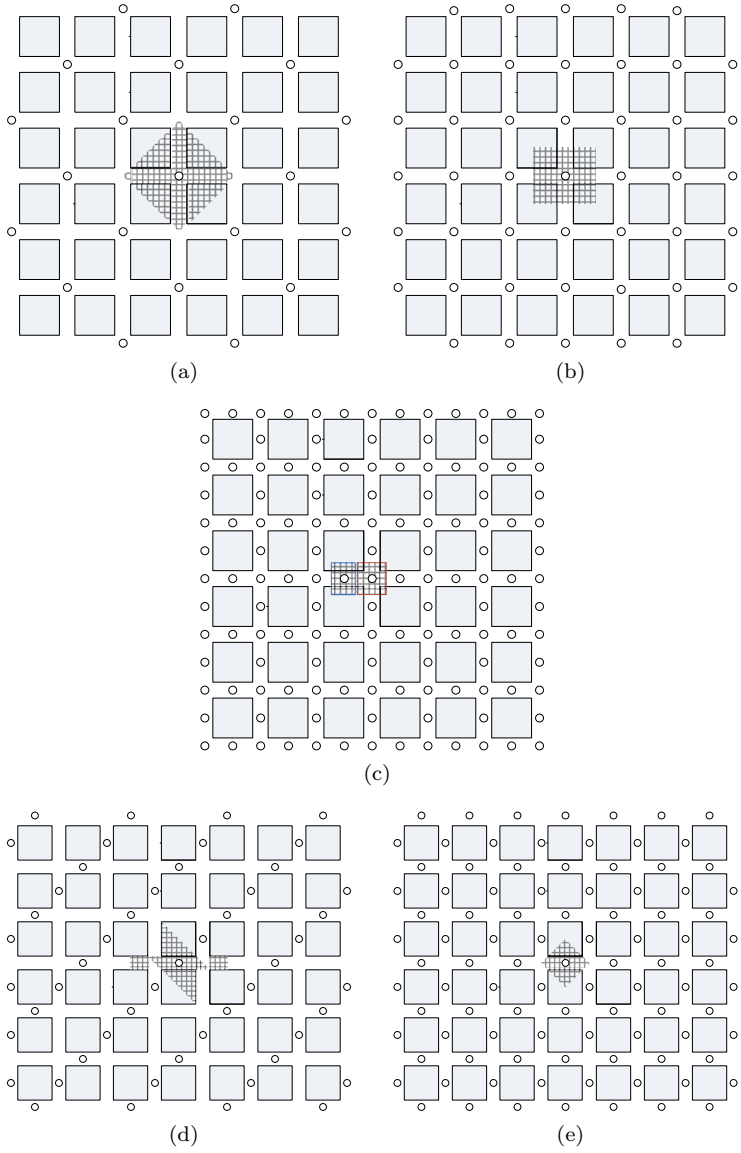

Figure 3.6 Manhattan grid city model (aerial view). (a) *Full square cell plan*, (b) *Half square cell plan*, (c) *Quarter square cell plan*, (d) *Linear-A cell plan*, and (e) *Linear-B cell plan*. The shaded region is the dominance area of the middle site which is considered for statistical analysis. The circular dots indicate the site locations.

Analysis methodology and simulation parameters

Due to homogeneity of the environment, the receiver points from the dominance area of the center cell site have been considered for statistical analysis and then normalized to 1 km^2 area. However, for the *Quarter square cell plan*, the propagation environment for sites located at the intersection is different than for the sites located between the intersection. Hence, for the analysis of *Quarter square cell plan*, the combined average statistics from the dominance region of middle site located at the intersection and the site located between two intersections is considered, as shown by the colored boxes in Fig. 3.6c. The methodology for calculating the capacity-efficiency of microcellular deployments is the same as that of homogeneous macrocellular deployments, described in Section 3.1.2.

Table 3.9 gathers the general list of simulation parameters specific to microcellular deployment. The microcells are deployed at street level at a height of 10 m above the ground. Moreover, all of the sites utilize an Omni-directional antenna with 1.8 dBi gain. Note that the effective isotropic radiated power (*EIRP*) in the maximum antenna gain direction is 34.8 dBm (33 dBm + 1.8 dBi = 34.8 dBm).

3.2.1 Capacity efficiency analysis

In this section, the results from the simulations in terms of coverage, radio channel conditions (*SINR*) and capacity are analyzed and discussed. It is pertinent to mention over here that all the results and analysis in this section are based on the performance metrics defined in Chapter 2 and elaborated in Section 3.1.

Fig. 3.7 shows the statistical 10^{th} percentile values for the received signal levels (i.e., coverage) and *SINR*, respectively, for the outdoor and different indoor floor levels. The x-axis indicates the cell density per km^2 and y-axis the corresponding Received Signal Strength [dBm] or *SINR* [dB]. For analysis, the indoor floor levels have been grouped into three classes; the *bottom floors*, *middle floors* and the *top floors*. The *bottom floors* bar presents the average of the 10^{th} percentile values on 1^{st} and 2^{nd} floor, the *middle floors* bar indicate the average of the 10^{th} percentile values on 4^{th} and 5^{th} floor, while the *top floors* bar shows the average of the 10^{th} percentile values on 7^{th} and 8^{th} floor.

From Fig. 3.7a, it can be seen that the outdoor receiver points experience quite high signal levels as compared to the indoor receivers, for all of the layouts. The black dotted line indicates the receiver noise floor level at -92 dBm. Unlike macrocellular deployment, the receiver points on the *top floors* experience lowest signal levels as compared to the rest of the floors. This is due to lower microcellular antenna height

Table 3.9 General microcellular simulation parameters.

Parameter	**Unit**	**Value**
Operating frequency	[MHz]	2100
Bandwidth, W	[MHz]	20
Transmit power per microcell base station	[dBm]	33
BS antenna type		Omni-directional
BS antenna beamwidth, $HPBW_{h/v}$	[°]	360°/90°
BS antenna gain, G_m	[dBi]	1.8
MS antenna type		Halfwave dipole
MS antenna gain	[dBi]	2.2
BS antenna height, h_{BS}	[m]	10
MS antenna height, h_{MS}	[m]	2
Receiver noise figure	[dB]	9
Receiver noise floor level, P_n	[dBm]	-92
Propagation environment		Manhattan
Propagation model		3D ray tracing
Building dimensions	[m]	110×110
Building height	[m]	40
Street width	[m]	30
Indoor layout		Open office
Outdoor-to-indoor wall penetration loss	[dB]	25

which reduces the EIRP in the direction of *top floors*. In the *square cell plans*, as the network is densified from *FS Omni* (26 cells/km^2) to *QS Omni* (129 cells/km^2), a slight improvement of approximately 2-3 dBs can be noticed, mostly on the bottom and middle floors. The improvement in the coverage level comes from the deployment of more base stations which results in smaller cell sizes, thereby reducing the path losses. The effect of site densification, on the indoor coverage levels, is observed to be quite marginal in the *linear cell plans* in the top floors, while the bottom and middle floors experience some improvement.

Fig. 3.7b presents the 10$^{\text{th}}$ percentile values, i.e. the statistics from the cell edge, for *SINR* in outdoor and indoor environment for different cell plans. Negative *SINR* values can be observed for both outdoor and indoor receiver points for all the layouts. This is due to the high interference levels from the co-channel cells at the cell border region. As the network is densified, the *SINR* performance degrades even further. In comparison with *square cell plans*, the *linear cell plans* provide better *SINR* perfor-

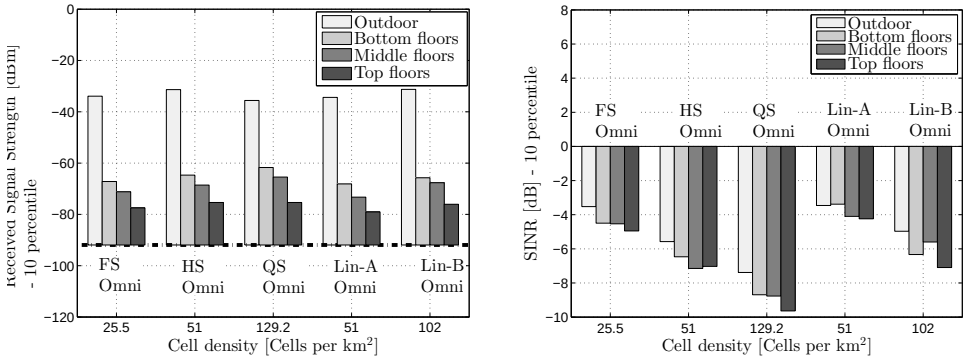

(a) (b)

Figure 3.7 10^{th} percentile (cell edge) values for (a) Coverage, and (b) Signal-to-Interference Noise ratio (*SINR*), for pure microcellular deployment with different deployment cell plans. The black dashed line in (a) indicates the thermal noise floor at -92 dBm.

mance by limiting the overall interferers. For the same cell density of 51 cells/km^2, the *Linear-A cell plan* exhibits much better *SINR* performance, both outdoor and indoor, as compared to *Half square cell plan*. Hence, site placement play an important role in determining the radio channel conditions at the cell edge. Table 3.10 maps the 10^{th} percentile *SINR* values (at the cell border region) to the cell spectral efficiency using basic shannon capacity theorem. As it is a direct mapping, the general trend follows that of *SINR* performance.

Table 3.11 provides the combined overview of the average cell and network area spectral efficiency, for the outdoor and indoor environments, for different cell plans. In a full load condition, the cell efficiency is shown to decrease as the network is densified. Initially for the *FS cell plan* (26 cells/km^2), the cell spectral efficiency is at the level of 0.9 bps/Hz for outdoor and 0.8 bps/Hz for indoor. This reduces to the level of 0.5 bps/Hz (44 % reduction) for outdoor locations and 0.4 bps/Hz (50 % reduction) for the indoor locations when the network is densified to the level of 129 cells/km^2 (*QS cell plan*). Similarly for the *linear cell plans*, the outdoor efficiency decreases from 1.3 bps/Hz (51 cells/km^2) to 0.9 bps/Hz (102 cells/km^2), while for the indoor the cell efficiency reduces to 0.7 bps/Hz from 1 bps/Hz (30 % reduction in both outdoor and indoor performance). Moreover, with a cell density comparable to that of *Half square cell plan* (51 cells/km^2), the *Linear-A cell* provides better cell spectral efficiency, both outdoor and indoor, due to better interference shielding. Next, look-

Table 3.10 Microcellular cell edge (10^{th} percentile values) spectral efficiency for outdoor and different indoor floor levels

	Cell spectral efficiency, η_{cell} [bps/Hz]			
	10^{th} percentile			
Cell layout	Outdoor	Bottom floors	Middle floors	Top floors
Full Square	0.46	0.44	0.44	0.4
Half Square	0.35	0.3	0.26	0.26
Quarter Square	0.23	0.18	0.17	0.15
Linear-A	0.54	0.55	0.48	0.47
Linear-B	0.4	0.3	0.3	0.26

Table 3.11 Average cell spectral and network area spectral efficiency for different microcell layouts

		$\bar{\eta}_{cell}$ [bps/Hz]		$\bar{\eta}_{area}$ [bps/Hz/km^2]	
Cell layout	ρ_{cell} [Cells per km^2]	Outdoor	Indoor	Outdoor	Indoor
Full square	26	0.9	0.8	23	20.4
Half square	51	0.7	0.5	35.7	25.5
Quarter square	129	0.5	0.4	64.5	51.6
Linear-A	51	1.3	1	66.3	51
Linear-B	102	0.9	0.7	91.8	71.4

ing at the network level capacity, the higher degree of resource reuse, due to denser deployments, results in an increase of the area spectral efficiency. It is interesting to note that due to strategic placement of the microcells, the *Linear-A cell plan* offers slightly higher outdoor network capacity and comparable indoor network capacity with 60 % less cells as compared to *QS cell plan*. However, in case of both *square cell plans* and *linear cell plans*, the indoor network area capacity is lower than outdoor capacity mainly due to associated coverage limitation on the top floors. In other words, densifying the microcell network helps in increasing the indoor network area capacity but not in direct proportion to cell density, as observed in outdoors. *Hence, similar to a pure macrocellular deployment, it is concluded that homogeneous microcellular network densification also suffers from inefficiency and coverage problems especially in urban indoor environment.*

Table 3.12 Area power consumption and energy efficiency for different microcell layouts

			E_{eff} [bps/Hz/kW]	
Cell layout	ρ_{cell} [Cells per km^2]	P_{km^2} [kW/km^2]	Outdoor	Indoor
Full square	26	3.9	5.9	5.1
Half square	51	7.7	4.7	3.3
Quarter square	129	19.4	3.3	2.7
Linear-A	51	7.7	8.6	6.6
Linear-B	102	15.3	6	4.7

3.2.2 Energy efficiency analysis

Power consumption of microocell base station

The power consumption for microcell base station can be calculated using similar model used for macrocellular base station proposed in [85]. However, the input parameters given therein, for calculating the power consumption of a microcell base station, results in higher power consumption value than what is reported in the recent datasheets of different network vendors [113, 114], typically between 100 - 220 W for a 30 dBm transmit power base station. Thus, to avoid any bias, the power consumption of the micro base station in the analysis is assumed at 150 W.

Table 3.12 gives the area power consumption and energy-efficiency of pure microcellular deployments with different cell plans. The area power consumption values have been mapped to corresponding energy efficiency values using (2.5). Looking at the energy-efficiency performance of *square cell plans*, the efficiency decreases, both in outdoor and indoor, as the network is densified. The reason is attributed to the high interference levels which decrease the average cell level capacities as the sites are brought closer together. Same trend is observed for *Linear cell plans*. However, in comparison, the *Linear cell plans* still offer relatively better outdoor and indoor energy-efficiency performance than *square cell plans* due to better strategic location.

3.2.3 Cost efficiency analysis

Cost structure of microocell base station

Table 3.13 gives the various cost items related to CAPEX and OPEX and their approximate values for deploying a microcell site. For microcells, the comparatively low price tag comes from the fact that due to small size factor and smaller coverage

Table 3.13 CAPEX and OPEX costs for microcellular base-station

CAPEX (*Initial costs*)	**Microcell BS**
Base station equipment	2.5 k€
Site deployment cost	0.5 k€
Total CAPEX	*3 k€*
OPEX (*Running costs*)	**Microcell BS**
Site rent (lease)	1 k€/year
Leased Line rent (backhaul)	2 k€/year
Operation and Maintenance	1.5 k€/year
Total OPEX	*4.5 k€/year*

footprint, the low-power radio implementation eliminates most of the equipment cost that are considered for macrocellular cell site. Hence, the cost of microcell is assumed to be 1/4 of macrocell base station cost. Further, as microcells are intended to be deployed on lamp posts or building walls etc., signficant cost savings can be achieved as compared to macrocells which usually require construction of large masts etc. Based on the cost values given in Table 3.13, the total cost for an omni-directional microcellular base station in NPV is estimated to be 32 k€, using (2.8).

Table 3.14 gives the total area cost and cost-efficiency of pure microcellular deployments with different cell plans. The cost-efficiency values have been computed using (2.7). Looking at the overall cost-efficiency performance of *square cell plans*, the general trend follows that of energy-efficiency pattern of microcellular deployments examined in the previous section. The cost efficiency, observed for both outdoor and indoor environment, decreases as the microcellular networks are densified. For the outdoor environment, this is attributed to the rising interference levels as the sites are brought closer together. For the indoor environment, the poor performance is due to coverage limitation in the upper floor levels of high-rise buildings in dense urban environment, arising mainly because of the street level deployment of microcells which result in low antenna gains as the floor levels increase.

3.3 Macro-Micro Heterogeneous Network Deployment

As evident from the discussion in the previous sections, both homogeneous macrocellular and microcellular deployments suffer from poor indoor capacity efficiency, in

Table 3.14 Total area cost and cost efficiency for different microcell layouts

			C_{eff} [bps/Hz/k€]	
Cell layout	ρ_{cell} [Cells per km^2]	T_{cost/km^2} [k€/km^2]	Outdoor	Indoor
Full square	26	832	0.03	0.02
Half square	51	1632	0.02	0.01
Quarter square	129	4128	0.01	0.01
Linear-A	51	1632	0.04	0.03
Linear-B	102	3264	0.03	0.02

comparison to outdoor environment, mainly due to poor indoor coverage. In the pure macrocellular deployment scenario the lower floors are coverage limited, while in the microcellular deployments the higher floors experience poor coverage due to lower height of microcellular antennas.

This section looks into heterogeneous co-channel macro-micro deployments as a possible solution to overcome the indoor coverage problem inherent in homogeneous legacy deployments. The performance of co-channel macro-micro deployment is evaluated, analyzed and contrasted against pure macrocellular and microcellular deployment specifically from the network densification point of view. Moreover, the analysis in this section is based on the system model and methodologies covered in Section 3.1 and 3.2. The general simulation parameters for macro- and micro- cellular deployments are kept the same except for the propagation model, which is based on dominant path model (DPM) instead of 3D ray tracing (3D RT), which was used for studies in the earlier sections.

In a co-channel macro-micro heterogeneous deployment scenario, the interference conditions at the receiver point differs from homogeneous macro/micro deployment scenario. Thus, for *SINR* calculations, two different cases are considered; *(a)* a receiver point connected to a macrocell and, *(b)* a receiver point connected to a microcell. The *SINR* in such a scenario is given by:

$$\Gamma_j^{Macro} = \frac{S_j^{Macro}}{\sum_i I_{i,j}^{Macro} + \sum_k I_{k,j}^{Micro} + P_n}$$
$$\Gamma_j^{Micro} = \frac{S_j^{Micro}}{\sum_i I_{i,j}^{Macro} + \sum_k I_{k,j}^{Micro} + P_n} \tag{3.9}$$

where $\Gamma_{j,}^{Macro}$ and $\Gamma_{j,}^{Micro}$ are the *SINR* conditions experienced by the j^{th} UE connected to the macrocell and microcell, respectively. In both cases, the receiver point is interfered by the corresponding co-channel macrocells and microcells.

For the purpose of comparison, the following deployment scenarios have been evaluated:

- *Pure macrocellular deployment*; Starting with inter-site distance (ISD) of 593 m (Macro 593), the network is densified to ISD 297 m (Macro 297).
- *Pure microcellular deployment*; Starting with *Full square cell plan* (FS Omni), the network is densified to *Half square cell plan* (HS Omni).
- *Heterogeneous macro-micro deployment*; In this scenario, the macrocellular network is jointly deployed with co-channel microcellular network. Initially, the macrocells are deployed with ISD 593 m and the microcells are deployed using *Full square cell plan* (Macro593+FS). The network is then densified at both macro- and micro- layer, where the macrocell ISD is decreased to 297 m and the microcells are brought closer to form *Half square cell plan* (Macro 297+HS).

Fig. 3.8 shows the performance comparison of heterogeneous and homogeneous deployment solutions with different levels of densification. Starting with the cell edge coverage performance (Fig. 3.8a), both outdoor and indoor coverage performance is shown to have noticeable improvement in heterogeneous deployment scenario. The improvement in the indoor coverage performance is attributed to the fact that the top and bottom floors are being jointly serviced by macrocell and microcell sites respectively. Next, coming to the cell edge *SINR* performance (Fig. 3.8b), the impact of deploying co-channel macro-micro network does not bring any positive improvement in the indoor radio channel conditions even though the indoor coverage conditions improve. This is due to the fact that as both macro-and micro- layers are deployed in co-channel configuration, the level of interference increases which negatively impacts the *SINR* performance not only in the indoor environment but also in the outdoor environment. The cell edge capacity efficiency (Fig. 3.8c) also follows the same trend as it relates directly to the radio channel conditions. From the average cell spectral efficiency point of view, in the intial deployment scenario (Macro593+FS), the outdoor performance improves slightly as compared to the standalong *Full square cell plan*, however, subsequent densification of macro-micro layer reduces the outdoor/indoor cell level capacities due to rising co-channel interference. Finally, looking at the network spectral efficiencies of different deployment scenarios, the dense macro-micro deployment (Macro297+HS) offers better outdoor/indoor network capacity gains due-

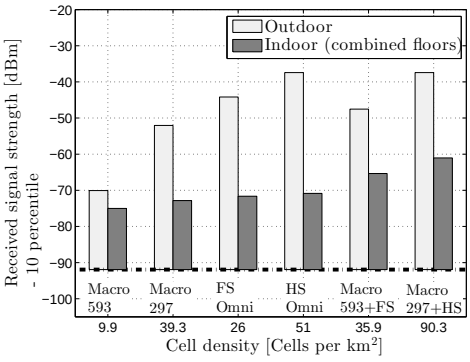

(a) Coverage (Cell edge)

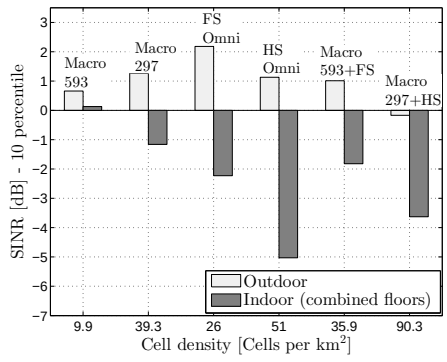

(b) Signal-Interference Noise ratio - (Cell edge)

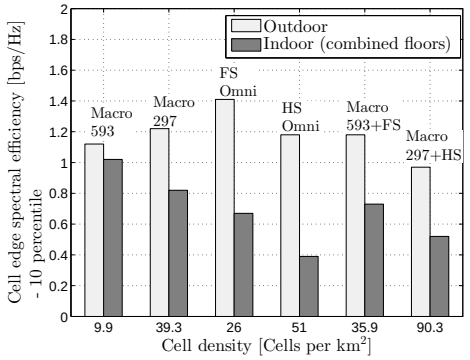

(c) Cell edge spectral efficiency

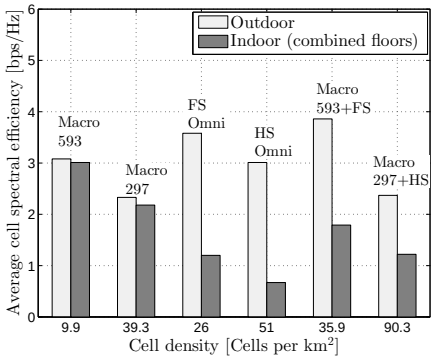

(d) Average cell level spectral efficiency

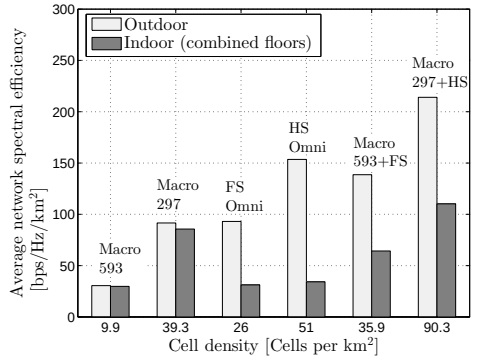

(e) Average network area spectral efficiency

Figure 3.8 Performance comparison of homogeneous and heterogeneous deployment scenarios.

to higher spatial re-use.

3.4 Chapter Conclusions

This chapter examined the techno-economic feasibility of utilizing legacy deployment solutions (macro-/micro-cellular technology) for fulfilling the exponentially rising capacity demand through network densification. The performance was evaluated and analyzed based on: (*i*) *homogeneous network deployment* (pure macro- or micro-cellular deployment) and (*ii*) *heterogeneous network deployment* (combined macro- and micro-cellular deployment), with varying cell densities per km^2.

In the *homogeneous network deployment* case, it is shown that under full load condition, both macrocellular and microcellular deployments suffer from cell level capacity degradation as the network is densified. Furthermore, from the coverage point of view, in a dense urban environment with high rise buildings, the macrocellular densification suffer from poor indoor coverage mainly in the lower floor levels. This is mainly caused by increasing antenna downtilting, to avoid, inter-cell interference, as the cell sites are brought closer together. The coverage limitation, in part, affects the attainable capacity in the indoor environment, which results in the indoor network area capacity to saturate as the network is densified. In the microcellular deployment scenario, the top floor levels suffer from coverage limitation due to lower *EIRP* and high path loss, resulting from street-level deployment of microcell sites. In both macrocellular and microcellular deployment scenarios, densifying the network helps in increasing the indoor network area capacity, even though the cell level capacity is shown to degrade. However, the relative increase in the network capacity is not in direct proportion to cell density, as in outdoor environment. From the energy and cost-efficiency point of view, the poor indoor capacity performance has also a direct impact on the energy and cost efficiency in both macrocellular and microcellular networks, as lower network area capacity in the indoor environment results in higher energy consumption and cost per bit.

The *heterogeneous network deployment* or so called *hierarchical cellular structure*, is shown to overcome the inherent indoor coverage problem of the *homogeneous network deployment*, in urban areas with high rise buildings. The coverage levels improve due to the fact that lower floor levels are served by street-level microcells, while top floors are served by roof-top macrocells. Nevertheless, the hierarchical deployment of macro-microcellular network deployment brings only slight improvement in the indoor network area capacity. The increased interference levels from co-channel deployment of macro- and micro-cells reduces the cell level capacities both in the outdoor and

indoor environment, which limits the network level capacity gains. This can be improved by utilizing advanced interference cancellation and mitigation techniques e.g. *base station coordination* or *beamforming* etc.

As a bottom line, if the target of the operator is to provide only outdoor service, the legacy deployment solutions might still be good and viable options option to go with. However, for the indoor environment, where the capacity demand is exponentially increasing, densification of outdoor legacy deployment solutions to extreme levels, might not be feasible due to associated indoor network capacity in-efficiencies, as already discussed in this chapter, coverage problems owing to high building penetration losses in modern buildings, and also due to the zoning restrictions in some regions. Addressing the rising indoor capacity demand is thus likely to require dedicated indoor deployments, e.g. indoor picocell or femtocells, that will provide local indoor capacity within the network. Chapter 4 looks into the ultra-dense deployment of indoor femtocells and evaluates the techno-economics feasibility of deploying such extremely dense indoor networks for meeting the indoor capacity demands of the future.

Chapter 4

Indoor Femtocell-based HetNet Deployment Solutions

As recently elaborated in e.g. [3–5], the amount of mobile data traffic is expected to grow by a factor 1000 by the year 2020. Such massive mobile data growth cannot be supported and delivered using traditional legacy deployment solutions (macro-/micro-cellular networks) alone [4] but a heterogeneous network with multiple network layers all the way down to pico and femto access points is likely to be deployed. This poses also considerable challenges from radio network planning and operation perspectives. Of particular importance is the ability to provide enhanced indoor coverage and capacity as more and more of the mobile data is arising and consumed indoors [4, 5].

Contemplating on the relative share of today's indoor/outdoor data traffic, there is a global consensus among mobile operators and wireless infrastructure vendors that majority of the overall mobile data traffic, approximately 65-70 %, is generated by indoor users [107]. Hence, it can be assumed that the indoor users generate significant portion of mobile operators revenue. However, despite this fact, poor indoor coverage from outdoor deployments has been and still is the topmost complaint that the mobile operators are struggling with [115]. Outdoor signals incur high losses when penetrating into the indoor environment via external walls. Traditionally, the values have been in the range of 5 dB - 15 dB, however, more recent measurement based studies have reported building penetration losses up to 35 dB in modern constructions [13, 14]. Apart from the capacity and coverage limitations, the *Energy-* and *Cost- inefficiencies* associated with legacy outdoor deployment solutions, as observed in Chapter 3, represents a key concern for mobile operators[1]. This necessitates a shift from current *Outside-In* approach to a new deployment paradigm that puts more

[1]Recently, political initiatives have put strigent requirements on mobile operators to reduce their CO_2 emissions [11]. Also from the cost perspective, the energy consumption of the radio access networks contribute significantly, towards mobile operator OPEX (operational expenditures). Roughly 80 % of the energy consumed by the RAN comes from the base stations [10].

focus on the service provisioning from indoor perspective. As such, indoor deployment of small cells has been identified as a cost-efficient solution that offers wireless carriers a sustainable evolutionary pathway to meet the indoor capacity demands of the future [79, 116]. An increasing trend among the operators opting for such small cell deployments has been recently observed.

For the *Beyond 4G* (B4G) networks, the experts envision that in order to fulfill the surging capacity demands of 1000x or more, an extremely dense network of small cells in inevitable that provides seamless coverage and mobility, thus giving rise to a concept known as *DenseNets*. Network densification, based on ultra-dense deployment of small cells, is being considered as one of the key flavors of the emerging 5G cellular networks that will truly address the 1000x data challenge [79, 116]. A large share of these deployments will be *indoor*, as this is the arena where majority of the data traffic is believed to originate from in future. While the outdoor basic macro layer is still always needed for high mobility outdoor users, such massive scale indoor deployments may also shift the current *Outside-In* deployment strategy towards a new paradigm based on *Inside-Out* approach where not only the indoor users but potentially also some low-mobility outdoor neighborhood users can be served by indoor base-stations [117]. Among other small cell solutions, femtocells are on the list of candidate technologies that will enable successful realization of DenseNets. Indoor femtocells access points (FAPs) are low power nodes, with very small coverage footprint, that use the conventional DSL connection as their backhaul. Due to being located inside the buildings, they are well positioned for delivering proper indoor coverage. However, because of the small coverage footprint, (typically 2-5 times smaller foot-print than microcell and 10-15 times smaller than macrocells), a very dense deployment of femtocells will be needed in order to have a ubiquitous indoor coverage. Such dense deployment triggers cost and energy efficiency concerns for mobile operators.

This Chapter examines the techno-economical aspects of ultra dense network deployment based on indoor small cell (femtocell) solution. The performance is evaluated in comparison with legacy deployment solutions (macrocell, microcell). The impact of varying wall penetration losses on the performance of ultra dense small cells in a suburban environment is investigated in Section 4.1. Section 4.2 examines the potential of using indoor dense small cell deployments for indoor and indoor-to-outdoor service provisioning in suburban and urban environment. Next, the techno-economical comparison of ultra-dense small cell networks and legacy deployment solutions, for indoor service provisioning, in a suburban environment is made in Section 4.3. Finally, the impact of small cell backhaul limitation on the overall capacity performance

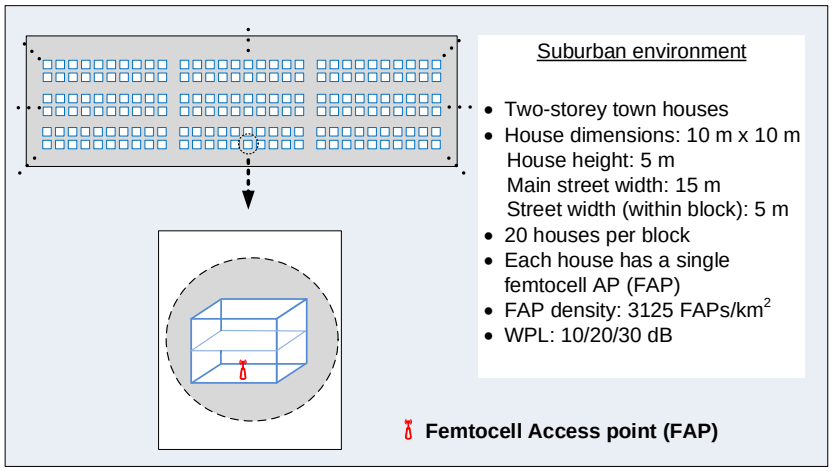

Figure 4.1 Suburban scenario (aerial and 3D view) used in the analysis; the dotted lines imply continuous blocks of houses. The femtocells are deployed inside each house (dense deployment) and assumed to be on the first floor.

is examined in Section 4.4. All the results and analysis presented in this chapter are based on the author's work reported in [68, 69, 72].

4.1 Performance Analysis of DenseNets with Modern Buildings

This section looks into the impact of modern buildings and their increased wall penetration losses on three different mobile network deployment strategies, namely; (*i*) pure macrocell deployment, (*ii*) pure femtocell deployment, and (*iii*) heterogeneous co-channel macro-femto network deployment. The pure macrocellular deployment is evaluated in order to compare the legacy deployment solution with small cells based solution in a suburban enviroment.

4.1.1 System model and assumptions

Scenario description

The analysis is done in a general suburban locality with rectangular residential building blocks arranged in a grid pattern; see Fig. 4.1. A block consists of 20 town houses and each house has dimensions of 10 m x 10 m, a height of 5 m and comprises of

2 floors. The street width between two consecutive houses within a block is taken to be 5 m, whereas the inter-block separation is 15 m. For the indoor floor plan, an open space is assumed with no room partitions i.e. no hard obstructions for the signal propagation except for the ceiling/floor and exterior walls, as shown in Fig. 4.1

Deployment strategies

- *Macrocellular deployment*; The macrocells are deployed using a hexagonal layout with an intersite distance (ISD or $\bar{d}_{site}$) of 1732 m, which is stemming from 3GPP specifications for a suburban deployment [118]. Assuming a regular hexagonal cell, the dominance area of a cell, A_{cell} is calculated using (3.1), which in turn gives the cell density, ρ_{cell}, per km^2. For an ISD of 1732 m, the resulting macrocell density is approximately 3.5 cells/km^2.

- *Femtocell deployment*; A very dense deployment of indoor femtocell access points (FAPs) is assumed wherein every residential house has a femtocell deployed on the ground floor; see Fig. 4.1. Hence, the FAP density for the considered scenario is 3125 FAPs/km^2. Moreover, the femtocells are assumed to be operating in an OSG (open subscriber group) mode [119], in which a non-FAP-member user equipment (UE) can also be connected to the FAP if it enters its dominance area.

- *Macro-Femtocell co-channel deployment*; This third strategy is basically the combination of the previous two deployment strategies. The femtocells are deployed within the dominance area of macrocells and both operate on the same carrier (hence called co-channel deployment).

Wall and floor penetration losses

To account for the outdoor-to-indoor propagation loss, three different exterior wall penetration losses (WPL) of 10 dB, 20 dB and 30 dB were considered. These values have been selected to model the building penetration losses for both older and modern constructions, for instance, a loss of approximately 5-15 dB has been observed for older buildings, while for modern constructions the measured WPL range lies between 25-35 dB, in the 2100 MHz band [14].

Typically, in macrocellular scenario, the effect of floor, in a two storey town house, is almost negligible as the main mode of propagation is via external walls. However, in the femtocell scenario, the floor penetration loss does have an effect on the upper floor coverage. Hence, the floor penetration loss for a typical town house was taken

Table 4.1 General simulation parameters of suburban macro/femto deployment study

Parameter	Unit	Value
Operating frequency	[MHz]	2100
Bandwidth, W	[MHz]	20
Macrocell sites		19 sites (3.5 cells/km^2)
Femtocells Access Points (FAPs)		1 FAP/house (893 cells/km^2)
Transmit power	[dBm]	43 (Macrocell sector), 20 (FAP)
BS antenna type		Directional (Macro), Omni (FAP)
BS antenna beamwidth, $HPBW_{h/v}$	[°]	Directional (65°/6°), Omni (360°/90°)
BS antenna gain, G_m	[dBi]	Omni (1.8), Directional (18)
UE antenna type		Halfwave dipole
UE antenna gain	[dBi]	2.2
BS antenna height, h_{BS}	[m]	Macro (30), Femto (2)
UE antenna height, h_{MS}	[m]	2
Receiver noise figure	[dB]	9
Receiver noise floor level, P_n	[dBm]	-92
Propagation environment		suburban
Propagation model		3D ray tracing
Building dimensions	[m]	10×10
Building height	[m]	5
Indoor layout		Open space
External wall penetration loss	[dB]	10, 20, 30

to be 4 dB.

General simulation parameters

Table 4.1 gathers the list of general simulation parameters. The femtocells are assumed to employ an omni-directional antenna, which is typically used in commercially available FAPs. The effective isotropic radiated power (EIRP) in the maximum antenna gain direction is 61 dBm (43 dBm + 18 dBi = 61 dBm) for macrocells and 21.8 dBm (20 dBm + 1.8 dBi = 21.8 dBm) for the FAPs. Moreover, to determine the receiver thermal noise floor, a 20 MHz bandwidth is assumed (stemming from 3GPP Long Term Evolution, LTE).

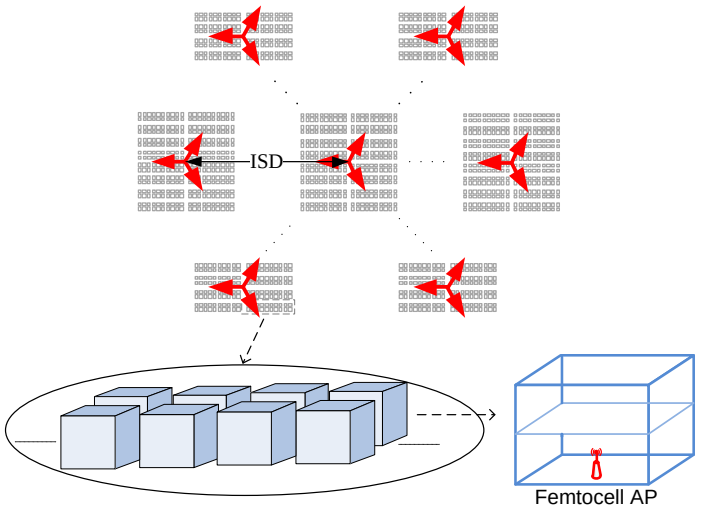

Figure 4.2 Suburban scenario used in the analysis; the dotted lines imply continuous blocks of houses. The red arrows indicate the orientation of the macrocell sectors (only one tier of macrocells is shown, whereas the analysis considers two tiers of macrocell interferers). The femtocells are deployed inside each house (dense deployment) and assumed to be on the first floor.

4.1.2 Analysis methodology

This section expands on the analysis methodology and capacity efficiency metrics described in Chapter 2. Due to homogeneity of the environment, only the receiver points and femtocells falling within the dominance area of the center macrocell site have been considered for statistical analysis and then normalized to 1 km^2 area, as shown in Fig. 4.2. Moreover, the distribution of receiver points across all the houses (and floors) is uniform. Receiver spacing for outdoor is 5 m, while for the indoor the spacing is 2.5 m.

As evident from (2.4), the cell/area spectral efficiency depends directly on the distribution of *SINR* (Γ) within a cell area. The amount of interference a UE receiver experiences at a given time is largely determined by the deployed network architecture.

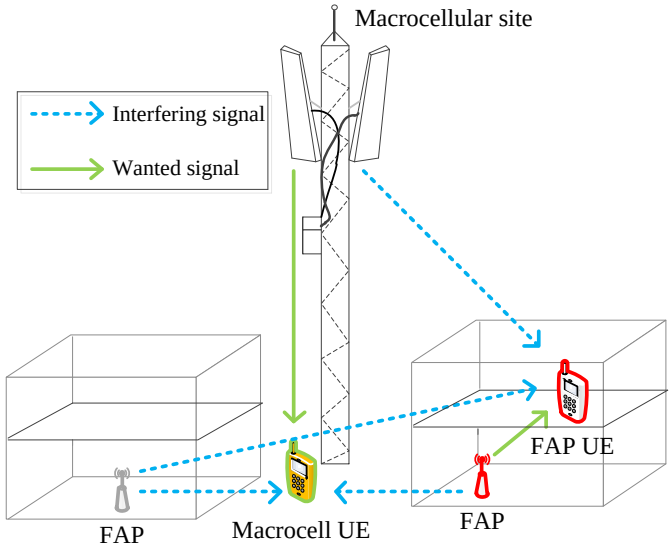

Figure 4.3 Radio channel (interference) conditions experienced by UEs in a co-channel macro-femto network (Other macrocell tiers not shown).

Fig. 4.3 shows an example of UE interference conditions in a typical macro-femto network architecture. Depending on the underlying deployment strategy, a UE may experience interference from either co-channel macro layer, co-channel femto layer or from both macro and femto layers. The mathematical expression for calculating *SINR* (Γ) in each of the deployment strategy is given as follows:

Interference conditions; Macro-only deployment

In Macro-only deployment case, the UE experiences interference from other co-channel macrocells. The *SINR* in such a scenario is given by:

$$\Gamma_j = \frac{S_j^{Macro}}{\sum_i I_{i,j}^{Macro} + P_n} \tag{4.1}$$

where S_j^{Macro} is the received signal power of the serving macrocell at j^{th} UE. $I_{i,j}^{Macro}$ is the received power of the i^{th} macrocell interferer at j^{th} UE, and P_n denotes the noise floor which includes also the UE receiver noise figure.

Interference conditions; Femto-only deployment

In femto-only deployment case, the UE experiences interference from other co-channel femtocells. These are usually the femtocell access points deployed in the nearby neighbouring houses or rooms (if multiple femtocell APs are deployed within a building). The *SINR* in such a scenario is given by:

$$\Gamma_j = \frac{S_j^{Femto}}{\sum_k I_{k,j}^{Femto} + P_n} \tag{4.2}$$

where S_j^{Femto} is the received signal power of the serving FAP at the j^{th} UE. $I_{k,j}^{Femto}$ is the received power of k^{th} femtocell interferer at j^{th} UE, and P_n denotes again the effective noise floor.

Interference conditions; Macro-Femto deployment

For the co-channel Macro-Femto deployment scenario, two different UE cases are considered; *(a)* a UE connected to a femtocell and, *(b)* a UE connected to the macrocell. In both cases the UE is interfered by other co-channel macro and femtocell transmit-

ters. The *SINR* conditions experienced by a UE in such a scenario is given by:

$$\Gamma_j^{Macro} = \frac{S_j^{Macro}}{\sum_i I_{i,j}^{Macro} + \sum_k I_{k,j}^{Femto} + P_n}$$
$$\Gamma_j^{Femto} = \frac{S_j^{Femto}}{\sum_i I_{i,j}^{Macro} + \sum_k I_{k,j}^{Femto} + P_n} \tag{4.3}$$

where $\Gamma_{j,}^{Macro}$ and $\Gamma_{j,}^{Femto}$ are the *SINR* conditions experienced by the j^{th} UE connected to the macrocell and FAP, respectively. In both cases, the UE is interfered by the corresponding co-channel macro- and femtocell transmitters.

4.1.3 Capacity efficiency analysis

In general, received useful signal power and SINR are the most important performance indicators that provide primary information on how well a system/network is performing under given radio channel conditions. From the overall cell site capacity perspective, the performance at the cell edge is of significance as these regions, due to being far away from the serving base station, experience worse coverage and radio channel conditions. Hence, the focus in this subsection is first on the worst 10^{th} percentile values, which represent the conditions at the cell edge regions, thus reflecting the system coverage.

Fig. 4.4 shows the outdoor and indoor 10^{th} percentile values for a) received signal power (i.e., coverage) and b) SINR, for the three deployment strategies under different external wall penetration losses. The x-axis indicates the wall penetration loss [dB], and y-axis the corresponding received signal power [dBm] or SINR [dB]. Starting with the coverage analysis (Fig. 4.4a), it can seen that for *Macro-only outdoor scenario*, the coverage improves slightly as the external wall penetration loss increases from 10 dB to 20 dB. This is due to more signal power being reflected back into the street than being allowed to penetrate inside the house/building. Subsequent increase in WPL, however, brings no improvement. For the *Macro-only indoor coverage*, the result is quite consistent i.e., increase in WPL results in the signal being attenuated more as it penetrates into the indoor environment. At 30 dB WPL, the cell edge houses suffer heavy coverage limitation in the Macro-only strategy.

Coming next to the *femto-only* strategy, the *outdoor coverage* is much better than Macro-only strategy (∼16 dB higher received signal level) in the 10 dB WPL scenario. The reason can be attributed to very dense deployment of FAPs, which results

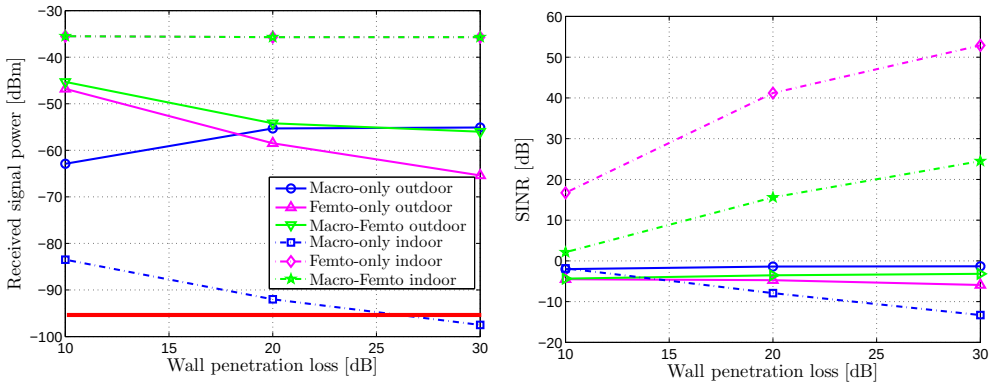

(a) (b)

Figure 4.4 10^{th} percentile (cell edge) values for (a) Coverage, and (b) Signal-to-Interference Noise ratio, for different deployment strategies and wall penetration losses. The red line in (a) indicates the thermal noise floor at -92 dBm

in outdoor UEs being served by the nearby FAPs from the indoor locations. For the 20 dB and subsequent 30 dB WPL values, the outdoor coverage level of femto-only deployment strategy drops below that of Macro-only deployment strategy because the femto AP signals penetrating outside experience higher and higher attenuation from the external wall. For the *indoor environment*, the WPL does not have any impact on the indoor coverage, as the FAPs are located inside the houses/buildings and within close vicinity of the UEs, resulting in high average received signal powers (approximately -35 dBm, irrespective of WPL) due to low path loss. In the *co-channel Macro-Femto* deployment strategy, for the lower 10 dB WPL value, the *outdoor* UEs are served by the strong nearby femtocell AP but for 20 dB and 30 dB WPL values, the macro signal level is stronger and thus the UEs are served by the macro-layer. The *indoor* UEs at the cell edge are always served by the indoor FAP due to stronger signal power received from the FAP.

The corresponding radio channel conditions in terms of SINR for all three deployment strategies in different wall penetration loss scenarios are shown in Fig. 4.4b. In *Macro-only* deployment strategy, the WPL does not affect the outdoor performance much. For all three WPLs, the SINR is below 0 dB at the cell edge. For the indoor environment, in the initial 10 dB WPL scenario, the radio channel conditions are actually slightly better than in outdoor environment, primarily due to better interference shielding from other co-channel macrocells. However, as the wall penetration

loss is increased to 20 dB and onwards up to 30 dB, the radio channel conditions start to degrade due to coverage limitation in the indoor environment. This implies that for providing adequate coverage at the cell edge, and if only macro-layer is deployed for service provisioning, the macrocell sites need to be either densified substantially or the height of the macrocell sites needs to be increased for improving path loss and thereby the indoor coverage. These options are both very costly and difficult to realize, hence already motivating towards indoor femto deployments.

Examining next the *femto-only* strategy, the outdoor radio channel conditions seem to suffer from severe interference from the neighbouring FAPs and the *SINR* performance starts to degrade as the WPL increases, due to decreasing signal strength from the indoor FAPs (see Fig 4.4a). However, for the indoor performance, the WPL actually favors the FAPs by making them more isolated from co-channel neighbouring femto APs. The higher the wall attenuation, the better the femtocells are isolated, which results in increased indoor SINRs.

In the two-tier *Macro-Femto* deployment case, the outdoor SINR performance is at the level of Femto-only deployment, however as the WPL increases, radio channel conditions start to improve due to better coverage conditions at the cell edge. Comparatively, the SINR level lies below Macro-only deployment strategy for 30 dB WPL scenario even though the UEs in both strategies experience the same coverage conditions as shown in Fig. 4.4a. This is because of the additional interference that the outdoor UEs experience from the nearby indoor FAPs in case of Macro-Femto network. The same phenomenon of additional interference is also observed by the indoor UEs which are served by the indoor FAPs. The additional interference from the co-channel macro-layer results in degradation of the SINR performance in the indoor environment. However, the increasing wall penetration loss somewhat helps in isolating the femtocells, thereby improving the radio channel conditions (SINR) as shown in Fig. 4.4b.

Fig. 4.5 maps the SINR values to cell-edge capacity/spectral efficiency values using (2.4). As shown, the Femto-only and Macro-Femto deployment strategies perform much better in the indoor environment and yield comparatively better cell edge spectral efficiencies than Macro-only deployment, while for the outdoor environment the overall performance of all the strategies is very similar, and fairly low (below 1 bps/Hz). The increasing wall penetration loss helps in achieving highest indoor cell spectral efficiency for Femto-only deployment yielding up to ∼18 bps/Hz spectral efficiency in 30 dB WPL case while the corresponding spectral efficiency with 10 dB WPL value is only 5.6 bps/Hz. The Macro-Femto deployment strategy delivers up to ∼8 bps/Hz in 30 dB WPL case while the corresponding efficiency is only 1.4 bps/Hz

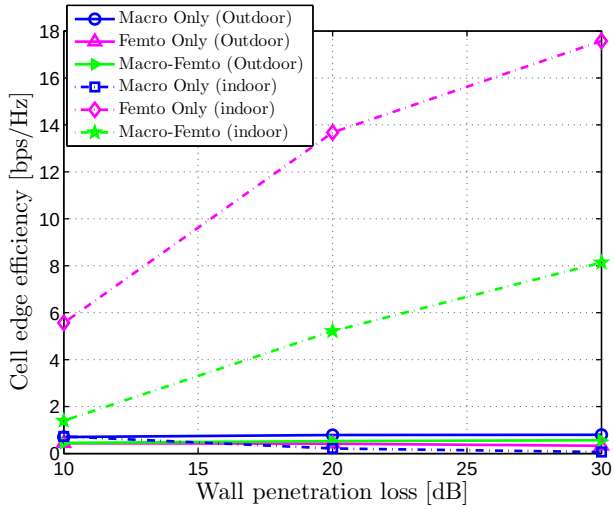

Figure 4.5 10^{th} percentile (cell edge) cell spectral efficiency values for different deployment strategies and wall penetration losses.

in the 10 dB WPL case.

Table 4.2 and Table 4.3 gathers and summarizes next the obtained *average cell and network area spectral efficiencies* in the different deployment strategies for both outdoor and indoor users and under different building penetration losses, respectively. The network area spectral efficiencies have been calculated using (2.3). The average cell spectral efficiency performance follows the same pattern as that of cell edge performance with Femto-only network providing better average cell spectral efficiency for the indoors with highest wall penetration loss, and is followed by two tier co-channel Macro-Femto deployment solution. With lowest WPL value, i.e. 10 dB, the difference in the indoor average cell performance is small, however, as the wall penetration loss increases, so does the difference in achievable average cell spectral efficiencies between Femto-only network and Macro-Femto network.

Investigating next the obtained average *area spectral efficiencies*, a huge difference can be observed between *Macro-only deployment* compared with *Femto-only* and *Macro-Femto deployment*. The reason is simply attributed to the extremely dense femtocells which are deployed in every house, i.e., 3125 femtocells/km^2 as compared to 3.5 macrocells/km^2. The extreme densification of the femtocells actually results in extreme spatial frequency reuse providing very steep *network capacity gains* even though the average *cell-level* capacities are relatively low for femtocells as compared to Macro-only deployment for the outdoor scenario. Furthermore, due to better iso-

Table 4.2 Average Cell spectral for different deployment strategies

Deployment strategy	$\bar{\eta}_{cell}$ [bps/Hz]					
	10 dB WPL		20 dB WPL		30 dB WPL	
	Outdoor	Indoor	Outdoor	Indoor	Outdoor	Indoor
Macro-only	2.43	2.9	2.35	2.28	2.35	2.21
Femto-only	0.8	7.6	1	15.7	1.2	19.5
Macro-Femto 2 Tier	1.3	6.4	2.1	12.8	2.2	14.5

Table 4.3 Average network area spectral efficiency for different deployment strategies

Deployment strategy	$\bar{\eta}_{area}$ [bps/Hz/km^2]					
	10 dB WPL		20 dB WPL		30 dB WPL	
	Outdoor	Indoor	Outdoor	Indoor	Outdoor	Indoor
Macro-only	8.4	10.1	8.1	7.9	8.1	7.7
Femto-only	2602	23800	3197	48940	3632	60840
Macro-Femto 2 Tier	4007	20080	6410	40090	6926	45460

lation provided by high wall penetration losses, the indoor network capacity increases significantly for both femto-only and Macro-Femto deployment strategies because in both cases the indoor UEs are served by the femtocells. Hence, from the network area spectral efficiency point of view, it can be concluded that femtocells are the best choice for providing indoor connectivity due to better coverage, radio channel conditions and also huge capacity gains. Moreover, as the femtocells are deployed inside the customer premises, the indoor coverage problems that arise due to high external wall penetration losses in legacy macro networks can be effectively eliminated. In fact, mobile operators can eventually exploit the high wall penetration losses to their advantage by deploying the indoor femto networks which will be better isolated from the interfering outdoor transmitter and, likewise, the outdoor UEs can be protected from the nearby indoor co-channel femtocell interferers, thus resulting in an increase in the total cell and network level capacities.

4.1.4 Energy efficiency analysis

The energy-efficiency performance metric defined in Chapter 2, depends upon two key inputs; (*i*) network area capacity and (*ii*) total area power consumption. For estimating the total area power consumption it is imperative that the power con-

sumption of an individual base station is modelled accurately. A base station site comprises of a base station unit, also known as the base transceiver station (BTS), which has the capability to transmit and receive radio signals to and from the mobile subscribers, together with possible associated units like cooling and air-conditioning in macro devices, and to provide connectivity towards the core network. Due to the clearly different deployment purposes of macrocells and femtocells, also the base station architectures for these types of networks are different. Hence, two separate power consumption models, discussed in [85] and [120], are utilized for estimating the power consumption of macrocell base station and femtocell access point, which are explained as following:

Macrocellular base station power consumption model

The power consumption model for macrocell base station has been described in detail in Chapter 3. The input parameters for the macro base station power consumption model are given in Table 3.5. Based on the parameters in Table 3.5, the total power consumption of a macro base station can be evaluated yielding approximately 1113 W.

Femtocell Access Point (FAP) power consumption model

The power consumption model proposed in [120] defines three power consumption components within a femtocell access point/base station. A microprocessor is responsible for operations and management related to radio protocols, baseband processing and backhaul connection with the core network, an FPGA board taking care of encryption and authentication related protocols and a radio frequency (RF) block consisting of a power amplifier and a transceiver. Thus, the power consumption of a femtocell access point, P_{BS}^{Femto}, can be evaluated using the following model [120]:

$$P_{BS}^{Femto}\,[W] = P_{MP} + P_{FPGA} + P_{TRX} + P_{Amp} \tag{4.4}$$

The power amplifier power consumption is determined using (3.8). As the femtocell technology targets the consumer market segment, the internal electronics components of the access points, especially the PA, are not necessarily as power efficient as those of macrocellular base stations to keep the FAP price tag within affordable range. Thus, the PA efficiency in FAP's is typically relatively low. For the analysis a 20 % power amplifier efficiency has been assumed for the femtocell AP. Table 4.4 gathers the rest of the parameters, applied from [120], for evaluating the power consumption of the femtocell AP. Based on the parameters in Table 4.4, the total power consumption of a femtocell base station can be evaluated and yields roughly 10.1 W.

Table 4.4 Input parameters for the femtocell BS power consumption model

Component/Equipment	Unit	Value
Transmit power at the antenna, P_{TX}	[Watts]	0.1
Power Amplifier efficiency, η_{Amp}	[%]	20
Power consumption of Transceiver, P_{TRX}	[Watts]	1.7
Power consumption of Microprocessor, P_{MP}	[Watts]	3.2
Power consumption of FPGA, P_{FPGA}	[Watts]	4.7

Energy-efficiency results and analysis

Thus far the performance analysis of different deployment strategies focused on the coverage, interference and capacity metrics. It was tentatively concluded that due to dense deployment of femtocells the network can expect very steep system capacity gains. However, one big question that remains is the *energy consumption* of such extremely dense network. Generally speaking, the cost structure of a mobile operator can be categorized into *a) Investment/Capital expenditure (or CAPEX)* and *Running/Operational expenditure (or OPEX)*. Furthermore, it is generally acknowledged in the mobile industry that energy consumption makes up a substantial portion of mobile operators expenditures. Thus, reducing the OPEX through improved network level energy efficiency is a key objective for today's network operators. Hence, this section will look at the energy efficiency (EE) aspects of the considered deployment strategies and also study the impact of wall penetration losses on the achievable energy efficiency.

Fig. 4.6 shows the obtained energy-efficiency performance of the three deployment strategies, for both outdoor and indoor users and under different wall penetration losses using (2.5). Focusing first on the *outdoor environment*, it can be established that the impact of increasing wall penetration loss on dedicated indoor solution (Femto-only deployment) and hybrid Macro-Femto solution is constructive while for the pure outdoor solution it is having a (slightly) degrading effect on the energy-efficiency. Among the three deployment strategies, the most energy efficient strategy is the Macro-Femto deployment supporting an average network throughput of ∼211 bps/Hz per 1 kW power consumption, under 30 dB WPL, followed by Femto-only network (E_{eff}∼115 bps/Hz/kW). For achieving the same level of efficiency, the Macro-only network will have to improve its area spectral efficiency by ∼12 times.

Looking next at the *indoor performance*, the Femto-only network outperforms all other strategies in terms of energy-efficiency by offering the highest average network

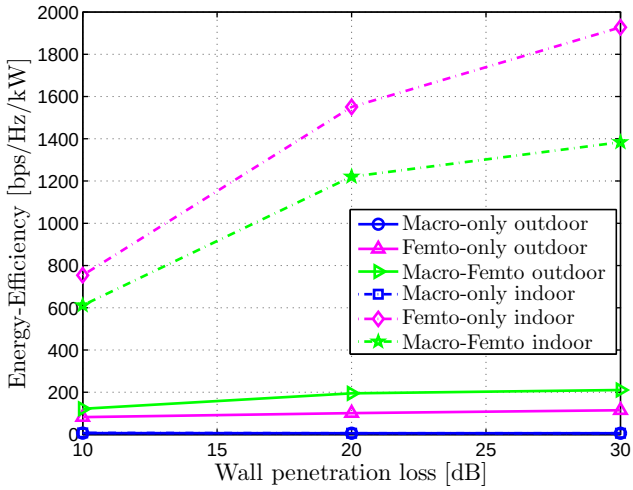

Figure 4.6 Energy-Efficiency performance of different deployment strategies and wall penetration losses.

throughput of 1928 bps/Hz per 1 kW of power consumption under WPL of 30 dB. To reach the 'Femto-only' network efficiency, the Macro-Femto network should improve its system capacity by ∼1.4 times (e.g. through better interference management or coordination), while the lowest performing Macro-only strategy should improve its area efficiency by ∼100 times to reach the same energy efficiency of 1928 bps/Hz/kW. Such area efficiency improvement is virtually impossible, demonstrating again the potential of (co-channel) small-cell deployments in providing the exponentially increasing amount of mobile data with sustainable energy-efficiency.

4.2 Indoor and Indoor-to-Outdoor Service Provisioning

As mentioned in the beginning of the chapter, 5G networks will most likely encompass extremely dense deployments of small cells, typically in the indoor scenarios. It is believed that majority of these small cells will be purchased and deployed either by end users in their homes in a 'plug and play' fashion, or by enterprises in commercial buildings with no or minimal assistance from the mobile operators, thereby enabling significant savings for the operators in terms of CAPEX and OPEX. Moreover, owing to a very small coverage footprint, the extreme density of these small cells will enable

very tight frequency reuse, resulting in large *network capacity* gains, thus, fulfilling the indoor capacity demands in a cost-efficient manner.

For the outdoor service provisioning, the operators have so far been relying on outdoor installations (mostly macro- layer), while deploying microcells only in hotspot areas. Outdoor deployments, unfortunately, come with a substantial price tag for the wireless carriers, with major cost items being site rental, RF engineering and backhaul connectivity. The associated high CAPEX and OPEX, nowadays, are a key concern for cost aware mobile operators that are striving to provide better services at lower cost in a highly competitive markets, where 'flat business model ' prevail. Fortunately, there is an option for mobile operators to bring their infrastructure cost down significantly. Indoor small cells despite having limited coverage foot-print, tend to radiate/spill their signals into the neighborhood outdoor environment. These signals usually originate from small cells located in the nearby buildings. By enabling the indoor small cells to operate in an open subscriber group (OSG) mode and thus provide service in their immediate outdoor vicinities, mobile operators can significantly lower their infrastructure costs by benefiting from zero *site rental*, *RF engineering* and *backhaul connectivity* costs, and thereby providing connectivity to outdoor users/customers with lower incurred costs. Similar concept of indoor-to-outdoor service provisioning has been presented by Qualcomm as '*Neighborhood Small Cells* (NSC)' in [116, 117]. Furthermore, key challenges related to deployment, mobility management and RRM (radio resource management) of NSC have been discussed quite nicely in [117].

In the previous section, the impact of different wall penetration loss on the overall (outdoor and indoor) performance for three different deployment strategies was examined. This section evaluates the impact of different wall penetration losses on the performance evaluation of indoor DenseNets, from indoor-to-outdoor service provisioning perspective. For the performance evaluation, two different propagation environments are considered; *suburban* and *dense urban*. The scenario for the *suburban* is depicted in Fig. 4.1, while scenario illustration for the urban environment is given in Fig. 4.7. In each of the environment, the femtocells access points (FAPs) are extremely densely populated and operate in an *open subscriber group* (OSG) configuration. In the OSG mode, the outdoor macrocell users can also attach to the indoor femtocells, in locations where the indoor femtocells are dominant and vice versa. In the suburban scenario, three different wall penetration losses; 10 dB, 20 dB and 30 dB have been considered. The values have been selected to model the exterior wall penetration losses of typical town houses with older and modern constructions [13]. While for the urban environment, in turn, a downtown (city center) area with tall buildings

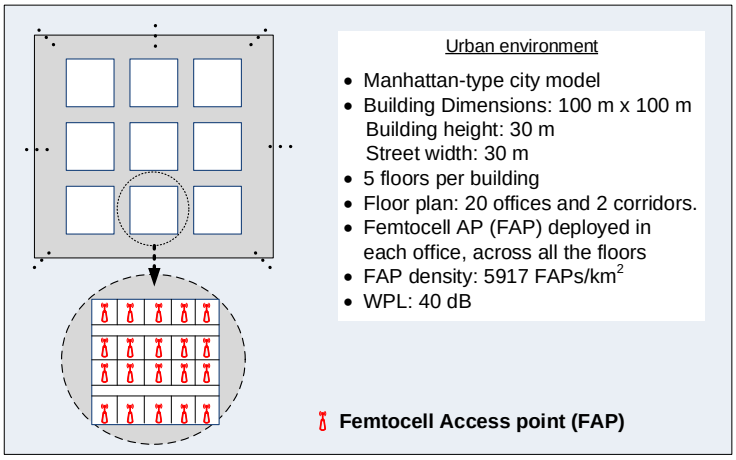

Figure 4.7 Urban scenario (aerial and 3D view) used in the analysis; the dotted lines imply continuous blocks of buildings. The femtocells are deployed in each room, across all the floors.

is assumed. The external wall penetration loss in such urban buildings is believed to be even higher, due to presence of steel columns etc., hence the WPL in this case is selected to be 40 dB. Moreover, from the deployment point of view, in a suburban environment, a single femtocell is assumed per residential home which results in a cell density of 3125 FAPs/km^2. In the urban environment, due to larger buildings, 20 FAPs per floor are assumed (1 FAP in every office room), which gives an extremely high cell density of 5917 FAPs/km^2. The results and analysis discussed in this section are based on the analysis methodology established in earlier section.

Fig. 4.8 shows the spectral efficiency and energy efficiency performance for indoor deployed DenseNets in suburban and urban environments for different wall penetration loss scenarios. From the indoor users' perspective, the high wall penetration loss is actually shown to improve the capacity performance in the suburban environment. The reason is simply due to better shielding, with increasing WPL, from neighbouring interfering femtocells access points that are installed in other houses, as shown also by the SINR performance in Fig. 4.8a. Owing to very high frequency reuse (resulting from ultra dense indoor deployments), along with better interference shielding due to high wall penetration loss yielding high cell level capacities, the area capacity in the indoor environment increases proportionally. For the urban environment, on the other hand, due to the dominant interferers being present inside the building, the cell level capacities are deteriorated, resulting in lower cell spectral efficiency as

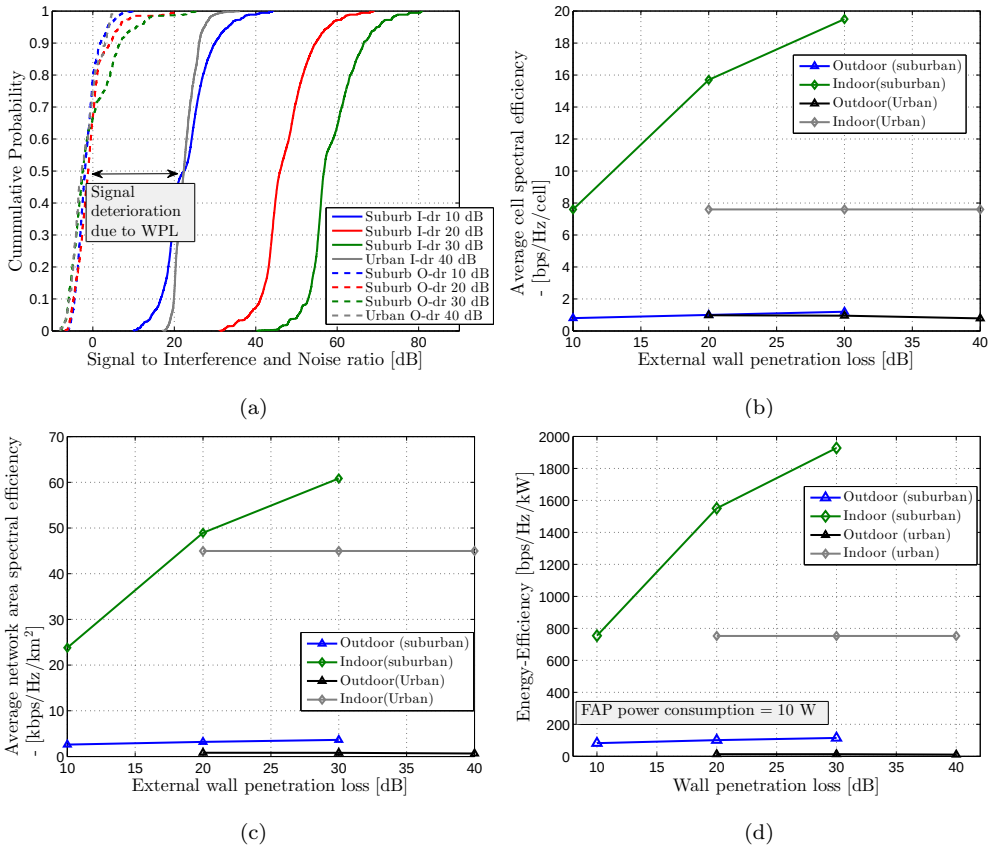

Figure 4.8 Performance analysis of femtocells based DenseNets for outdoor and indoor users in suburban and urban environments with different wall penetration losses; (a) *Signal to Interference and Noise ratio*, (b) *Average cell spectral efficiency*, (c) *Average network spectral efficiency*, and (d) *Network energy efficiency*. (In (a); I-dr = Indoor, O-dr = Outdoor)

compared to suburban scenarios. Furthermore, the lower cell level capacity, in urban scenario, also naturally decreases the achievable network capacity. Hence, slightly lower network spectral efficiency performance can be witnessed in the urban environment, as compared to suburban 20 dB and 30 dB wall penetration loss scenarios. For comparison purposes, the wall penetration loss of 20 dB and 30 dB are also plotted for the urban scenario. Furthermore, in the urban indoor environment, as the dominant interferers are already present inside the building, the wall penetration loss does not have any essential impact on the cell-, network- and energy efficiency performance.

Looking next at the *indoor-to-outdoor* service provisioning performance, the achievable outdoor capacity gain from dense indoor femtocell deployments is comparatively

lower. The reason, as mentioned earlier, is attributed to the high wall penetration loss that actually deteriorates the signal quality of indoor transmitters, as clearly shown in Fig. 4.8a, thereby reducing cell throughput. Comparing the network spectral efficiency and network energy efficiency with densest pure macro-layer configuration (120 cells/km^2) in Chapter 3, the indoor ultra dense femtocell deployment still offers 400 times more indoor area capacity and 12 times more outdoor area capacity in suburban 30 dB WPL scenario, while in the urban environment, the relative indoor/outdoor area capacity gain is 300 times and 2.2 times respectively in the 40 dB external wall penetration scenario. Similarly, from the energy efficiency point of view, owing to the extremely high frequency reuse and significantly low power consumption per femtocell AP (in the order of 10W), the amount of bits transferrable per kW, in suburban 30 dB scenario, is 600 times and 20 times more than in the densest macrocellular configuration, for indoor and outdoor respectively.

Hence, it is concluded that for indoor users, the dense femto-cell deployment provides enormous network level capacity gain, and reduces also the energy per communicated bit substantially, compared to densified macro network. Furthermore, mobile operators can provide certain services to the outdoor users from indoor access points, however, in order to guarantee higher bit rates, the operators will be required to deploy dedicated outdoor installations as well. Furthermore, the indoor-to-outdoor service provisioning will obviously work only in small streets or neighbourhoods, as the indoor small cells, due to lower transmit power levels, will only be able to cover areas in the vicinity of the buildings. Any outdoor location, wider than few tens of meters might experience coverage limitation if there is no dedicated outdoor access layer available. Indoor-to-outdoor service provisioning solution using Indoor DenseNets can thus be considered as a good complement to the outdoor network, as a means of, e.g., offloading capacity in times when the outdoor layer is overloaded with users during busy hours.

4.3 Techno-economical Analysis and Comparison of Legacy and Ultra-dense Small Cell Networks

So far, in the previous sections it was observed that ultra-dense small cell networks can generate enormous indoor system capacity due to extremely high degree of spatial reuse. This section now looks at the techno-economical aspects of the indoor ultra-dense networks. The performance of ultra-dense small cells (based on indoor femtocells) is analyzed and compared with densification of legacy deployment solutions (macrocell

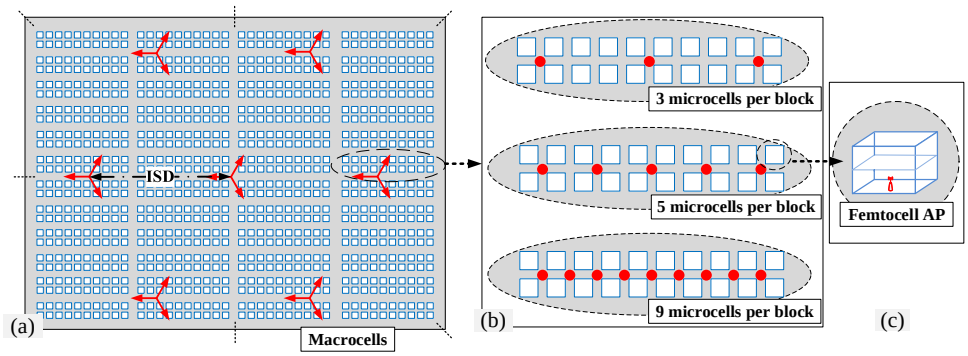

Figure 4.9 Suburban scenario used in the analysis. (a) *Macrocellular deployment*; actual site separation depends on the ISD. The red solid line arrows indicate the orientation of the macrocell sectors (only one tier of macrocells is shown, whereas the analysis considers two tiers of macrocell interferers). (b) *Microcellular deployment*; showing three deployment cases based on densification level. (c) *Femtocell deployment*; The femtocells are deployed in each house (ultra-dense deployment) and assumed to be on the ground floor.

.

and microcell) in a suburban environment. Specifically, the coverage, capacity, energy and cost efficiency of the considered deployment strategies are analyzed and compared from indoor service provisioning perspective. In Chapter 3, the densification of legacy deployment solutions in dense urban environment was shown to be in-efficient in terms of indoor capacity efficiency. The main objective of this section is to examine whether indoor femtocells would be a feasible pathway for mobile operators to evolve their networks in order to address the indoor capacity requirements in an energy- and cost-efficient manner.

4.3.1 Deployment strategies

For the techno-economical analysis, four competing deployment strategies are considered as alternative solutions for indoor service provisioning, namely; *Macrocellular only deployment*, *Microcellular only deployment*, *Femtocell only deployment* and a hybrid *Macro-Femto co-channel deployment*.

Macrocellular deployment

The macrocells are deployed using a hexagonal layout, as shown in Fig. 4.9a. To evaluate the indoor performance of macrocellular network from network densification point of view, three intersite distances (ISD or $\bar{d}_{site}$) are considered; 1732 m (baseline), 866 m, 433 m.

Microcellular deployment

Microcells are relatively low power base stations that are installed outdoors to cover a small hot spot area (up to 100 - 250 m). Due to their compact size and discrete form, they are well suited for installation on lamp posts, building side walls etc. For the analysis, the microcells are deployed at the street intersections of the neighborhood, as shown in Fig. 4.9b. For evaluating the performance and economical benefits of microcellular densification, three deployment cases are considered; (*i*) 3 microcells per block, (*ii*) 5 microcells per block, in which a microcell is located on every second intersection and (*iii*) 9 microcells per block, which is the densest deployment scenario, wherein a microcell is located on every intersection of the neighborhood block.

Femtocell deployment

For the *femtocell deployment*, an ultra-dense deployment of indoor femtocell access points (FAPs) is assumed wherein every residential house has a femtocell deployed on the ground floor; see Fig. 4.9c. Moreover, the femtocells are assumed to be operating in an OSG (open subscriber group) mode, in which a non-FAP-member user equipment (UE) can also be connected to the FAP if it enters its dominance area.

Macro-Femtocell co-channel deployment

The fourth deployment strategy is basically the hybrid combination of the macrocellular deployment strategy and femto cell deployment. The femtocells are deployed within the dominance area of macrocells and both operate on the same carrier (hence called co-channel deployment). The techno-economical analysis of the Macro-Femto deployment scenario is done for all three considered ISDs of macrocellular deployment. It is pertinent to note that in all the three macrocellular deployment cases, the femtocell density remains the same. Furthermore, for simplicity, no coordination between macrocell base station and femtocell base station, nor between different femtocell base stations is assumed.

The cell density, ρ_{cell}, per km^2 is generally calculated as the inverse of cell area. Table 4.5 gives the cell area and cell densities for different deployment scenarios.

4.3.2 System model and assumptions

The scenario is based on the general suburban locality described in Section 4.1 and depicted in Fig. 4.1. While assuming a modern construction throughout the area, a wall penetration loss of 30 dB is assumed. Inside the residential houses, the floor

Table 4.5 Cell densities for different deployment scenarios

Deployment strategy	Cell Area [km^2]	Cell density
***Macrocellular only*:**		
Macrocell - ISD 1732 m	0.29	3.5 cells/km^2
Macrocell - ISD 866 m	0.07	13.9 cells/km^2
Macrocell - ISD 433 m	0.02	55.4 cells/km^2
***Microcellular only*:**		
3 microcells per block	0.0021	468.8 cells/km^2
5 microcells per block	0.0013	781.3 cells/km^2
9 microcells per block	0.0007	1406.3 cells/km^2
Femtocell only	0.00032	3125 cells/km^2
***Macro-Femto HetNet*:**		
Macrocell - ISD 1732 m	Macro (0.29), Femto (0.00032)	3128.5 cells/km^2
Macrocell - ISD 866 m	Macro (0.07), Femto (0.00032)	3138.9 cells/km^2
Macrocell - ISD 433 m	Macro (0.02), Femto (0.00032)	3180.4 cells/km^2

penetration loss is taken to be 4 dB, which is typical value for town houses [13].

Table 4.6 gathers the the simulation parameters used in the analysis. Note that the effective isotropic radiated power (EIRP) in the maximum antenna gain direction is 61 dBm (43 dBm + 18 dBi = 61 dBm) for macrocells, 35 dBm (30 dBm+5dBi = 35 dBm) for microcells and 22.2 dBm (20 dBm + 2.2 dBi = 22.2 dBm) for the FAPs. Moreover, to determine the receiver thermal noise floor, a 20 MHz bandwidth is assumed (stemming from 3GPP Long Term Evolution, LTE).

4.3.3 Capacity efficiency analysis

In this section, the results from the simulations in terms of coverage, radio channel conditions (*SINR*) and capacity are analyzed and discussed. It is pertinent to mention over here that all the results and analysis in this section are based on the performance metrics defined in Chapter 2 and elaborated in Section 3.1 for legacy deployment solutions (macrocell and microcell) and Section 4.1 for femtocells based deployment solutions. The *SINR* for pure macrocell/microcell deployment is calculated using (3.1), while for femtocell deployment scenarios, the *SINR* for pure femtocell and macro-femto co-channel deployment is given by (4.2) and (4.3), respectively.

Fig. 4.10 shows the indoor 10$^{\text{th}}$ percentile values for a) received signal power (i.e., coverage) and b) SINR (radio channel condition), for the four deployment strategies.

Table 4.6 General simulation parameters

Parameter	**Unit**	**Value**
Operating frequency	[MHz]	2100
Bandwidth, W	[MHz]	20
Transmit power at the antenna port	[dBm]	Macrocell: 43, Microcell: 30, Femtocell: 20
BS antenna type		Directional (Macro), Omni (Microcell and FAP)
BS antenna beamwidth, $HPBW_{h/v}$	[°]	Directional (65°/6°), Omni (360°/90°)
BS antenna gain, G_m	[dBi]	Macrocell: 18, Microcell: 5, Femtocell: 2.2
UE antenna type		Halfwave dipole
UE antenna gain	[dBi]	2.2
BS antenna height, h_{BS}	[m]	Macrocell:30, Microcell: 4, Femtocell: 2
UE antenna height, h_{MS}	[m]	2 (relative to floor level)
Receiver noise figure	[dB]	9
Receiver noise floor level, P_n	[dBm]	-92
Propagation environment		suburban
Propagation model		Dominant Path Model
Building dimensions	[m]	10×10
Building height	[m]	5
Indoor floor plan		Open space
External wall penetration loss	[dB]	30

The x-axis indicates the respective cell densities for each of the deployment strategy, and y-axis the corresponding received signal power [dBm] or SINR [dB]. Starting with the coverage analysis (Fig. 4.10a), it is shown that deployment strategies based on the indoor deployed femtocell solutions offer much stronger signal strength, even at the cell border regions, as compared to the outdoor deployed macro and micro based networks. The reason for such high signal strength is simply due to the fact that femtocell APs, due to being in close proximity of the indoor receiving points, offer quite low path loss to the receivers. Moreover, the signals coming from outdoor macro and micro sites are attenuated signficantly due to high wall penetration loss, which further increases the path loss between outdoor sites and indoor receiving

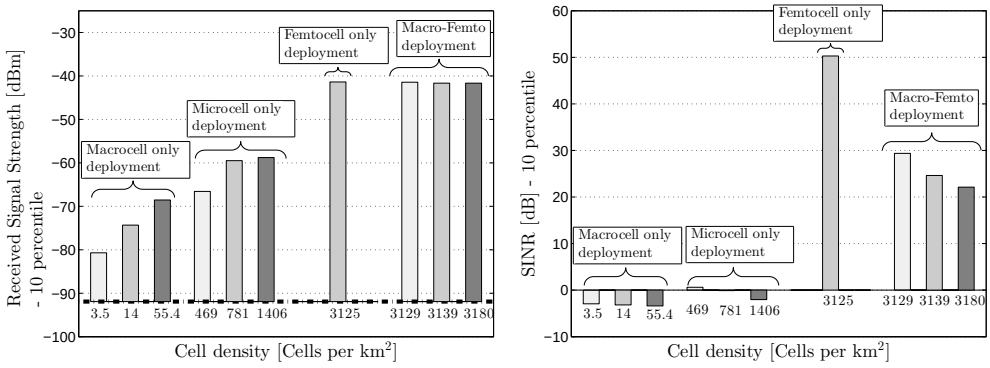

Figure 4.10 10^{th} percentile (cell edge) values for (a) Indoor coverage, and (b) Indoor Signal-to-Interference and Noise ratio, for different deployment strategies. The black dashed line in (a) indicates the thermal noise floor at -92 dBm

points. Although, the effect of wall penetration loss can be decreased by densifying the outdoor macro- or micro- layers, nevertheless, the coverage level still lags behind that of femto based solutions. From Fig. 4.10a, it is quite clear that the femtocell AP dominates the indoor coverage even with dense outdoor macro-layer deployed.

The corresponding radio channel conditions in terms of SINR for all four deployment strategies are shown in Fig. 4.10b. A very similar trend in the SINR performance is shown. Femtocells APs, due to being located inside the residential houses, are well isolated from other co-channel femtocells, located in neighboring houses. For the femto- only deployment case, the signals coming from the co-channel femtocell interferers are attenuated upto 60 dB due to the wall penetration losses, which results in quite high SINR performance (upto 50 dB) in the indoor environment. However, when a co-channel heterogeneous network is considered, the femto AP isolation is partially degraded due to additional interference from the outdoor macro-layer and hence degradation in the radio channel conditions can be witnessed. Thus, the outdoor network densification in case of homogeneous and heterogeneous deployment strategies is shown to further degrade the radio channel conditions indoors, due to closing in of the interfering sites.

Next, coming to the capacity efficiency analysis, Table 4.7 gives the indoor *cell-edge spectral efficiency* along with *average cell and area capacities* for different deployment strategies. The SINR values, analyzed in the previous subsection, are directly

Table 4.7 Cell edge efficiency, Average cell spectral & area spectral efficiency for different deployment strategies, evaluated for indoor users

Deployment strategy	**Cell edge efficiency** [bps/Hz]	$\bar{\eta}_{cell}$ [bps/Hz]	$\bar{\eta}_{area}$ [bps/Hz/km^2]
***Macrocellular only*:**			
Macrocell - ISD 1732 m	0.59	2	7
Macrocell - ISD 866 m	0.57	1.74	24
Macrocell - ISD 433 m	0.54	1.76	98
***Microcellular only*:**			
3 microcells per block	1.12	2.7	1267
5 microcells per block	1	2.4	1877
9 microcells per block	0.7	1.97	2768
Femtocell only	16.7	18.97	59280
***Macro-Femto HetNet*:**			
Macrocell - ISD 1732 m	9.76	13.57	42440
Macrocell - ISD 866 m	8.19	11.07	34750
Macrocell - ISD 433 m	7.36	9.78	31100

mapped to the cell spectral efficiency values using (2.4). As shown, the Femto-only and Macro-Femto deployment strategies perform much better in the indoor environment and yield comparatively better cell edge spectral efficiencies than the outdoor macro- and micro- only deployments. Densifiying the outdoor networks (macro, micro) clearly has a negative impact mainly on the indoor cell edge capacities, due to radio channel degradation, in all of the deployment strategies. The same trend is also observed for *average cell level capacities*. Investigating, next, the obtained average *area spectral efficiencies*, a huge difference can be seen between outdoor macro- and micro- only deployment compared with Femto-only and Macro-Femto deployments. The reason is attributed to the extremely dense femtocells which are deployed in every house. The extreme densification of the femtocells actually results in extreme spatial frequency reuse providing very steep *network capacity gains*. Furthermore, due to better isolation provided by high wall penetration losses, the indoor network capacity increases significantly for both femto-only and macro-femto deployment strategies because in both cases the indoor UEs are served by the femtocells. *Hence, from the network area spectral efficiency point of view, it is observed that femtocells are the best choice for providing indoor local area service due to better coverage, radio channel conditions and also huge capacity gains.* Moreover, as the femtocells are deployed

Table 4.8 Energy efficiency for different deployment strategies

Deployment strategy	**Area power consumption** [kW/km^2]	**Energy efficiency** [bps/Hz/kW]
***Macrocellular only*:**		
Macrocell - ISD 1732 m	1.2	5.8
Macrocell - ISD 866 m	4.8	5
Macrocell - ISD 433 m	19.2	5.1
***Microcellular only*:**		
3 microcells per block	70.3	18
5 microcells per block	117.2	16
9 microcells per block	211	13.1
Femtocell only	31.3	1894
***Macro-Femto HetNet*:**		
Macrocell - ISD 1732 m	32.5	1306
Macrocell - ISD 866 m	36.1	963
Macrocell - ISD 433 m	50.5	616

inside the customer premises, the indoor coverage problems that can arise due to high external wall penetration losses in legacy outdoor networks can be effectively eliminated.

4.3.4 Energy and Cost efficiency analysis

Based on the power consumption models and corresponding input values, as described in Chapter 3 for legacy deployment solutions and Section 4.1 for femtocellular access point, the power consumption for macrocellular base station, microcellular base station and femtocell access point operating in full load condition is computed to be 1113 W, 150 W and 10.1 W, respectively.

Table 4.8 gathers the energy-efficiencies for different deployment strategies. Looking at the *area power consumption* values, the power consumption increases with increasing outdoor base stations (macro and micro) density over 1 km^2. It is also interesting to note that despite having extreme cell density (3125 FAPs per km^2), the area power consumption of femtocells per km^2 is relatively not that high. As an example case; comparing femtocell deployment with pure macrocellular deployment (ISD 433 m), it is shown that with approximately 160 times more cell sites, the area power consumption of femtocell deployment is just 1.6 times more per km^2.

Table 4.9 CAPEX and OPEX costs for different types of base-stations

CAPEX (*Initial costs*)	**Macrocell BS**	**Microcell BS**	**Femtocell AP**
Base station equipment	10 k€	2.5 k€	0.1 k€
Site deployment cost	5 k€	0.5 k€	0 k€
Total CAPEX	*15 k€*	*3 k€*	*0.1k€*
OPEX (*Running costs*)	**Macrocell BS**	**Microcell BS**	**Femtocell AP**
Site rent (lease)	5 k€/year	1 k€/year	0 k€/year
Leased Line rent (backhaul)	2 k€/year	2 k€/year	0.5 k€/year
Operation and Maintenance	7 k€/year	1.5 k€/year	0 k€/year
Total OPEX	*14 k€/year*	*4.5 k€/year*	*0.5 k€/year*

Furthermore, when compared to microcell deployments e.g., 3 cells per block, the femtocell area power consumption is approximately half. The reason for this is the extremely low power consumption per femtocell AP as compared to the outdoor base stations (approximately, 90 % smaller power consumption than microcells site and 99% smaller than macrocells site).

From the *energy efficiency* point of view, the femtocell based deployments clearly dominate this arena as well. Owing to the high capacity gains achieved from ultra-dense deployment, the amount of bits transferrable per kW is significantly high for femtocells. In other words, the energy consumption per transferring one bit of data goes down in ultra-dense deployment of femtocells. Moreover, the network densification of outdoor deployment networks does not bring any significant capacity gain that can offset the high power consumption of the network. Hence as a preliminary conclusion; *the ultra-dense deployment of femtocells seem to be an energy-efficient pathway for mobile operators to provide indoor service.*

Next, coming to the economics and the cost-efficiency results of the four deployment strategies. Table 4.9 gives the various cost items related to CAPEX and OPEX and their approximate values for macrocell, microcell and femtocell cell site. The cost of femtocell AP, which are mainly targeted towards the residential consumer market, is selected to be comparable to commercially available WLAN AP. From operational expenses point of view, due to relatively small size factor, the microcells tend to have lower OPEX costs as compared to macrocells, while the only running cost incurred in operating a femtocell is the backhaul connectivity. For the analysis, the backhaul for femtocells is assumed to be via residential DSL connection (the annual rate is based on flat rate of 40 € per month, which is typical monthly connection fee for high speed

Table 4.10 Cost efficiency for different deployment strategies

Deployment strategy	**Total cost per Area** [k€/km^2]	**Energy efficiency** [bps/Hz/k€]
***Macrocellular only*:**		
Macrocell - ISD 1732 m	121	0.06
Macrocell - ISD 866 m	482	0.05
Macrocell - ISD 433 m	1924	0.051
***Microcellular only*:**		
3 microcells per block	15002	0.08
5 microcells per block	25002	0.075
9 microcells per block	45000	0.062
Femtocell only	10313	5.75
***Macro-Femto HetNet*:**		
Macrocell - ISD 1732 m	10434	4.1
Macrocell - ISD 866 m	10795	3.2
Macrocell - ISD 433 m	12237	2.5

residential internet connection in Europe, e.g. [121]). As such, the approximate costs of macrocell, microcell and femtocell base station in net present value (NPV) is calculated to be 104 k€, 32 k€and 3.3 k€, respectively. Based on the approximate costs of different base station types, the *Total cost per Area* and *Cost efficiency* performance values for each of the deployment strategies are summarized in Table 4.10. Similar to the findings observed for energy-efficiency, we can see that the capacity gain achieved through ultra-dense deployment of femtocells, together with lower cost per femtocell AP, actually brings down the cost of deployment of ultra dense femtocell networks, which further reduces the *cost per bit*. Interesting thing to note here is the marginal difference in the cost-efficiency of macrocell and microcell deployments.

4.4 Impact of Backhaul Limitation on Femtocell Capacity Performance

The findings from the techno-economical analysis in the previous section indicate that the indoor femtocell based solution provide lowest 'cost' and 'energy' consumption per bit, as compared to the legacy deployment solution, for indoor service provisioning. It is pertinent to note over here that the analysis have so far been based on the assump-

tion of 'no backhaul limitation for femtocell access points'. In reality, however, the indoor femtocells are connected to the core network of the mobile operator via fixed broadband residential internet connection e.g., ADSL (Asynchronous Digital Subscriber Line), FTTH (Fiber to the Home) etc. The connectivity speed of these fixed line connection depends on the end users (customers) subscription. Hence, the actual performance of femtocell access point, in practice, is limited by the fixed broadband connection line of the residence. In this section, the impact of backhaul limitation on the network capacity performance of femtocell deployment strategy is evaluated and compared with legacy deployment solutions (macrocell and microcell), which are assumed to have no such constraint.

Table 4.11 and Table 4.12 give the average cell and corresponding network level capacities, respectively, for each of the deployment strategies under different operating bandwidths. The femtocell deployment is constraint by four backhaul (B/H) capacity constraints, while for the legacy deployment solutions no such backhaul limitation is assumed. Clearly, from cell capacity point of view, it can be seen that the capacity of femtocell deplomet is severely limited by the backhaul even though the air-interface may be able to offer higher throughput due to better radio channel conditions. From the network area capacity point of view, at low operating bandwidth (5 MHz), the femtocells still offer better cost and energy efficiency compared to the legacy deployment solutions even if the femtocell backhaul offers very limited connectivity (2 Mbps). On the other hand, as the operating bandwidth increases, the legacy deployment solutions start to offer higher network capacity gains (especially the microcellular deployments) compared to femtocells with low backhaul connectivity. Nevertheless, in deployment scenarios where the femtocells are connected to atleast 32 Mbps connection, the network level throughput increases beyond what is offered by the legacy solutions. Hence, it is concluded that the actual network level gains from deploying dense femtocells will highly depend upon the backhaul connectivity.

4.5 Chapter Conclusions

This chapter analyzed and compared the dense deployment of indoor femtocell-based solutions and legacy deployment solutions (macro-/micro-cell deployments) from technical and economical aspects.

First, the performance of ultra-dense indoor femtocell based deployment solution was benchmarked with legacy macrocell deployment in a suburban environment with different wall penetration losses recently encountered in modern buildings. From coverage point of view, it was shown that the homogeneous macrocellular deployments

Table 4.11 Average cell level capacity for different deployment strategies

Deployment Strategy	Average Cell Capacity [Mbps]				
	5 MHz	10 MHz	20 MHz	40 MHz	100 MHz
Macrocell only:					
ISD 1732 m	10	20	40	80	200
ISD 866 m	8.7	17.4	34.8	69.6	174
ISD 433 m	8.8	17.6	35.2	70.4	176
Microcell only:					
3 cells/block	13.5	27	54	108	270
6 cells/block	12	24	48	96	240
9 cells/block	9.85	19.7	39.4	78.8	197
Femtocell only:					
B/H: 2 Mbps	2	2	2	2	2
B/H: 8 Mbps	8	8	8	8	8
B/H: 32 Mbps	32	32	32	32	32
B/H: 100 Mbps	94.85	100	100	100	100

suffered from heavy indoor coverage limitations resulting from increased wall penetration losses, while the femtocell based solutions (pure femtocell and macro-femtocell deployments) performed substantially better in terms of indoor coverage. From the overall system capacity- and energy efficiency point of view, the femtocell based solutions performed quite consistently in modern building constructions. Hence, to counter the growing concerns of the mobile operators related to 'zero-energy' and other modern buildings, it is concluded that an attractive solution is to deploy dedicated indoor solutions like femtocells.

Next, the performance of ultra-dense indoor femtocells was compared with legacy macrocellular and microcellular based solution, as an alternative means of providing indoor service. Four key performance metrics were considered for the analysis; *coverage*, *capacity*, *energy-* and *cost efficiency*. Moreover, a key study item was the network densification of outdoor base stations and those deployments compared with ultra-dense indoor femtocell deployments. From the coverage point of view, femtocells based solutions (both femto only and macro-femto) provided much better indoor signal levels compared to outdoor legacy deployments. Unlike, the performance of legacy deployment solutions observed in Chapter 3, owing to the extremely high spatial re-use coupled with low power consumption and low cost per femtocell access

Table 4.12 Average network level capacity for different deployment strategies

Deployment Strategy	Average Network Capacity [Gbps]				
	5 MHz	10 MHz	20 MHz	40 MHz	100 MHz
Macrocell only:					
ISD 1732 m	0.04	0.07	0.14	0.3	0.7
ISD 866 m	0.12	0.24	0.5	1	2.4
ISD 433 m	0.5	1	2	3.9	9.8
Microcell only:					
3 cells/block	2.8	5.6	11.3	22.5	56.3
6 cells/block	3.9	7.8	15.6	31.3	78.1
9 cells/block	4.9	9.8	19.7	39.4	98.4
Femtocell only:					
B/H: 2 Mbps	6.3	6.3	6.3	6.3	6.3
B/H: 8 Mbps	25	25	25	25	25
B/H: 32 Mbps	100	100	100	100	100
B/H: 100 Mbps	296.4	312.5	312.5	312.5	312.5

point, the femtocell based solutions offer extremely high overall indoor network area capacity and energy- and cost-efficiency for indoor service provisioning. Even, in the deployment scenario case, where the backhaul of femtocell is limited in terms of bit rate, the overall network capacity gain is much more, as compared to legacy deployment solutions, due to extremely dense deployment. Hence, it is concluded that to counter the growing concerns of the mobile operators related to the exponentially increasing amounts of mobile data towards the 5G era, one strong solution is to deploy dense layer of dedicated indoor solutions like femtocells which offer a cost-effective and energy-efficient solution.

Apart from the indoor service provisioning, the coverage in the outdoor vicinity of the building, provided by the indoor femtocell access points, can be utilized by mobile operators to offload the macrocellular traffic in busy hours, thereby adding addtional capacity to the system without investing in expensive network infrastructure. However, it is important to note that indoor femtocells cannot replace the outdoor infrastructure. For outdoor user service provisioning, a dedicated outdoor deployment will always be required. Chapter 5 then looks at an outdoor deployment solution, based on the distributed antenna system (DAS), as a candidate solution for high-speed service provisioning in the outdoor environment.

Chapter 5

Outdoor Distributed Antenna Systems

THE majority of the future data traffic demand, as highlighted in the preceding chapters, will originate from the indoor locations and will be localized to certain geographical areas, mainly 'dense urban areas' and not the whole network. In Chapter 4, it was shown that the indoor based small cell solutions serve as a key technology to provide the indoor capacities with high speed data services. Nevertheless, the evolution of outdoor network elements for enhanced outdoor users is still partially unresolved. In Chapter 3, the densification of legacy deployment solutions (macro-/micro-cell) was shown to provide better outdoor network level capacity compared to the indoors, however, the cell level capacity degraded significantly with increasing level of densification due to co-channel interference.

For the outdoor service provisioning, due to relatively low traffic volume and high mobility users, mobile operators may still continue, for sometime, to rely on the macrocellular layer to provide wide area coverage. This trend, however, will not last for long, as the recent advancements in wireless connectivity e.g., for vehicles, *supporting different applications ranging from infotainment and security to navigation etc.*, will put stringent requirements on the mobile operators infrastructure also outdoors[1,2]. Consumers will expect the same level of quality of user experience (QoE) within their vehicles as that experienced outside the vehicle, i.e., they will expect access to infotainment services, inside their vehicles, to have the same degree of reliability and uptime as they do when they tune into FM radio. Such innovations will demand high bit rates with '*anywhere anytime availability*', which the legacy outdoor deployments inherently lack. Traditional macrocellular deployments are only able to

[1]By year 2024, approximately 90 % of the new cars will have embedded connectivity [122]

[2]Current smartphone usage statistics; 58 % users in US and 47 % in Europe report using apps while driving [123]

provide peak bit rates to relatively few users in a certain geographic location. The reason is attributed to the fact, that due to large coverage areas of macrocells, the users located near the cell site experience much better radio channel conditions and lower path loss as compared to the users at the cell edge, thus resulting in quite uneven distribution of the achievable data rates throughout the cell coverage area, as illustrated in Fig. 5.1. For next generation high speed services, the distance between the eNode-B and UE has to be small enough to have minimum path loss and thus provide high SINR. Massive MIMO with large antenna arrays is one way to go, which is also a key topic being researched for 5G [124]. Another method is to bring the base station antennas closer to the users.

Outdoor small cells can effectively address the inherent problem of macrocells. Due to their relatively small coverage footprint, the users are always within their vicinity, which helps in reducing the path loss. However, the problem with outdoor small cells is that in order to have a continuous coverage, small cells in sizeable numbers need to be deployed quite close to each other, which poses problems for high mobility users. In the indoor environment, where the location of indoor users rarely change, the indoor small cell solutions are able to provide better service. In contrast, the situation in the outdoor environment is completely different as majority of the outdoor subscribers are high mobility users. Deploying several hundreds of outdoor small cells to cover a certain downtown area can result in large number of handovers, thus resulting in network signalling overload which eventually will result in connection drops. Thus, in order to provide high speed data services to high mobility users, especially in downtown areas where majority of the capacity demand will be concentrated, operators will need to deploy solutions that offer both flavors of macro and small cells i.e., re-designing their networks using solutions that prevent bad coverage, poor radio link quality arising from interference and most importantly unsuccessful handovers for high mobility users.

Outdoor distributed antenna systems (ODAS) technology inherently offers such solution, wherein distributed remote antenna nodes, usually deployed on a public utility poles (e.g., street lights) are clustered to form one large cell. Hence, through the distributed antenna nodes the UE can experience highly stable signal strength throughout the DAS cell coverage area. Depending upon the size of the cell, the number of nodes per DAS cell may vary from 5 to 100 or even more. Compared to a small cell, which typically has a cell range of 100 - 500 m, a DAS cell may cover one street block or a whole neighbourhood. In the past, most of the DAS deployments had been limited to the indoor environments, usually deployed in large malls, academic institutions (campus areas) or enterprise buildings with few outdoor instal-

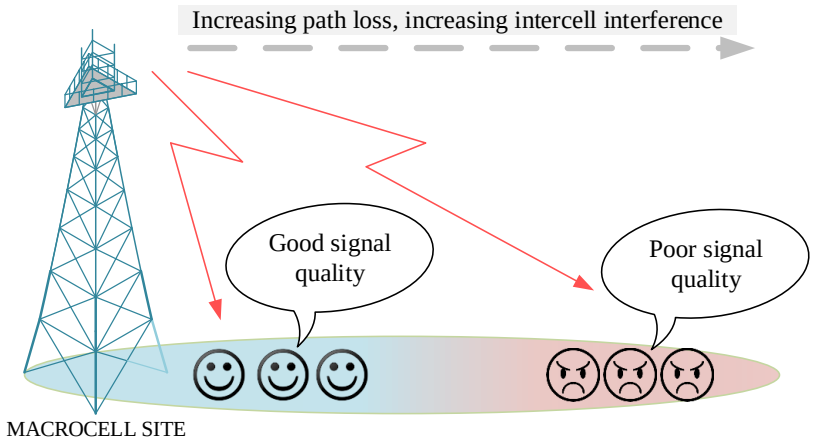

Figure 5.1 Macrocellular pathloss phenomenon; good signal quality near the cell site and poor signal quality at the cell edge.

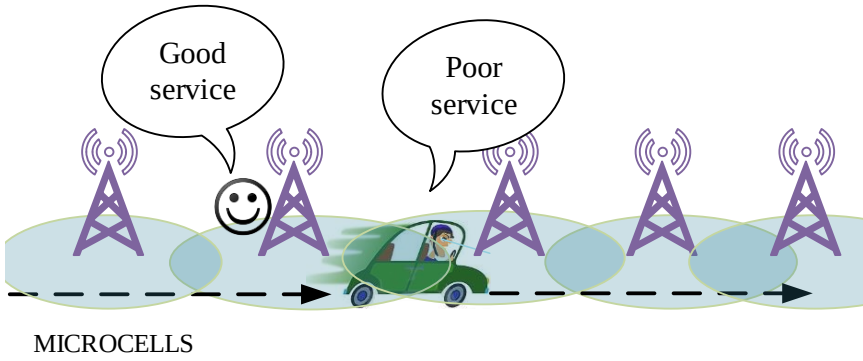

Figure 5.2 Outdoor small cell scenario; frequent handovers in short period of time can result in signaling overload thereby causing connection drops (poor QoE) for fast moving vehicles.

lations. More recently, DAS deployments have started to make their way into the outdoor deployment arena, with majority of the deployments taking place so far in the North America and Far East Asia

This chapter looks into different deployment strategies for outdoor DAS in order to establish new insight and understanding on the effective methodology to deploy the ODAS solution. The different ODAS deployment strategies are compared with the baseline stand-alone small cells, as an alternative solution for provisioning of high bit rates. Specifically, two key metrics are taken into account; *coverage* and *spectral-efficiency* for the performance comparison. Finally, an advanced form of outdoor DAS concept, *Dynamic DAS*, is introduced and analyzed , that offers an efficient and capacity-adaptive solution to provide on-demand outdoor capacity in urban areas by dynamically configuring the remote antenna units to either act as individual small cells or distributed nodes of a common central cell.

The text, results and analysis presented in this chapter are based on the author's published work in [70–72].

5.1 Outdoor DAS Deployment Strategies

Unlike macrocells, urban small cells and outdoor distributed antenna systems are planned to provide service in a targeted area with concentrated demand for capacity. Hence, in order to restrict the coverage foot-print of a stand-alone small cell or an individual DAS node, the antennas are typically deployed on utility poles, street lights etc. along the public right of way (streets, roads, pedestrian walkway etc.) well below the average rooftop level. As such, both small cells and ODAS operate in a microcellular environment, where the surrounding environment (especially the buildings) define the cell pattern. In general, this allows for virtually unlimited number of ways to deploy microcells (stand-alone small cells and DAS nodes). However, careless deployment, without any specific layout and planning, will result in irregular interference patterns, leading to highly unstable network performance behavior, thereby yielding low overall cell and system level capacity. Hence, proper cell planning is required to maximize the utility and quality of the microcellular network. *It is emphasized that both stand-alone small cell and outdoor DAS, in this chapter, are considered as microcells.*

As a comparison point for the performance with ODAS deployment strategies, stand-alone small cells deployment is assumed as the baseline. In the analysis, the stand-alone cells are deployed at every second intersection (see Fig. 5.3) and each cell covers one full block in all four directions along the street.

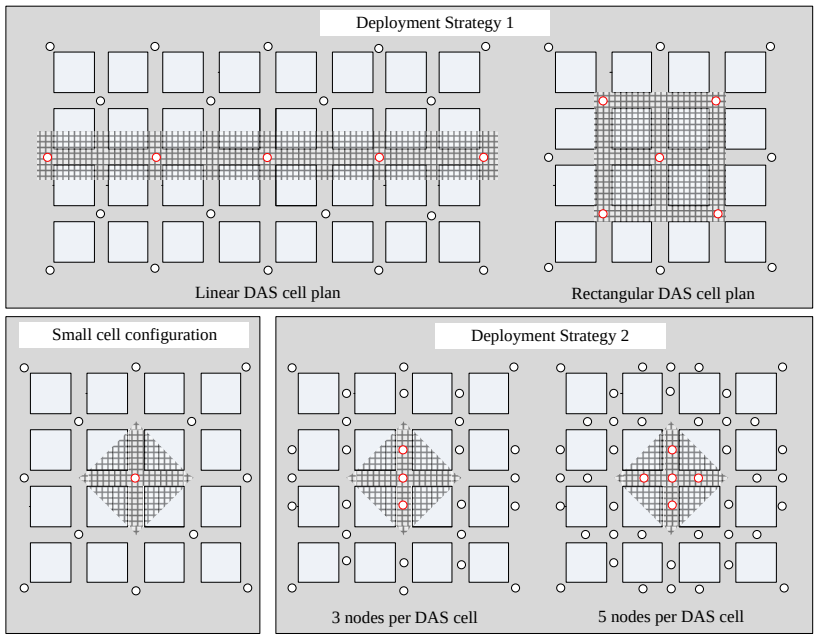

Figure 5.3 Deployment scenarios for small cell configuration and outdoor distributed antenna systems with different deployment strategies. The red circular dots, within the gauze wire patterns, depict remote antenna nodes belonging to a DAS cell, while the remaining dots show interfering nodes. The actual simulation area is cropped to focus on the center DAS/small cell. Approximate cell shape for each configuration is shown by the gauze wire pattern.

In order to introduce the ODAS deployment solution into the network, the following two strategies have been considered:

5.1.1 Strategy 1: *cell clustering*

In strategy 1, the already deployed small cells are grouped into clusters and each cluster is configured to act as a single DAS cell, transmitting the same signal. In essence, the antenna elements/nodes [per km^2] remain unchanged. However, the cell size increases as more nodes are combined into the DAS cell, which essentially reduces the cell density [per km^2]. Furthermore, to streamline the DAS planning process, two cell plans are defined; (*i*) Linear cell plan and, (*ii*) Rectangular cell plan. The cell plans are selected such that they can be easily tessellated together in microcellular environment to form a seamless network coverage area with no gaps.

Table 5.1 Cell densities for different deployment scenarios

Deployment strategy	Cell density	Node density
Small cell deployment	30 cells/km^2	30 nodes/km^2
***DAS deployment, Strategy 1*:**		
Linear cell plan	6 cells/km^2	30 nodes/km^2
Rectangular cell plan	6 cells/km^2	30 nodes/km^2
***DAS deployment, Strategy 2*:**		
3 nodes per DAS cell	30 cells/km	90 nodes/km^2
5 nodes per DAS cell	30 cells/km	150 nodes/km^2

The concept is similar to the cell plans used for nominal planning of macrocellular sites e.g. *hexagonal, clover-leaf, square* cell layouts [125]. Although, the number of nodes per DAS cell can be arbitrary, for the analysis purpose only 5 nodes per DAS cell have been assumed. The deployment strategy 1, using *Linear* and *Rectangular* cell plans, is shown in Fig. 5.3.

5.1.2 Strategy 2: *increasing DAS nodes*

In strategy 2, new antenna elements (AEs) are introduced within the coverage area of existing small cell to form a DAS cell configuration. Thus, the cell size remains constant, but now the antenna density [per km^2] increases. This means that despite of introducing new AEs into the network, the cell density [per km^2] remains the same. For the purpose of analysis only 3 and 5 AEs per DAS cell are considered, as illustrated in Fig. 5.3.

Table 5.1 gives the cell and node densities for different deployment scenarios. In case of stand-alone small cell, a node refers to the cell site, and in case of DAS it refers to the remote antenna element.

5.2 System Model and Assumptions

The analysis is done in a dense urban area. Hence, to imitate such an environment a Manhattan grid city model is utilized, as shown in Fig. 5.3, which can be regarded as a good approximation of major downtowns around the world. Each building has dimensions of 100 m x 100 m, a height of 25 m and comprises of 5 floors. The street width between two consecutive buildings within a block is taken to be 30 m, which also corresponds to inter-block separation. For the indoor floor plan, an open space

Table 5.2 General simulation parameters for DAS simulations

Parameter	**Unit**	**Value**
Operating frequency	[MHz]	2100
Bandwidth, W	[MHz]	20
Transmit power	[dBm]	33
Node antenna type		Omni directional
Node antenna beamwidth, $HPBW_{h/v}$	[°]	360°/90°
Node antenna gain	[dBi]	5.5
UE antenna type		Omni directional
UE antenna gain	[dBi]	2.2
Node antenna height	[m]	8,
UE noise figure	[dB]	9
UE noise floor level, P_n	[dBm]	-92
Propagation environment		Dense Urban
Propagation model		Dominant Path Model
Building dimensions	[m]	100×100
Building height	[m]	25
Indoor floor plan		Open space
External wall penetration loss	[dB]	30

is considered with no internal wall partitions i.e. no hard obstructions for the signal propagation except for the ceiling/floor and exterior walls. Furthermore, assuming modern constructions throughout the urban environment, a building penetration loss (BPL) of 30 dB is again assumed. Similar penetration loss values for modern buildings have been reported in [13], for the 2100 MHz band.

Table 5.2 gathers the rest of the simulation parameters. 'UE' in the table refers to 'user equipment' i.e. the mobile receiver. It is pertinent to mention here that the total transmit power per node remains the same irrespective of the deployment scenario. Hence, the effective isotropic radiated power (EIRP) in the maximum antenna gain direction is 38.5 dBm (33 dBm + 5.5 dBi = 38.5 dBm). Moreover, to determine the receiver thermal noise floor, a 20 MHz bandwidth is assumed (stemming from 3GPP Long Term Evolution, LTE).

5.3 Methodology for Performance Analysis

According to (2.4) it is evident that the cell/area spectral efficiency depends directly on the distribution of Γ i.e. *SINR - which defines the radio channel condition.* The level of useful signal and interference that a UE receiver experiences at a given time is largely determined by the deployed network architecture. This is elaborated in more detail next.

5.3.1 Interference conditions; small cell deployment

In a stand-alone small cell deployment scenario, the UE experiences interference from other co-channel small cells (SC); mostly from line of sight (LOS) cells. The *SINR* in such a scenario is given by:

$$\Gamma_j^{SC} = \frac{S_j^{SC}}{\sum_i I_{i,j}^{SC} + P_n} \tag{5.1}$$

where S_j^{SC} is the received signal power of the serving cell at j^{th} UE. $I_{i,j}^{SC}$ is the received power of the i^{th} small cell interferer at j^{th} UE, and P_n denotes the noise floor which includes also the UE receiver noise figure.

5.3.2 Interference conditions; DAS deployment

In case of DAS configuration, the received signal power from a serving DAS cell is actually the superposition of the received signal powers from all the individual nodes belonging to the serving DAS cell, i.e., the signal powers from all the nodes within a DAS cell are effectively combined at the receiver, while the signal power received from other co-channel DAS nodes is treated as interference. The total *SINR* that a UE experiences in a DAS configuration is given by:

$$\Gamma_j^{DAS} = \frac{\sum_{k \notin i} S_{k,j}^{DAS}}{\sum_{i \notin k} I_{i,j}^{DAS} + P_n} \tag{5.2}$$

where $S_{k,j}^{DAS}$ is the received signal power at the j^{th} UE, from the k^{th} node in the serving DAS cell and $k \notin i$. $I_{i,j}^{DAS}$ is the received power of the i^{th} node, of the interfering cell, at j^{th} UE, and P_n denotes the noise floor which includes also the UE receiver noise figure. It is pertinent to mention over here, that in real networks, achieving coherent

combining of the useful signal energy at the receiver may necessitate accurate phase alignment of the signals of the serving DAS cell already on the transmitter side. Here, we do not address that issue explicitly but simply seek to understand the principal performance behavior of such distribute antenna system.

5.4 Analysis of Outdoor DAS Deployment Strategies

In this section the performance of each of the DAS deployment strategies, introduced in Section 5.1, is evaluated and analyzed in terms of *coverage* and *spectral efficiency*. This will provide technical insight into which deployment strategy will be best suited for mobile operators in order to provide high speed data services.

Similar to the analysis in the previous chapters, due to homogeneity of the environment, the receiver points from the dominance area of the center cell (small cell/ DAS cell) are considered for statistical analysis and the analysis results are further normalized to 1 km^2 area. For simulating a continuous cellular network effect, all the interfering tiers that have significant contribution to the interference level in the dominance area of a serving cell have been taken into account. Moreover, the distribution of receiver points outdoors and across all the buildings (floors) is uniform.

5.4.1 Coverage and interference analysis

Fig. 5.4 shows the 10^{th} percentile values for (a) received signal power (i.e., coverage) and (b) SINR (radio channel condition), for the four deployment strategies. The x-axis indicates the respective cell densities for each of the deployment strategy, and y-axis the corresponding received signal power [dBm] or SINR [dB]. Starting with the coverage analysis (Fig. 5.4a), it can be seen that in all the deployment strategies the indoor environment experiences poor coverage as compared to the outdoors. Several reasons can be attributed to this; (*i*) the signal propagation from outdoor to indoor environment experiences heavy external wall penetration loss which degrades the signal strength by 30 dB, (*ii*) due to relatively low antenna height installation, the EIRP towards top floors of the buildings is smaller as compared to the lower floors or street level, thus resulting in coverage limitation. However, there is a slight impact of introducing DAS configuration in the network, as the network coverage levels in the indoor environment tend to improve slightly. This is because of the superposition of the received signals, from different DAS nodes, at the receiver end. Overall, the cell edge conditions in the *outdoor environment* tend to be at the same level and

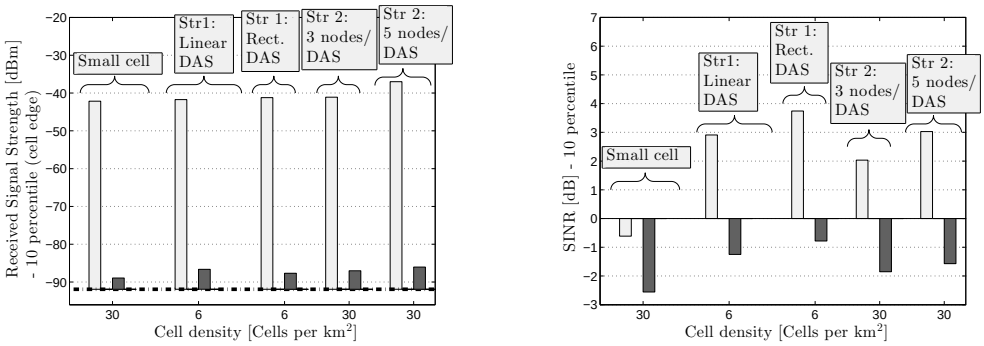

Figure 5.4 10^{th} percentile (cell edge) values for (a) Coverage, and (b) Signal-to-Interference Noise ratio, for different deployment strategies. The black dashed line in (a) indicates the thermal noise floor at -92 dBm. Moreover, the light and dark shaded bars indicate the *outdoor* and *indoor* performance, respectively, for each of the deployment scenario. (Str1: Strategy 1, Str2: Strategy 2)

substantially higher as compared to the indoor, with *5 nodes per DAS* cell configuration (employing strategy 2), bringing improvement as compared to the rest of the deployment strategies.

Now coming towards the radio channel conditions, which are shown by the bar graph in Fig. 5.4b, a clear performance difference between stand-alone small cell deployment and DAS deployment is evident. The reason for poor SINR performance in the small cell deployment is simply attributed to the fact that due to the close proximity of the co-channel sites (mainly LOS sites), the interference level increases at the cell edge. While in the DAS deployments this problem is reduced using the two different deployment strategies. In strategy 1, although the node density is the same as that of stand-alone small cell deployment, the DAS configuration effectively clusters nearby co-channel sites into a DAS node, thereby eliminating the dominant interference. Furthermore, in strategy 1, as the number of nodes increases within a DAS cell, the cell size also increases, which consequently relocates the effective interference further away. Also, the distributed nodes spread across the large DAS cell, reinforces the signal strength thereby reducing the path loss. In strategy 2, due to similar cell size as that of small cell deployment, the distance to the nearest co-channel interferer remains the same, however, the interference in this strategy is mitigated with increased signal strength from remote antenna nodes spread across

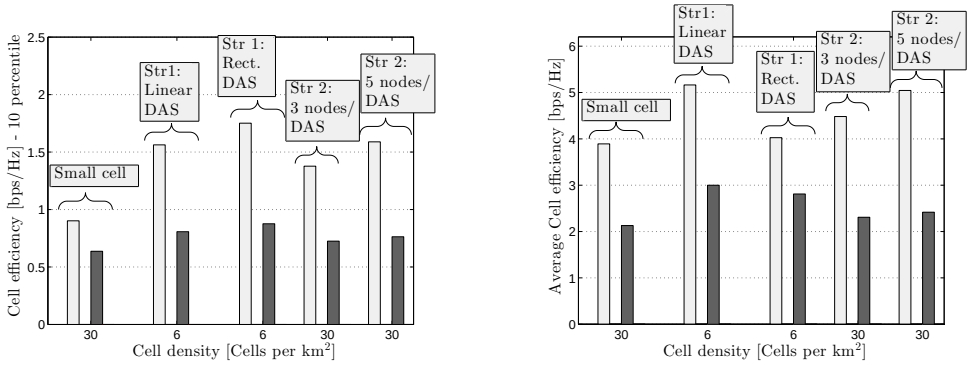

Figure 5.5 Capacity efficiency statistics; (a) 10^{th} (cell edge) spectral efficiency [bps/Hz], and (b) average cell spectral efficiency [bps/Hz]. The light and dark shaded bars indicate the *outdoor* and *indoor* performance, respectively, for each of the deployment scenario.(Str1: Strategy 1, Str2: Strategy 2)

the cell area. Overall, from outdoor coverage and radio channel conditions point of view, DAS configurations deployed using strategy 1 offer best performance.

5.4.2 Cell and area spectral efficiency analysis

Fig. 5.5 gives the indoor and outdoor *cell-edge spectral efficiency* along with *average cell capacities* for different deployment strategies considered in the analysis. The SINR values, analyzed in the previous section, are directly mapped to the cell spectral efficiency values using (2.4) taking into account the overall analyzed cell area. From the figure, overall, DAS configurations offer much better outdoor cell edge capacity performance as compared to small cell deployments, due to better interference management, while the indoor capacity values are fairly similar for all the configurations (stand-alone and DAS). The same trend is also observed for *average cell level capacities*. Investigating, next, the obtained average *network spectral efficiencies*, Fig. 5.6, due to relatively smaller cell size the small cell deployment as well as the DAS strategy 2 offer much higher area capacity as compared to the DAS deployments employing strategy 1. The small cell size results in higher cell density per km^2 which translates into higher spatial frequency reuse. To sum up, distributed antenna systems deployed using strategy 1 offer better cell edge capacity performance, due to better interference management, which can lead to higher data data rates per UE. However, such

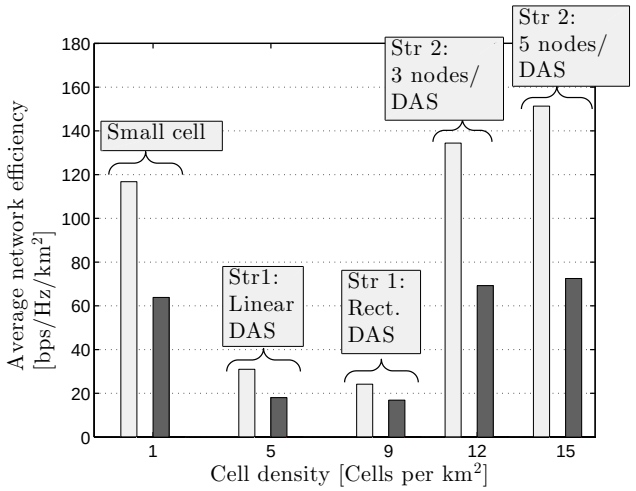

Figure 5.6 Average network efficiency statistics [bps/Hz/km^2] for each of the deployment scenario. The light and dark shaded bars indicate the *outdoor* and *indoor* performance. (Str1: Strategy 1, Str2: Strategy 2)

strategy does not maximize the spatial reuse of frequencies, and thus the network or area capacity is somewhat limited, while the deployment strategy 2 offers a balanced performance in terms of cell and area level capacities.

5.5 Capacity Limitation of Traditional DAS and the Dynamic DAS Concept

In a typical cellular network, the overall network traffic fluctuates during the time of the day. An idle or low load is usually experienced for example, during late night or early morning, while high/peak load is observed during day time or early evening, as shown in Fig. 5.7. Also the traffic pattern varies separately for outdoor (after office hours - *on highways, boulevards etc.*) and for the indoor environments (during office hours and evenings). Hence, there is an inherent need to *provide capacity dynamically* outdoors whenever needed.

Traditional DAS systems work on static configuration i.e., the clustering of the antenna nodes are pre-configured at the base station hub and thus cannot efficiently deliver capacity in highly dynamic outdoor hotspot regions where the traffic varies geographically with time. Hence, most of the resources are wasted. In order to –

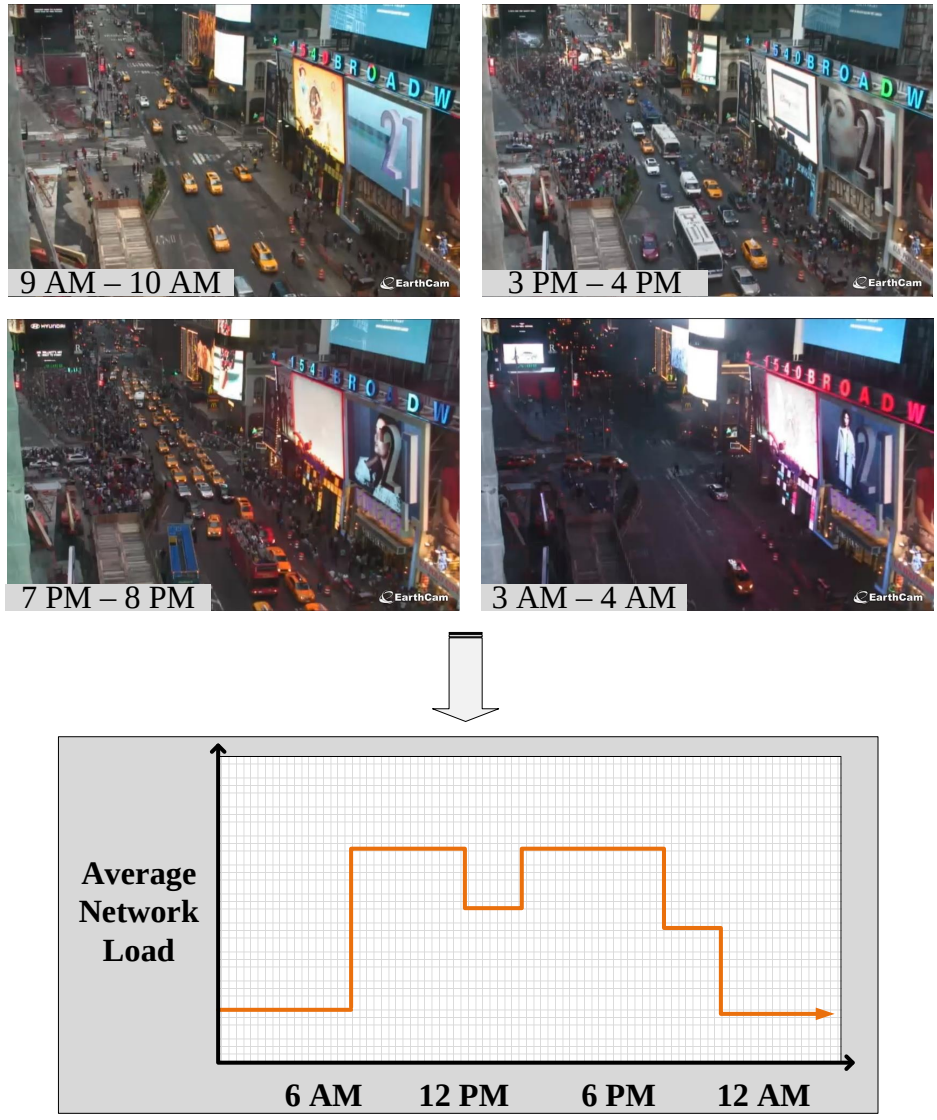

Figure 5.7 Traffic variation pattern during different time periods at Broadway Avenue, New York, USA. (Images courtesy of EarthCam.com)

–address the exponentially increasing outdoor data traffic, the DAS network will need to dynamically reconfigure itself based on the instantaneous load, thus delivering the resources to parts of the network that experience high traffic load. The recent *cloud RAN* (C-RAN) technology aim to offer the capabilities, where tens or even hundreds of small cells or remote antenna units are connected via high speed and low latency backhaul links to a central hub site which houses the centralized processing servers [126], much like the traditional DAS system. In essence, the C-RAN is analogous to a *Dynamic Distributed Antenna system*, that offers pooling of its resources at the central hub site and dynamically concentrates them to geographic areas with high capacity requirements e.g. sport arenas, high streets etc. C-RAN technologies are one of the hot topics that are being considered as key enablers for upcoming 5G networks [79].

In the following section, the performance of dynamic DAS is analyzed in low and high traffic scenarios with two different antenna configurations. The aim is to show the potential of the proposed dynamic DAS concept to efficiently provide on-demand capacity, based on outdoor mobile traffic condition, in a dynamic manner.

5.5.1 Dynamic DAS operation modes

For the performance evaluation of dynamic DAS, two scenarios are considered, based on network traffic load periods in a certain geographic location:

Low traffic load period

During low traffic conditions, the DAS system configure as itself as a super microcell. In super microcell mode, the distributed antenna nodes are configured to transmit the same signal, which results in the UE experiencing highly stable signal strength throughout the DAS cell coverage area. This leads to better radio channel conditions thereby resulting in higher achievable bit rates.

High/Peak traffic load period

In peak load conditions with lots of devices needing service, the dynamic DAS configures the remote antenna nodes (or DAS nodes) to act as multiple independent small microcells. As such, the different nodes are configured to transmit independent signals. This increases the amount of spatial reuse which in turn increases the local-area capacity. Hence, during peak load conditions when more users are trying to access the network, the dynamic DAS efficiently delivers the network resources to those parts of the network that experience high-traffic load.

Fig. 5.8 illustrates the dynamic DAS configurations in both scenarios. It is perti-

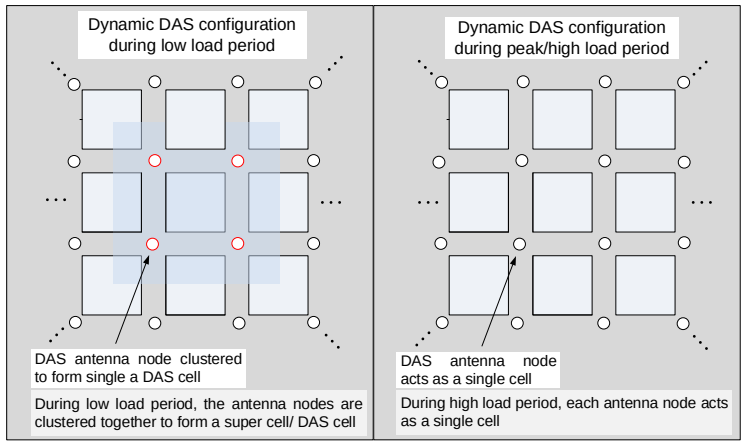

Figure 5.8 Dynamic distributed antenna system configurations during; (a) *Peak network load time period*, and (b) *low network load time period*. The blue shaded region in (b) shows the coverage area of a super microcell (DAS cell). Furthermore, the red colored circles in (b), are the nodes that form a single cluster of DAS cell nodes.

nent to mention over here that although the main aim of the chapter is to show the performance of dynamic DAS in outdoor dense urban environment, indoor aspects should not be forgotten. Thus, to be inline with the future deployment trend, the interference contribution from the co-channel ultra dense indoor small cell deployment also has to be taken into account when evaluating the performance of dynamic DAS in outdoor setting. Therefore, a femtocell access point is assumed in every office within each building. The *coverage* and *spectral efficiency* performance in indoor environment are out of the scope of this chapter.

5.5.2 System model and assumptions

Scenario description

The performance analysis of dynamic DAS in different traffic conditions, is evaluated in the dense urban environment described in Section 5.3.1. For the indoor floor plan, instead of open office, a 3GPP office model is considered, as shown in Fig. 5.9. It is pertinent to mention over here that the indoor floor plan is only relevant from the indoor transmitters point of view, that act as interferers to outdoor deployment infrastructure.

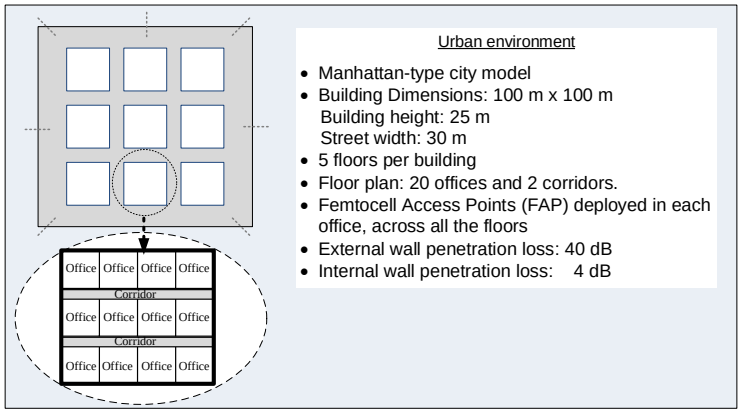

Figure 5.9 Dense urban scenario used in the analysis. The indoor floor plan is based on the 3GPP office model.

Antenna model and configuration

The dynamic DAS, as mentioned in the previous section, is deployed in the microcellular environment. In dense urban environment this gives rise to the street canyon effect. The signals traveling in a street canyon tend to travel much further as compared to the signal traveling in free space [127]. This is due to the tunneling effect caused by the side walls which direct the signals into the alley. As a consequence,the effect of distant interfering tiers especially the LOS tiers, which were negligible before, starts to become more visible. Thus, in order to combat the street canyon effect, two antenna configurations have been considered. The first antenna configuration is the baseline configuration utilizing an Omni-directional antenna (typical for microcellular deployment), while the second configuration utilizes a wide beam directional antenna with extreme downtilt configuration (i.e., 90° mechanical downtilt, where the main lobe in pointing directly downwards). The reason for having a wide beam antenna relates to the deployment aspects of microcells. As mentioned earlier, the microcells are typically deployed on street lamp post or other public utilities. Hence, the operators are bound, by the practical deployment as well as the local city council laws, to use small antennas that can be easily deployed without affecting the aesthetics of the locality. The size of a directional antenna depends on the beamwidth; as the narrow beam antennas require a large number of antenna array elements and vice versa. Therefore, in order to keep the antenna size small, a directional antenna with 90° vertical and horizontal half-power beamwidth, has been assumed in the simulations. The modeling of the directional antenna is based on an extended 3GPP antenna model

Table 5.3 General simulation parameters for Dynamic DAS simulations

Parameter	Unit	Value
Operating frequency	[MHz]	2100
Bandwidth, W	[MHz]	20
Transmit power per antenna node	[dBm]	33
Node antenna type		Omni- and Directional
Node antenna beamwidth, $HPBW_{h/v}$	[°]	360°/90° (Omni config.)
	[°]	90°/90° (downtilt config.)
Node antenna gain	[dBi]	5.5 (Omni) and 7 (Directional)
UE antenna type		Omni directional
UE antenna gain	[dBi]	2.2
Node antenna height	[m]	8,
UE noise figure	[dB]	9
UE noise floor level, P_n	[dBm]	-92
Propagation model		Dominant Path Model
Backhaul capabilities		No backhaul limitation assumed

proposed in [92].

Table 5.3 gather the rest of the simulation parameters. 'UE' in the table refers to 'user equipment' i.e. the mobile receiver. It is pertinent to mention here that the total transmit power per node remains the same irrespective of the dynamic DAS operation mode. Hence, the effective isotropic radiated power (EIRP) in the maximum antenna gain direction for the Omni-directional antenna configuration case is 38.5 dBm (33 dBm + 5.5 dBi = 38.5 dBm) and 40 dBm (33 dBm + 7 dBi = 40 dBm) for the down-tilt configuration. Moreover, to determine the receiver thermal noise floor, a 20 MHz bandwidth is assumed (stemming from 3GPP Long Term Evolution, LTE).

5.5.3 Methodology for evaluating the dynamic DAS concept

The level of useful signal and interference that UE receiver experiences, at a given time, in dynamic DAS system is largely determined by the operation mode, which is elaborated as follows:

Interference condition; individual microcell mode

When the nodes in the DAS are configured to act as an individual microcell (MC), the UE within a certain cell experiences interference from other co-channel interfering cells (outdoor microcells or indoor FAPs); mostly from line of sight (LOS) cells. The *SINR* in such a scenario is given by:

$$\Gamma_j = \frac{S_j^{MC}}{\sum_i I_{i,j} + P_n} \tag{5.3}$$

where S_j^{MC} is the received signal power of the serving microcell at j^{th} UE. $I_{i,j}$ is the received power of the i^{th} interferer cell at j^{th} UE, and P_n denotes the noise floor which includes also the UE receiver noise figure.

Interference condition; super microcell mode

In case of super microcell or DAS configuration mode, the received signal power within the super microcell coverage area is actually the superposition of the received signal powers from all the individual nodes belonging to the super cell, i.e. the signal powers from all the nodes within a DAS cell are effectively combined at the receiver. The received signals from other co-channel cells (interfering microcell nodes or indoor FAPs) are treated as interference. The total *SINR* that a UE experiences in a DAS configuration is given by:

$$\Gamma_j = \frac{\sum_{k \notin i} S_{k,j}^{DAS}}{\sum_{i \notin k} I_{i,j} + P_n} \tag{5.4}$$

where $S_{k,j}^{DAS}$ is the received signal power at the j^{th} UE, from the k^{th} node in the serving DAS cell and $k \notin i$. $I_{i,j}$ is the received power of the i^{th} interfering cell, at j^{th} UE, and P_n denotes the noise floor which includes also the UE receiver noise figure.

5.5.4 Performance analysis of Dynamic DAS concept

This section looks into the performance of the dynamic DAS with different antenna configurations under *low* and *high* network load scenarios. The key performance metrics used in the analysis are *coverage*, *SINR* and *spectral efficiency*.

Due to the homogeneity of the environment, only the receiver points belonging to the dominance area of nodes located within the blue shaded region, shown in Fig. 5.8, are considered in the analysis. Moreover, the distribution of outdoor receiver points

is uniform.

Coverage and interference analysis

Fig. 5.10 shows the statistical values in terms of 10^{th} percentile (cell edge), 50^{th} percentile (Median) and 90^{th} percentile (peak) values for; (a) *received signal power (i.e., coverage)* and (b) *SINR (radio channel condition)*, for the dynamic DAS operating modes and with different antenna configurations. The y-axis indicates the corresponding received signal power [dBm] or SINR [dB]. Starting with the coverage performance (Fig. 5.10a); in both antenna configurations (Omni- and extreme tilt), the received signal levels tend to improve as the dynamic DAS configures the remote antenna nodes to form a super microcell. This is because in super microcell mode, the received signals from different DAS nodes are superposed at the receiver end, which not only tends to improve the median and peak values but also the received signal level at the cell edge (10^{th} percentile). Comparing the omni (no-tilt) with directional (90° DT) antenna configuration; due to the main beam tilted downwards, the coverage levels in the extreme tilt configuration are lower than in the baseline no-tilt configuration. This helps in reducing in the inter-cell interference and hence improves the radio channel conditions which is discussed next.

Fig. 5.10b shows the *SINR* performance bar graph for dynamic DAS modes with different antenna configurations. During the peak time period, when the number of users within the specific location increases, the network load rises. Hence, in order to accommodate more users within that geographic locality, the dynamic DAS network, through a server located in a central hub site, dynamically configures its remote antenna nodes to act as separate small cells. As such, the cell density within that geographic location increases, which translates into higher frequency reuse in that area, thereby accommodating more users, as will be shown in next section. The tradeoff, however, in such a scenario is that due to closely spaced co-channel sites, the inter-cell interference increases which degrade the radio channel conditions. In real networks, this cell-level performance reduction, stemming mostly from cell-edge users, can partially be compensated through inter-cell interference coordination (ICIC) and collaborative scheduling. However, in dense urban environment with high-rise buildings, the situation is exacerbated, due to *street canyon effect*. As mentioned in the earlier section, the street/urban canyon effect allows the signal level to propagate further than is possible in free space. As a result, the distance interferers become dominant as well, thereby further degrading the *SINR* performance. To counter the urban canyon phenomenon, an effective method is to steer the main antenna beam away from the street alley and instead focus it down towards the street. This reduces the *EIRP* along the

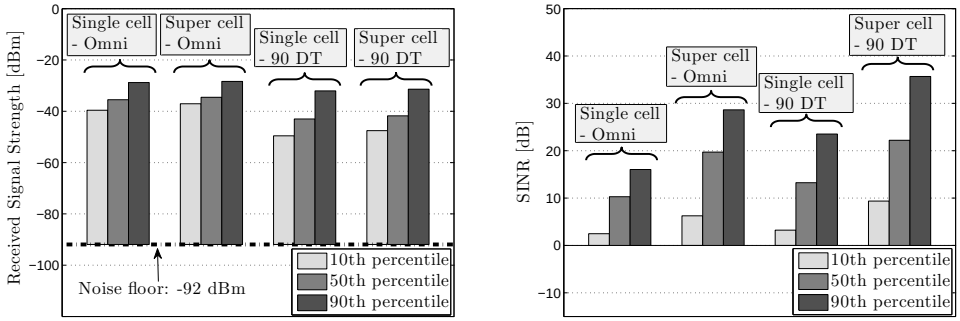

(a) (b)

Figure 5.10 10^{th} percentile (cell edge), 50^{th} percentile (median) and 90^{th} percentile (peak) values for outdoor (a) Coverage, and (b) Signal-to-Interference Noise ratio, for dynamic DAS under different operation modes and with different antenna configurations. Under high traffic conditions the dynamic DAS configures the nodes to operate as individual microcells, whereas in low traffic time period, the nodes are reconfigured to operate as one super microcell/DAS cell.

canyon thereby reducing the inter-cell interference in adjacent/neighboring LOS cells. The reduction in inter-cell interference translates into better *SINR* performance, as shown by the comparison of '*Individual microcells - Omni*' configuration with '*Individual microcells* - 90° *DT*' configuration in Fig. 5.10b. Subsequently, when the number of active users within a geographic location decreases, the network load goes down and hence, the DAS network re-configures itself into super microcell mode. The result is that the neighboring/adjacent nodes are clustered together to form a single cell, which not only improves the coverage level but also reduces the inter-cell interference within the cell. Hence an improvement can be seen in the *SINR* performance, as shown by '*Super cell*' configurations in Fig. 5.10b. In both dynamic DAS operation modes, the 90° DT configuration outperforms the Omni- no tilt configuration, due to effective interference control.

Cell and Area spectral efficiency analysis

Fig. 5.11 gives the capacity efficiency statistics for the dynamic DAS operation modes with different antenna configurations. The *SINR* values, analyzed in the previous section, are directly mapped to the *cell spectral efficiency*, shown in Fig. 5.11a, using (2.4). The gain in cell spectral efficiency, that can be achieved when the nodes are

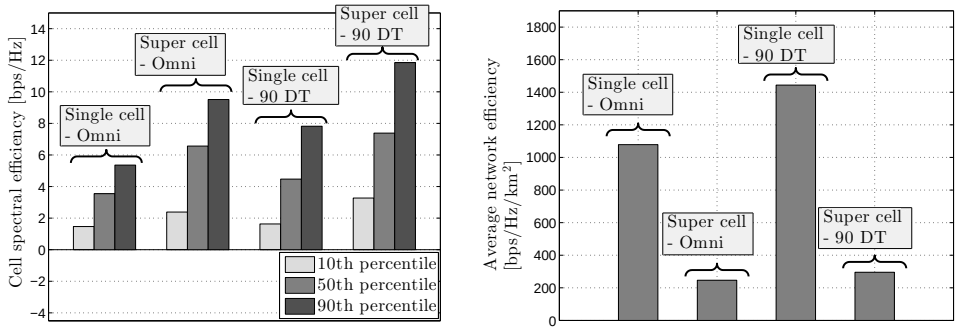

(a) (b)

Figure 5.11 Capacity efficiency statistics; (a) 10^{th} percentile (cell edge), 50^{th} percentile (median) and 90^{th} percentile (peak) values for outdoor cell spectral efficiency [bps/Hz], and (b) Average area spectral efficiency [bps/Hz/km^2] for dynamic DAS under different operation modes and with different antenna configurations.

clustered into DAS cell configuration, is approximately 1.5 times more than in the peak load scenario, when the nodes operate as separate small cells, (with both antenna configurations). Hence, in low load scenarios, the dynamic DAS network can offer high speed services to high mobility users with fewer numbers of handovers, due to the fact that the associated DAS nodes form one large cell. Coming to the area spectral efficiency performance; during peak load, the average gain in the area capacity, that is achievable through configuring each node as a small cell, is approximately 4.5 times more than the super microcell mode. This means that during peak load, the network is able to handle more users. From the handover point of view, during peak hours, the probability of high mobility users along the boulevards or high streets, where the majority of the data traffic is typically concentrated, is quite low - due to crowded roads. Hence, the frequency of handovers during peak hours, when the DAS nodes are acting as separate small cells, also reduces.

From the overall performance, the extreme tilt configuration, due to better interference management, exhibits higher cell and area spectral efficiency as compared to the baseline configuration.

5.6 Chapter Conclusions

This chapter examined the outdoor distributed antenna systems as an alternative solution for flexible capacity provisioning in outdoor environment.

First, the technical aspects of different deployment strategies for traditional outdoor distributed antenna system (ODAS) were analyzed and compared with standalone small cell deployment. For the deployment of ODAS, two strategies were considered based on the number of DAS nodes deployed. In strategy 1, the existing small cell sites were configured to act as single DAS cell, while in strategy 2, new antenna nodes were introduced into existing network. For the performance comparison of the ODAS strategies with standalone small cell deployment, two key metrics were considered; *coverage* and *capacity*. From the coverage point of view, both solutions, stand-alone small cells and DAS technology, offered comparative signal levels in the outdoor environment. From the cell level capacity-efficiency point of view, due to better interference management, distributed antenna systems offered better performance, especially at the cell edge. However, the deployment strategy 1 for outdoor DAS suffered from network level capacity inefficiency due to lower degree of spatial frequency reuse. Strategy 2 on the other hand provided a balanced approach, providing good cell level capacities while at the same time offering network capacities comparable to or even better than small cell deployments. However, the downside of Strategy 2 is that the total cost of deployment increases proportionally as new antenna nodes are added to the network.

Next, an advanced form of outdoor distributed antenna system, *Dynamic DAS* concept, was investigated, which dynamically adapts the system level capacity based on the outdoor traffic conditions. The basic premise behind the Dynamic DAS is that the outdoor mobile traffic variates during the time period of the day. Hence, to efficiently address the capacity demand, the remote antenna nodes are configured to act as a single micro cell during low traffic period, or multiple independent micro cells during high traffic period to increase the degree of spatial reuse and hence accomodate more users within the system. The potential of *Dynamic DAS* in an outdoor dense urban environment was shown under low and high network load conditions using cell- and network- level capacities as the performance evaluation metrics.

Chapter 6

Conclusions

6.1 Concluding Summary

Network densification has been identified as a key methodology to fulfill the surging data capacity demands in the long run. This dissertation examined the performance of network densification based on different deployment solutions in terms of *capacity*, *energy-* and *cost-efficiency*, from both indoor and outdoor service provisioning view points. For all the deployment scenarios, the network was assumed to be operating in a full load condition, which is the worst case scenario. By doing so, the considered deployment solutions are pushed to their extreme capacity limits. The ultimate aim of the dissertation was to get technical insight and understanding of DenseNets and their performance limits in the long run, and to draw cricitical conclusions on the choice of deployment scheme that can assist mobile operators in deciding the best evolution strategy for their network in the future.

Starting with the densification of classical deployment solutions used by the operators (based on macro-/micro-cellular technologies), the results revealed that the legacy solutions suffer from poor coverage and network capacity in-efficiencies in the indoor environment. The coverage limitation is more severe in the macrocellular deployment scenario, when building penetration losses increase beyond 20 dB. The indoor capacity in-efficiency also negatively impacted the energy- and cost- efficiency performance of the legacy solutions. Furthermore, the performance results showed that if the target of the operator is to provide only outdoor service, the legacy deployment solutions might still provide adequate service for the time being. However, for the indoor environment, where the capacity demand is exponentially increasing, addressing those demands by densifyinig the outdoor legacy deployments to extreme levels might not be feasible due to zoning restrictions and because of the observed inefficiencies.

When it comes to deployment solutions based on indoor small cells, the results

showed that the dedicated indoor solutions with densely deployed femto-cells are much more spectrally- and energy-efficient approach to address the enormous indoor capacity demands, compared to conventional (legacy) deployment solutions. Unlike outdoor deployments, the deployment of indoor femtocells, due to being located inside the building, provide superior indoor coverage and are not affected by increasing building penetration losses. Moreover, the results also showed that a heterogeneous macro-femtocells solutions provide superior outdoor cell edge performance as compared to homogeneous macrocellular deployment. Although, the dissertation focuses only on indoor femtocell deployments, the study can also be generalized to include other competing indoor small cell solutions like WiFi, in which case the traffic from outdoor layers is offloaded to WiFi networks. Hence, it is concluded that to counter the growing concerns of the mobile operators related to the exponentially increasing amounts of mobile data towards the 5G era and also modern buildings with higher wall penetration losses, an appealing solution is to deploy dedicated indoor small cell solutions like femtocells, WiFi etc. which offer a cost-effective and energy-efficient solution for indoor capacity demands. Also from indoor-to-outdoor service provisioning point of view, the mobile operators can partially leverage the indoor based femtocells to provide certain neighborhood coverage to low mobility outdoor users, thereby offloading some of the traffic from outdoor layer. This strategy can result in significant cost savings for mobile operators.

Finally, from the outdoor service provisioning view point, the dissertation looked at the prospect of using outdoor distributed antenna systems (ODAS) as an alternative solution to provide outdoor coverage and capacity. The results showed that due to being deployed on a street-level the ODAS solution is well suited to provide almost uniform coverage and better cell edge capacity performance. However, the traditional ODAS solution was shown to be in-efficient in terms of adopting to data traffic variation in the outdoor environment. Hence, an advanced form of 'dynamic DAS' concept was investigated that offers an efficient and capacity-adaptive solution to provide outdoor capacity, on-demand, in urban areas by dynamically configuring the remote antenna units to either act as individual small cells or distributed nodes of a common central cell.

6.2 Future Work

Improvement is a journey with no destination...

In general, the evaluation of simulation results is tightly coupled with the corresponding system models and assumptions. In this thesis, the network densification

was studied utilizing legacy (macro-/micro-cellullar) solutions, indoor femtocell-based solutions and outdoor distributed antenna systems. The performance of these solutions were evaluated in ideal and static propagation conditions in urban and suburban environments. Hence, it is pointed out that the results and conclusions presented in this dissertation are strictly-speaking valid only for the assumed deployment scenarios.

At the time of writing this section, there are several open questions regarding the work in the thesis field. A small list of enhancements to the simulation studies have been highlighted below which could be included in the future work:

- In this thesis, the performance of different deployment strategies was evaluated assuming no-intercell interference coordination (ICIC) mechanism between homogeneous cells or heterogeneous cells. Hence, future work should look into incoorporating the (ICIC) mechanism and observing the system capacity trend as the network is densified. Furthermore, from spectrum management point of view, it will be interesting to analyze the deployment case of dividing the spectrum between macro, micro and femtocells i.e. using adjacent channels for different layers of HetNet in order to eliminate the inter-layer interference.

- It will be interesting to see the impact of collaborative multicell processing techniques and advanced antenna systems (e.g. Massive MIMO and beamforming) on the performance of different deployment scenarios.

- All the simultions in this thesis were done in the UMTS Band 1 (2.1 GHz). Recently studies advocating mobile communications in the cm-wave or mm-wave bands have been published [75, 76, 128]. It will be interesting to evaluate the techno-economic performance of ultra-dense networks in the cm-wave or mm-wave bands.

- The dynamic DAS concept was evaluated based on two extreme ends (low and high network load) with simple propagation modeling based analysis. Further studies should concentrate on not only energy- and cost efficiency analysis but also on the system-level simulations, which take into account the switching criteria/algorithm of dynamic DAS, based on actual network load conditions.

- The cost efficiency analysis in the dissertation is based on simple cost model assuming Greenfield deployment. In practice, however, the cost modeling can be much more complex e.g., a) operators may already have some site assets, from their existing older networks, which they can capitalize on, b) operators might get into an agreement with other operators over site sharing or even spectrum

sharing in order to enhance their capacity etc. Further studies, can concentrate on a much more detailed techno-economic modeling that take into account the different deployment aspects as found in practice.

Bibliography

[1] *Cisco Visual Networking Index (VNI) report on Global Mobile Data Traffic Forecasts*, Annual Report, Cisco Systems Inc., 2014.

[2] J. Zander, "Challenge 2020 - 1000 times more capacity at todays cost & energy," http://zandercom.com/web/talks/, Dec 2012, [Online: accessed 5-May-2015].

[3] *Enhance mobile networks to deliver 1000 times more capacity by 2020*, White Paper, Nokia Networks, 2014.

[4] *5G Radio Access: Research and Vision*, White Paper, Ericsson, 2013.

[5] *The 1000x Mobile Data Challenge*, White Paper, Qualcomm Inc., 2013.

[6] V. Donald, "Advanced mobile phone service: The cellular concept," *The Bell System Technical Journal*, vol. 58, no. 1, pp. 15–41, Jan 1979.

[7] *ICT Sustainability Outlook: An Assessment of the Current State of Affairs and a Path Towards Improved Sustainability for Public Policies*, Report, BIO Intelligence Service and Alcatel-Lucent, 2013.

[8] *Sustainable Energy Use in Mobile Communication*, White Paper, Ericsson, 2007.

[9] M. Pickavet, W. Vereecken, S. Demeyer, P. Audenaert, B. Vermeulen, C. Develder, D. Colle, B. Dhoedt, and P. Demeester, "Worldwide energy needs for ICT: The rise of power-aware networking," in *Proc. 2nd International Symposium on Advanced Networks and Telecommunication Systems (ANTS)*, Dec 2008, pp. 1–3.

[10] F. Richter, A. Fehske, and G. Fettweis, "Energy Efficiency Aspects of Base Station Deployment Strategies for Cellular Networks," in *Proc. IEEE 70th Vehicular Technology Conference (VTC)*, Sep 2009, pp. 1–5.

[11] European Commission, "EU Commissioner calls on ICT industry to reduce its carbon footprint by 20% as early as 2015," http://europa.eu/rapid/press-release_MEMO-09-140_en.htm, Mar 2009, [Online: accessed 5-May-2015].

[12] *DIRECTIVE 2010/31/EU of the European Parliament and of the Council*, Official Journal of the European Union, 2010.

[13] A. Asp, Y. Sydorov, M. Valkama, and J. Niemelä, "Radio signal propagation and attenuation measurements for modern residential buildings," in *Proc. IEEE Globecom Workshops (GC Wkshps)*, Dec 2012, pp. 580–584.

[14] A. Asp, Y. Sydorov, M. Keskikastari, M. Valkama, and J. Niemelä, "Impact of Modern Construction Materials on Radio Signal Propagation: Practical Measurements and Network Planning Aspects," in *Proc. IEEE 79th Vehicular Technology Conference (VTC)*, May 2014, pp. 1–7.

[15] J. Lempiäinen and M. Manninen, *Radio Interface System Planning for GSM/GPRS/UMTS*. Kluwer Academic Publishers, 2001.

[16] J. Laiho, A. Wacker, and T. Novosad, *Radio Network Planning and Optimisation for UMTS, 2nd ed.* John Wiley & Sons Ltd, 2006.

[17] I. Rodriguez, H. Nguyen, N. Jorgensen, T. Sorensen, and P. E. Mogensen, "Radio Propagation into Modern Buildings: Attenuation Measurements in the Range from 800 MHz to 18 GHz," in *Proc. IEEE 80th Vehicular Technology Conference (VTC)*, Sept 2014, pp. 1–5.

[18] W. C. Jakes, *Microwave Mobile Communications*. IEEE Press, New York, 1972.

[19] W. R. Young, "Advanced mobile telephone service: introduction, background and objectives," *The Bell System Technical Journal*, vol. 58, p. 1–14, Jan 1979.

[20] H. J. Schulter and W. A. Cornell, "Multi-area mobile telephone service," *IRE Transactions on Communications Systems*, vol. 9, p. 49, Jun 1960.

[21] K. Araki, "Advanced mobile telephone service: introduction, background and objectives," *Rev. of the Electrical Communication Laboratory*, vol. 16, p. 357–373, Jun 1968.

[22] R. Frenkiel, "A high capacity mobile radiotelephone system model using a coordinated small zone approach," *IEEE Transactions on Vehicular Technology*, vol. 19, no. 2, pp. 173–177, May 1970.

[23] P. T. Porter, "Supervision and control features of a small zone radiotelephone systems," *IEEE Transactions on Vehicular Technology*, vol. 20, no. 3, pp. 75–79, Aug 1971.

[24] N. Yoshikawa and T. Nomura, "On the design of a small zone land mobile radio system in UHF band," *IEEE Transactions on Vehicular Technology*, vol. 25, no. 3, pp. 57–67, Aug 1976.

[25] V. Palestini, "Evaluation of overall outage probability in cellular systems," in *Proc. IEEE 39th Vehicular Technology Conference (VTC)*, May 1989, pp. 625–630.

[26] R. Steele, "Towards a high-capacity digital cellular mobile radio system," *IEE Communications, Radar and Signal Processing*, vol. 132, no. 5, pp. 405–415, Aug 1985.

[27] R. Steele and V. Prabhu, "High-user-density digital cellular mobile radio systems," *IEE Communications, Radar and Signal Processing*, vol. 132, no. 5, pp. 396–404, Aug 1985.

[28] K. Wong and R. Steele, "Transmission of digital speech in highway microcells," *Journal of the Institution of Electronic and Radio Engineers*, vol. 57, no. 6, pp. 246–254, Nov 1987.

[29] S. El-Dolil, W.-C. Wong, and R. Steele, "Teletraffic performance of highway microcells with overlay macrocell," *IEEE Journal on Selected Areas in Communications*, vol. 7, no. 1, pp. 71–78, Jan 1989.

[30] T.-S. Chu and M. Gans, "Fiber optic microcellular radio," *IEEE Transactions on Vehicular Technology*, vol. 40, no. 3, pp. 599–606, Aug 1991.

[31] W. C. Y. Lee, "Efficiency of a new microcell system," in *Proc. IEEE 42nd Vehicular Technology Conference (VTC)*, May 1992, pp. 37–42.

[32] L. Greenstein, N. Amitay, T.-S. Chu, L. Cimini, G. Foschini, M. Gans, C.-L. I, A. Rustako, R. Valenzuela, and G. Vannucci, "Microcells in personal communications systems," *IEEE Communications Magazine*, vol. 30, no. 12, pp. 76–88, Dec 1992.

[33] X. Lagrange, "Multitier cell design," *IEEE Communications Magazine*, vol. 35, no. 8, pp. 60–64, Aug 1997.

[34] J. Sarnecki, C. Vinodrai, A. Javed, P. O'Kelly, and K. Dick, "Microcell design principles," *IEEE Communications Magazine*, vol. 31, no. 4, pp. 76–82, Apr 1993.

[35] I. Chih-Lin, L. Greenstein, and R. Gitlin, "A microcell/macrocell cellular architecture for low- and high-mobility wireless users," *IEEE Journal on Selected Areas in Communications*, vol. 11, no. 6, pp. 885–891, Aug 1993.

[36] M. Murata and E. Nakano, "Enhancing the performance of mobile communications systems," in *Proc. IEEE 2nd International Conference on Universal Personal Communications: Gateway to the 21st Century*, vol. 2, Oct 1993, pp. 732–736.

[37] A. Yamaguchi, H. Kobayashi, and T. Mizuno, "Integration of micro and macro cellular networks for future land mobile communications," in *Proc. IEEE 2nd International Conference on Universal Personal Communications: Gateway to the 21st Century*, vol. 2, Oct 1993, pp. 737–742.

[38] J. Shapira, "Microcell engineering in cdma cellular networks," *IEEE Transactions on Vehicular Technology*, vol. 43, no. 4, pp. 817–825, Nov 1994.

[39] D. M. Grieco, "The capacity achievable with a broadband cdma microcell underlay to an existing cellular macrosystem," *IEEE Journal on Selected Areas in Communications*, vol. 12, no. 4, pp. 744–750, May 1994.

[40] S. A. Ahson and M. Ilyas, *Fixed Mobile Convergence Handbook*. CRC Press, 2010.

[41] S. C. Forum, http://www.smallcellforum.org, [Online: accessed 5-May-2015].

[42] *Enterprise femtocell deployment guidelines*, Technical report, SCF032.05.01, Small Cell Forum, 2014.

[43] *Deployment issues for urban small cells*, Technical report, SCF096.05.02, Small Cell Forum, 2014.

[44] *Deployment issues for rural and remote small cells*, Technical report, SCF156.05.01, Small Cell Forum, 2014.

[45] 3GPP Technical Report, *3G Home NodeB Study Item Technical Report*, 3GPP TR 25.820, version 8.2.0 , Release 8.

[46] ——, *Home Node B Radio Frequency (RF) Requirements (FDD)*, 3GPP TR 25.967, version 8.0.1 , Release 8.

[47] ——, *Evolved Terrestrial Radio Access (E-UTRA): FDD Home eNodeB (HeNB) Radio Frequency (RF) requirements analysis*, 3GPP TR 36.921, version 9.0.0 , Release 9.

[48] ——, *Evolved Terrestrial Radio Access (E-UTRA): TDD Home eNodeB (HeNB) Radio Frequency (RF) requirements analysis*, 3GPP TR 36.922, version 9.1.0 , Release 9.

[49] *4G Mobile Broadband Evolution: Release 10, Release 11 and Beyond - HSPA+, SAE/LTE and LTE-Advanced*, White paper, 4G Americas, 2012.

[50] Y. Liang, A. Goldsmith, G. Foschini, R. Valenzuela, and D. Chizhik, "Evolution of base stations in cellular networks: Denser deployment versus coordination," in *Proc. IEEE International Conference on Communications (ICC)*, May 2008, pp. 4128–4132.

[51] B. Badic, T. O'Farrrell, P. Loskot, and J. He, "Energy efficient radio access architectures for green radio: Large versus small cell size deployment," in *Proc. IEEE 70th Vehicular Technology Conference Fall (VTC)*, Sep 2009, pp. 1–5.

[52] F. Richter and G. Fettweis, "Cellular mobile network densification utilizing micro base stations," in *Proc. IEEE International Conference on Communications (ICC)*, May 2010, pp. 1–6.

[53] S. Tombaz, K. W. Sung, and J. Zander, "Impact of densification on energy efficiency in wireless access networks," in *Proc. IEEE Globecom Workshops (GC Wkshps)*, Dec 2012, pp. 57–62.

[54] K. Hiltunen, "Comparison of different network densification alternatives from the LTE uplink point of view," in *Proc. IEEE 22nd International Symposium on Personal Indoor and Mobile Radio Communications (PIMRC)*, Sep 2011, pp. 1601–1605.

[55] ——, "Comparison of Different Network Densification Alternatives from the LTE Downlink Performance Point of View," in *Proc. IEEE 74th Vehicular Technology Conference (VTC)*, Sep 2011, pp. 1–5.

[56] L. M. Correia, D. Zeller, O. Blume, D. Ferling, Y. Jading, I. Godor, G. Auer, and L. Van der Perre, "Challenges and enabling technologies for energy aware

mobile radio networks," *IEEE Communications Magazine*, vol. 48, no. 11, pp. 66–72, Nov 2010.

[57] G. Auer, V. Giannini, I. Godor, P. Skillermark, M. Olsson, M. Imran, D. Sabella, M. Gonzalez, C. Desset, and O. Blume, "Cellular energy efficiency evaluation framework," in *Proc. IEEE 73rd Vehicular Technology Conference (VTC)*, May 2011, pp. 1–6.

[58] M. Ericson, "Total network base station energy cost vs. deployment," in *Proc. IEEE 73rd Vehicular Technology Conference (VTC)*, May 2011, pp. 1–5.

[59] T. Le and M. Nakhai, "Possible power-saving gains by dividing a cell into tiers of smaller cells," *Electronics Letters*, vol. 46, no. 16, pp. 1163–1165, August 2010.

[60] H. Leem, S. Y. Baek, and D. K. Sung, "The effects of cell size on energy saving, system capacity, and per-energy capacity," in *Proc. IEEE Wireless Communications and Networking Conference (WCNC)*, Apr 2010, pp. 1–6.

[61] S. Tombaz, Z. Zheng, and J. Zander, "Energy efficiency assessment of wireless access networks utilizing indoor base stations," in *Proc. IEEE 24th International Symposium on Personal Indoor and Mobile Radio Communications (PIMRC)*, Sept 2013, pp. 3105–3110.

[62] K. Hiltunen, "Total power consumption of different network densification alternatives," in *Proc. IEEE 23rd International Symposium on Personal Indoor and Mobile Radio Communications (PIMRC)*, Sep 2012, pp. 1401–1405.

[63] Z. Frias and J. Pérez, "Techno-economic analysis of femtocell deployment in long-term evolution networks," *EURASIP J. Wirel. Commun. Netw.*, vol. 2012, no. 1, 2012.

[64] J. Markendahl and O. Mäkitalo, "A comparative study of deployment options, capacity and cost structure for macrocellular and femtocell networks," in *Proc. IEEE 21st International Symposium on Personal, Indoor and Mobile Radio Communications Workshops (PIMRC Workshops)*, Sep 2010, pp. 145–150.

[65] A. A. Widaa, J. Markendahl, and A. Ghanbari, "Toward capacity-efficient, cost-efficient and power-efficient deployment strategy for indoor mobile broadband," in *Proc. 24th European Regional Conference of the International Telecommunications Society*, Oct 2013.

[66] S. F. Yunas, T. Isotalo, J. Niemelä, and M. Valkama, "Impact of Macrocellular Network Densification on the Capacity, Energy and Cost Efficiency in Dense Urban Environment," *International Journal of Wireless and Mobile Networks (IJWMN)*, vol. 5, no. 5, pp. 99–118, Oct 2013.

[67] S. F. Yunas, T. Isotalo, and J. Niemelä, "Impact of network densification, site placement and antenna downtilt on the capacity performance in microcellular networks," in *Proc. 6th Joint IFIP/IEEE Wireless and Mobile Networking Conference (WMNC)*, Apr 2013, pp. 1–7.

[68] S. F. Yunas, A. Asp, J. Niemelä, and M. Valkama, "Deployment strategies and performance analysis of Macrocell and Femtocell networks in suburban environment with modern buildings," in *Proc. IEEE 39th Conference on Local Computer Networks (LCN'14)*, Sep 2014, pp. 643–651.

[69] S. F. Yunas, J. Niemelä, M. Valkama, and T. Isotalo, "Techno-economical analysis and comparison of legacy and ultra-dense small cell networks," in *Proc. IEEE 39th Conference on Local Computer Networks (LCN'14)*, Sep 2014, pp. 768–776.

[70] S. F. Yunas, M. Valkama, and J. Niemelä, "Cell planning for outdoor distributed antenna systems in dense urban areas," in *Proc. 16th International Telecommunications Network Strategy and Planning Symposium (NETWORKS'14)*, Sep 2014, pp. 1–7.

[71] ——, "Spectral Efficiency of Dynamic DAS with Extreme Down-tilt Antenna Configuration," in *Proc. IEEE 25th International Symposium on Personal, Indoor and Mobile Radio Communications (PIMRC'14)*, Sep 2014, pp. 1–6.

[72] ——, "Spectral and energy efficiency of ultra-dense networks under different deployment strategies," *IEEE Communications Magazine*, vol. 53, no. 1, pp. 90–100, Jan 2015.

[73] T. S. Rappaport, *Wireless Communications, 2nd edition.* Prentice-Hall, 2002.

[74] C. E. Shannon, "A Mathematical Theory of Communication," *The Bell System Technical Journal*, vol. 27, p. 379–423, Oct 1948.

[75] T. Rappaport, S. Sun, R. Mayzus, H. Zhao, Y. Azar, K. Wang, G. Wong, J. Schulz, M. Samimi, and F. Gutierrez, "Millimeter Wave Mobile Communications for 5G Cellular: It Will Work!" *IEEE Access*, vol. 1, pp. 335–349, 2013.

[76] P. Mogensen, K. Pajukoski, E. Tiirola, J. Vihriala, E. Lahetkangas, G. Berardinelli, F. Tavares, N. Mahmood, M. Lauridsen, D. Catania, and A. Cattoni, "Centimeter-Wave Concept for 5G Ultra-Dense Small Cells," in *IEEE 79th Vehicular Technology Conference (VTC)*, May 2014, pp. 1–6.

[77] L. Reading, http://www.lightreading.com/mobile/5g/ericsson-cto-5g-needs-broad-brush/d/d-id/711872.

[78] S. Talwar, D. Choudhury, K. Dimou, E. Aryafar, B. Bangerter, and K. Stewart, "Enabling technologies and architectures for 5G wireless," in *Proc. IEEE MTT-S International Microwave Symposium (IMS)*, Jun 2014, pp. 1–4.

[79] B. Bangerter, S. Talwar, R. Arefi, and K. Stewart, "Networks and Devices for the 5G era," *IEEE Communications Magazine*, vol. 52, no. 2, pp. 90–96, Feb 2014.

[80] C. Johnson, *Long Term Evolution in Bullets, 2nd edition.* www.lte-bullets.com, 2012.

[81] 3GPP Technical Report, *Evolved Terrestrial Radio Access (E-UTRA): Base station (BS) radio transmission and reception*, 3GPP TR 36.104, version 9.11.9 , Release 9.

[82] A. Damnjanovic, J. Montojo, Y. Wei, T. Ji, T. Luo, M. Vajapeyam, T. Yoo, O. Song, and D. Malladi, "A survey on 3GPP heterogeneous networks," *IEEE Wireless Communications*, vol. 18, no. 3, pp. 10–21, June 2011.

[83] V. Chandrasekhar, J. Andrews, and A. Gatherer, "Femtocell networks: a survey," *IEEE Communications Magazine*, vol. 46, no. 9, pp. 59–67, Sep 2008.

[84] *Small cells - what's the big idea*, White paper, Smal Cell Forum, 2012.

[85] M. Deruyck, W. Joseph, and L. Martens, "Power Consumption Model for Macrocell and Microcell Base stations," *Transactions on Emerging Telecommunications Technologies*, vol. 25, no. 3, pp. 320–333, Mar 2014.

[86] M. Deruyck, E. Tanghe, W. Joseph, and L. Martens.

[87] M. Deruyck, E. Tanghe, W. Joseph, W. Vereecken, M. Pickavet, L. Martens, and B. Dhoedt, "Model for power consumption of wireless access networks," *IET Science, Measurement and Technology*, vol. 5, no. 4, pp. 155–161, Jul 2011.

[88] T. Giles, J. Markendahl, J. Zander, P. Zetterberg, P. Karlsson, G. Malmgren, and J. Nilsson, "Cost drivers and deployment scenarios for future broadband wireless networks - key research problems and directions for research," in *Proc. IEEE 59th Vehicular Technology Conference (VTC)*, May 2004, pp. 2042–2046.

[89] T. Smura, "Techno-economic modelling of wireless network and industry architectures," Ph.D. dissertation, Aalto University, 2012.

[90] K. Johansson, A. Furuskar, P. Karlsson, and J. Zander, "Relation between base station characteristics and cost structure in cellular systems," in *Proc. IEEE 15th International Symposium on Personal, Indoor and Mobile Radio Communications (PIMRC)*, Sep 2004, pp. 2627–2631.

[91] 3GPP Technical Report, *Evolved Universal Terrestrial Radio Access (E-UTRA); LTE coverage enhancements*, 3GPP TR 36.814, version 11.0.0 , Release 11.

[92] F. Gunnarsson, M. Johansson, A. Furuskar, M. Lundevall, A. Simonsson, C. Tidestav, and M. Blomgren, "Downtilted Base Station Antennas - A Simulation Model Proposal and Impact on HSPA and LTE Performance," in *Proc. IEEE 68th Vehicular Technology Conference (VTC)*, Sep 2008, pp. 1–5.

[93] 3GPP Technical Report, *Physical layer aspects for evolved Universal Terrestrial Radio Access (UTRA)*, 3GPP TR 25.814, version 7.1.0 , Release 7.

[94] *Wireless InSite v 2.5 User's Manual*, Remcom Inc.

[95] J. Schuster and R. Luebbers, "Hybrid SBR/GTD radio propagation model for site specific predictions in an urban environment," pp. 84–92, Mar 1996.

[96] C. Balanis, *Advanced Engineering Electromagnetics*. John Wiley & Sons Ltd, 1989.

[97] *ProMan User's Manual*, AWE Communications.

[98] G. Wölfle, "Adaptive Propagation Models for the Planning of Wireless Communication Networks and for the Computation of the Reception Quality inside Building," Ph.D. dissertation, University of Stuttgart, 2000.

[99] R. Wahl and G. Wölfle, "Combined urban and indoor network planning using the dominant path propagation model," in *Proc. First European Conference on Antennas and Propagation (EuCAP)*, Nov 2006, pp. 1–6.

[100] G. Wölfle and F. Landstorfer, "Dominant paths for the field strength prediction," in *Proc. IEEE 48th Vehicular Technology Conference (VTC)*, May 1998, pp. 552–556.

[101] H. Alasti, K. Xu, and Z. Dang, "Efficient experimental path loss exponent measurement for uniformly attenuated indoor radio channels," in *Proc. IEEE SOUTHEASTCON*, Mar 2009, pp. 255–260.

[102] WINNER II Technical report, *WINNER II Channel Models part I- Channel Models*, IST-4-027756 WINNER II, D1.1.2.

[103] W. Yuanye, S. Kumar, L. Garcia, K. Pedersen, I. Z. Kovacs, S. Frattasi, N. Maretti, and P. E. Mogensen, "Fixed Frequency Reuse for LTE-Advanced Systems in Local Area Scenarios," in *Proc. IEEE 69th Vehicular Technology Conference (VTC)*, Apr 2009, pp. 1–5.

[104] M. J. Nawrocki, M. Dohler, and A. H. Aghvami, *Understanding UMTS Radio Network Planning.* John Wiley & Sons Ltd, 2006.

[105] J. Niemelä, T. Isotalo, and J. Lempiäinen, "Optimum antenna downtilt angles for macrocellular wcdma network," *EURASIP J. Wirel. Commun. Netw.*, vol. 2005, no. 5, pp. 816–827, 2005.

[106] H. Holma and A. Toskala, *LTE for UMTS – OFDMA and SC-FDMA Based Radio Access.* John Wiley & Sons Ltd, 2009.

[107] M. Paolini, "Mobile data move indoors," *Mobile Europe*, no. 215, pp. 22–25, Apr/May 2011.

[108] H. Chin, D. F. Kimball, S. Lanfranco, and P. M. Asbeck, "Wideband high efficiency digitally-assisted envelope amplifier with dual switching stages for radio base-station envelope tracking power amplifiers," in *Proc. IEEE MTT-S International Microwave Symposium Digest (MTT)*, May 2010, pp. 672–675.

[109] W. Yu-Chen, K. Chen, E. Naglich, and D. Peroulis, "A wideband 0.7 - 2.2 GHz tunable power amplifier with over 64% efficiency based on high-Q second harmonic loading," in *Proc. IEEE MTT-S International Microwave Symposium Digest (IMS)*, Jun 2013, pp. 1–4.

[110] *NSN Flexi Compact Base Station, Datasheet*, Nokia Networks and Solutions.

[111] J. Niemelä and T. Isotalo, *Coverage constrained Techno-economical comparison of Macro and Small Cell Planning Strategies*, Internal report, Dept. Electronics and Communications Engineering., Tampere University of Technology.

[112] M. Gudmundson, "Proc. Cell planning in Manhattan environments," in *Proc. IEEE 42nd Vehicular Technology Conference (VTC)*, May 1992, pp. 435–438.

[113] Alcatel Lucent, "9768 Metro Radio Outdoor B25 LTE 1W Data Sheet," http://resources.alcatel-lucent.com/?cid=161039, Sep 2014, [Online: accessed 5-May-2015].

[114] Airspan, "AirSynergy 3000, Data Sheet," https://www.airspan.com/wp-content/plugins/download-monitor/download.php?id=AirSynergy-3000-Brochure1.pdf, [Online: accessed 5-May-2015].

[115] P.-H. Lehne, "3rd nordic workshop of system & network optimization (snow)," in *Proc. Mobile Network Operator Challenges to Meet Future Demand for Mobile Broadband*, Apr 2012.

[116] N. Bhushan, J. Li, D. Malladi, R. Gilmore, D. Brenner, A. Damnjanovic, R. Sukhavasi, C. Patel, and S. Geirhofer, "Network densification: the dominant theme for wireless evolution into 5G," *IEEE Communications Magazine*, vol. 52, no. 2, pp. 82–89, Feb 2014.

[117] *Neighborhood Small Cells for Hyper Dense Deployments: Taking HetNets to the Next Level*, White Paper, Qualcomm Inc., 2013.

[118] 3GPP Technical Report, *Radio Frequency (RF) pattern matching location method in LTE*, 3GPP TR 36.809, version 12.0.0 , Release 12.

[119] R. Q. Hu and Y. Qian, *Heterogeneous Cellular Networks*. Wiley - IEEE Press, 2013.

[120] M. Deruyck, D. De Vulder, W. Joseph, and L. Martens, "Modelling the power consumption in femtocell networks," in *Proc. IEEE Wireless Communications and Networking Conference Workshops (WCNCW)*, Apr 2012, pp. 30–35.

[121] Unitmedia, http://www.unitymedia.de/privatkunden/kombipakete/2play-kombipakete, [Online: accessed 5-May-2015].

[122] *Connected cars: worldwide trends, forecasts and strategies 2014–2024*, Report, Analysys Mason, 2014.

[123] *The Connected Car: Consumer Interest and Current User Experience*, Automotive Consumer Insights (ACI) report, 2014.

[124] E. Larsson, O. Edfors, F. Tufvesson, and T. Marzetta, "Massive MIMO for next generation wireless systems," *IEEE Communications Magazine*, vol. 52, no. 2, pp. 186–195, Feb 2014.

[125] J. Itkonen, B. Tuzson, and J. Lempiäinen, "Assessment of Network Layouts for CDMA Radio Access," *EURASIP Journal on Wireless Communications and Networking*, vol. 2008, no. 1, 2008.

[126] *C-RAN: The Road Towards Green RAN*, White Paper, China Mobile Research Institute, 2011.

[127] V. Sridhara and S. Bohacek, "Realistic propagation simulation of urban mesh networks," *International Journal of Computer and Telecommunications Networking Computer Networks and ISDN Systems (COMNET)*, 2007.

[128] R. Baldemair, T. Irnich, K. Balachandran, E. Dahlman, G. Mildh, Y. Selen, S. Parkvall, M. Meyer, and A. Osseiran, "Ultra-dense networks in millimeter-wave frequencies," *IEEE Communications Magazine*, vol. 53, no. 1, pp. 202–208, January 2015.

Tampereen teknillinen yliopisto
PL 527
33101 Tampere

Tampere University of Technology
P.O.B. 527
FI-33101 Tampere, Finland

ISBN 978-952-15-3581-9
ISSN 1459-2045